Thermodynamics of liquid mixtures containing N-methyl-2-Pyrrolidone

Thesis
Submitted in fulfilment of the requirements for the degree of
MASTER OF SCIENCE
of
University of Natal

By

Pavanandan Kista Naicker

March 1997

DECLARATION

I hereby certify that the work presented in this thesis is the result of my own investigation under the supervision of Professor T. M. Letcher, and has never been submitted in candidature for a degree at any other university.

Pavanandan K. Naicker

I herby certify that the above statement is correct.

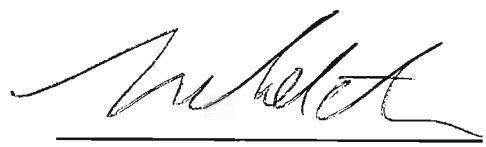

Prof. T. M. Letcher

Department of Chemistry,
University Natal,
Durban.

ACKNOWLEDGEMENTS

The author gratefully makes the following acknowledgements:

To the Mother Saraswathi from whom all knowledge flows, I am grateful for the guidance, strength and inspiration.

To Professor T. M. Letcher to whom I am eternally indebted for his guidance, supervision and encouragement during the course of this study.

To all the Technical staff : Greg, Jay, Logan, Raj, Dave and Jodie for all their help.

To Paul and Ashley for their help and cooperation.

To my parents who always insist, "go as far as you can". I thank them for their unwavering support and sacrifices.

To the FRD for financial support.

Finally to my wife for all her love, support and encouragement.

this thesis is dedicated
to
Sharushan

Abstract

This thesis involves a study of the thermodynamics of liquid mixtures containing N-methyl-2-pyrrolidone (NMP) and hydrocarbons or ethers. NMP is a polar liquid which is used in liquid extraction procedures for the separation of polar and nonpolar hydrocarbons. It was considered important enough to devote an entire thesis to the properties of NMP related to its interactions with simple hydrocarbons and ethers. The thesis consists of four parts:

Part one is devoted to liquid-liquid equilibria. Experimental results at 298.2 K, are presented for the mixtures: NMP + an aromatic hydrocarbon + an n-alkane. Firstly, the effect increasing the chain length of the alkane has on the liquid-liquid equilibria was investigated, by studying mixtures of the type: an n-alkane + toluene + NMP; where the n-alkane refers to n-hexane or n-nonane or n-tetradecane or n-hexadecane. Secondly, the effect of substitution on the benzene ring on the equilibria was studied by measuring the liquid-liquid equilibria for the mixtures: n-hexadecane + an aromatic hydrocarbon + NMP; where the aromatic hydrocarbon refers to toluene or o-xylene or m-xylene or p-xylene or mesitylene or ethyl benzene. The chain length of the n-alkane had a significant effect on the liquid-liquid equilibria. Methyl substitution on the benzene ring had a small effect on the liquid-liquid equilibria.

Part two is devoted to activity coefficients at infinite dilution. Experimental results at 298.15 K, determined using gas-liquid chromatography, are presented for the mixtures: NMP (solvent) + n-pentane or n-hexane or n-heptane or n-octane or cyclopentane or cyclohexane or cycloheptane or 1-hexene or 1-heptene or 1-octene or diethyl ether or diisopropyl ether. The magnitudes of the infinite dilution activity coefficients had the following order: n-alkanes > cycloalkanes > 1-alkenes > ethers.

Part three is devoted to excess molar enthalpies. Experimental results at 298.15 K are presented for the mixtures: NMP + an aromatic hydrocarbon. Here, an aromatic hydrocarbon refers to one of benzene or toluene or o-xylene or m-xylene or p-xylene or mesitylene or ethyl benzene. Isothermal flow microcalorimetry was used to determine the excess molar enthalpies. Increased methyl substitution on the benzene ring manifests itself as a reduction in the association between NMP and the aromatic hydrocarbon.

Part four is devoted to excess molar volumes. Experimental results at 298.15 K are presented for the mixtures: NMP + an aromatic hydrocarbon. Here, an aromatic hydrocarbon refers to one of benzene or toluene or o-xylene or m-xylene or p-xylene or mesitylene or ethyl benzene. Densitometry was used to determine the excess molar volumes. The excess molar volumes were negative for all the mixtures.

Contents

Chapter **Page**

Chapter **Page**

List of Tables

List of Figures

List of Symbols

Symbol

x_i = mole fraction of component i.

x_{ij} = mole fraction of component i in the phase rich in component j.

n^{25} = refractive index at 25 °C.

A_i = coefficient i in the Hlavatý equation.

B_i = coefficient i in the β equation.

C_i = coefficient i in the log equation.

x_I^o = fraction of n-alkane on the $x_2 = 0$ axis.

x_{II}^o = fraction of n-alkane on the $x_2 = 0$ axis.

x_i' = mole fraction of component i in the light phase.

x_i'' = mole fraction of i in the heavy phase.

μ_A = chemical potential of species A.

μ_A^* = chemical potential of species A in the standard state.

γ_A = activity coefficient of A.

γ_A^∞ = activity coefficient at infinite dilution of A.

γ_{13}^∞ = activity coefficient at infinite dilution of component 1 in component 3.

γ^∞ = activity coefficient at infinite dilution.

γ_i^∞ = activity coefficient at infinite dilution of i.

v_i = liquid molar volume of i.

R = gas constant = 8.3143 $J \cdot mol^{-1}$

λ_i = dispersion parameter of i.

q_i = induction parameter of i,
molecular surface area

τ_i = polar parameter of i,
adjustable parameters for UNIFAC,
period of oscillation.

α_i = acidity parameter of i.

β_i = basicity parameter i.

Symbol

ψ = parameter accounting for the difference in polarity between i and j

ξ = parameter accounting for the degree of hydrogen bonding.

d_{12} = Flory-Huggins combinatorial term.

aa = parameter used in the MOSCED obtained from literature.

γ_i^S = activity coefficient due to size.

γ_i^G = activity due to group interactions.

s_i = size fraction of i in the mixture.

γ_i^C = combinatorial term.

γ_i^R = residual term.

Φ_i = segment fraction of i.

θ_i = area fraction of i.

ℓ = parameter used in UNIFAC.

z = parameter used in UNIFAC.

r_i = molecular van der Waals volume.

u_i = parameter used in UNIFAC.

V_R = retention volume.

V_G = gas holdup volume.

V_3 = solvent volume.

K = partition coefficient.

V_N = net retention volume.

n_3 = number of moles of solvent.

p_1^o = solute vapour pressure.

U_o = outlet flow rate.

J_3^2 = Martin and James correction factor.

t_r = retention time of solute.

Symbol

t_G = retention time of unretained gas.

p_i = inlet pressure.

p_o = outlet pressure.

B_{11} = virial coefficient of the solute.

B_{12} = mixed virial coefficient.

V_1^{∞} = molar volume of component one at infinite dilution.

V_1^{o} = molar volume of the pure solute.

B = virial coefficient.

T_c = critical temperature.

V_c = critical volume.

n = number of carbon atoms.

I = Ionization energy of component.

A = constant in Antoine equation,
constant for density calculation.

B = constant in Antoine equation,
constant for density calculation.

C = constant in Antoine equation.

t = temperature in degrees Celsius,
time in seconds.

ΔH_{mix} = enthalpy of mixing.

H_m^E = excess molar enthalpy.

G_m^E = excess molar Gibbs energy.

p^o = pressure

P = power

I = current.

R = resistance

F = molar flow rate.

n_i = number of moles of i.

A_r = coefficients for the Redlich-Kister smoothing function.

Symbol

σ = standard deviation.

V_m^E = excess molar volume.

V_A^o = molar volume of pure A.

V_B^o = molar volume of pure B.

G^E = excess Gibbs function.

V = molar volume.

M = molar mass.

ρ = density.

ρ^{20} = density at 20 °C.

ρ^{25} = density at 25 °C.

T = temperature in degrees Kelvin.

Chapter 1
Introduction

This work investigates the thermodynamics of liquid mixtures containing N-methyl-2-pyrrolidone (NMP). NMP is a dipolar aprotic solvent that is used for the separation of low molecular weight monocyclic aromatic compounds from petroleum feedstock.[1,2,3] NMP is a heterocyclic molecule (see figure 1.1.).

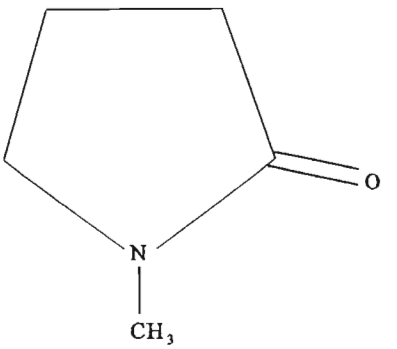

Figure 1.1 Structure of N-methyl-2-pyrrolidone,(NMP).

NMP has also been found to be an excellent dissociating solvent suitable for use in electrochemistry.[4,5,6] NMP has also been used as a dipolar aprotic medium for organic synthesis,[7] as well as a solvent for the study of aromatic radicals and electron-transfer reactions using pulse radiolysis,[8] and as a solvent for polymer casting.[9]
NMP is obviously a very important solvent.

On consulting the literature it was found that significant data on NMP was missing. In order to improve our knowledge of the interactions of NMP mixtures with hydrocarbons or with ethers, it was decided to measure some of the more important thermodynamic properties (see below) of NMP in these mixtures.

This thesis is divided into four parts:

Part one (chapter two) is devoted to the liquid-liquid equilibria of the mixtures NMP + an aromatic hydrocarbon + an n-alkane. Firstly, the effect increasing the chain length of the alkane has on the equilibria was investigated by studying mixtures of the type, an n-alkane + toluene + NMP, where the n-alkane is n-hexane or n-nonane or n-tetradecane or n-hexadecane. Very little of these data are already available in the literature, hence this work contributes to the literature. Secondly, the effect that substitution on the benzene ring has on the equilibria was studied by measuring the liquid-liquid equilibria for the mixtures n-

hexadecane + an aromatic hydrocarbon + NMP, where the aromatic hydrocarbon refers to toluene or o-xylene or m-xylene or p-xylene or mesitylene or ethyl benzene. This work contributes new data to the literature.

Part two (chapter three) is devoted to activity coefficients at infinite dilution for mixtures containing NMP. Experimental results at 298.15 K were presented for the mixtures: NMP (solvent) + n-pentane or n-hexane or n-heptane or n-octane or cyclopentane or cyclohexane or cycloheptane or 1-hexene or 1-heptene or 1-octene or diethyl ether or diisopropyl ether. New data are presented for cyclopentane, cycloheptane, 1-heptene, 1-octene, diethyl ether and diisopropyl ether. The data presented in this work together with existing data gives a picture of the thermodynamic effect of mixing. Gas-liquid chromatography was used to determine the activity coefficients at infinite dilution.

Part three (chapter four) is devoted to the study of excess molar enthalpies for the mixtures: NMP + an aromatic hydrocarbon. An aromatic hydrocarbon refers to benzene or toluene or o-xylene or m-xylene or p-xylene or mesitylene or ethyl benzene. Isothermal flow microcalorimetry was used to determine the excess molar enthalpies. New data is presented for the mixtures: NMP + toluene, NMP + m-xylene, NMP + p-xylene, NMP + mesitylene and NMP + ethyl benzene. The data presented in this work together with existing data from the literature show the effect that substitution on the benzene ring has on the excess molar enthalpy.

Part four (chapter five) is devoted to the excess molar volumes for the mixtures: NMP + an aromatic hydrocarbon. Aromatic hydrocarbon refers to benzene or toluene or o-xylene or m-xylene or p-xylene or mesitylene or ethyl benzene. Densitometry was used to determine the excess molar volumes. The measurements obtained here confirm some of the results found in the literature. The data presented in this work together with the data from the literature show the effect that substitution on the benzene ring has on the excess molar volume.

Chapter 2
Liquid-liquid equilibria

2.1. Introduction

Since the latter part of the last century liquid-liquid extraction has been extensively used in industry for the separation of liquid mixtures.[10] The separation of components by liquid-liquid extraction depends on the distribution of solutes between two liquid phases. A knowledge of liquid-liquid equilibria is vital for the design of extraction processes as such data not only eliminates the need for expensive pilot trials, but also gives an economic indication of solvent usage that is, the solvent loading capacity.[11] One such liquid-liquid extraction solvent is NMP, and it has been used to isolate aromatic hydrocarbons from hydrocarbon feedstock.[1]

Available literature on liquid-liquid equilibria of mixtures containing an n-alkane + an aromatic hydrocarbon + NMP only covers the mixtures presented in table 2.1; hence to provide a better picture for mixtures of this type the mixtures given in table 2.2 were investigated. The results presented in this work give a clear picture of the effect of methyl substitution on the benzene ring, on the liquid-liquid equilibria, as well as the effect of increasing the chain length of the n-alkane, on the liquid-liquid equilibria.

This chapter covers the experimental techniques available in the literature for determining liquid-liquid equilibria, followed by a brief description of the method and the graphical representation used in this work. Thereafter the results are presented for the liquid-liquid equilibria for the mixtures listed in table 2.2, followed by a discussion of the results.

Table 2.1. Available liquid-liquid equilibria data for mixtures of the type: an n-alkane + an aromatic hydrocarbon + NMP.

n-alkane	aromatic hydrocarbon	reference
heptane	toluene	12
tetradecane	toluene	13
heptane	benzene	14
tetradecane	benzene	13
tetradecane	xylene	13
tetradecane	ethylbenzene	13

Table 2.2. Systems for which liquid-liquid equilibria are determined at 298.2 K in this work.

n-hexane	+	toluene	+	NMP
n-nonane	+	toluene	+	NMP
n-tetradecane	+	toluene	+	NMP
n-hexadecane	+	toluene	+	NMP
n-hexadecane	+	o-xylene	+	NMP
n-hexadecane	+	m-xylene	+	NMP
n-hexadecane	+	p-xylene	+	NMP
n-hexadecane	+	mesitylene	+	NMP
n-hexadecane	+	ethyl benzene	+	NMP

2.2. Available techniques for determining liquid-liquid equilibria

Liquid-liquid equilibria can be determined by one of the following experimental techniques:[10]

2.2.1. Cell equilibration :

In this technique the constituents are vigorously stirred and then allowed to separate.[15] Once the phases are separated, samples are withdrawn from both phases and analysed, generally by gas chromatography (see figure 2.1). An advantage of this method is that it is direct and simple. However this method does present some difficulties in that sophisticated apparatus is required to analyse the phases. The accuracy of the gas chromatography technique is sometimes questionable as the peak area is often influenced by many factors.

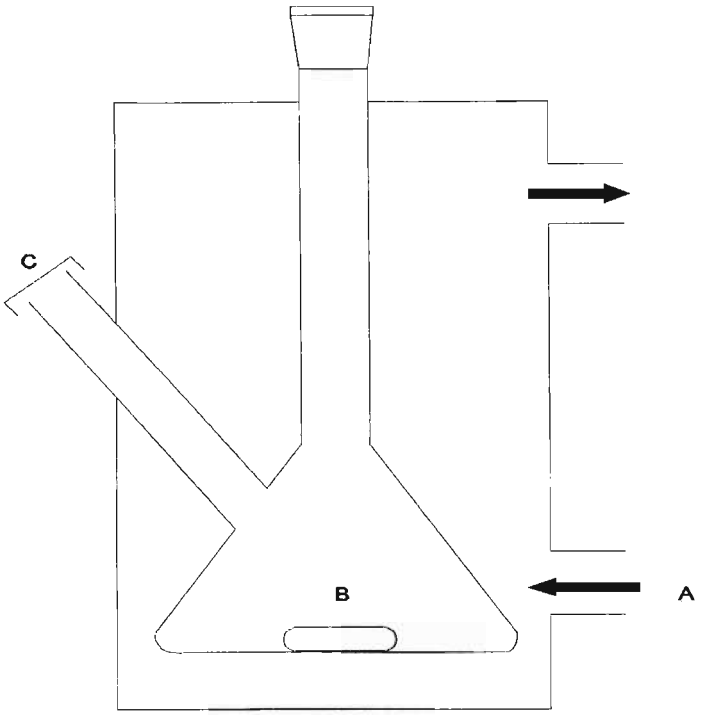

Figure 2.1. Simple cell for liquid-liquid equilibria determination.
(A) Temperature control (B) stirrer (C) septum.

2.2.2 Continuous measurement :

This technique involves the separation of the phases in a centrifuge.[16,17] Provision is made for the recirculation of the phases and for the online determination of composition. The type of detector used depends on the system investigated (see figure 2.2). An advantage of this method is that it does not require as much handling as cell equilibration. This technique does have a major drawback in that it requires sophisticated equipment and can be costly.

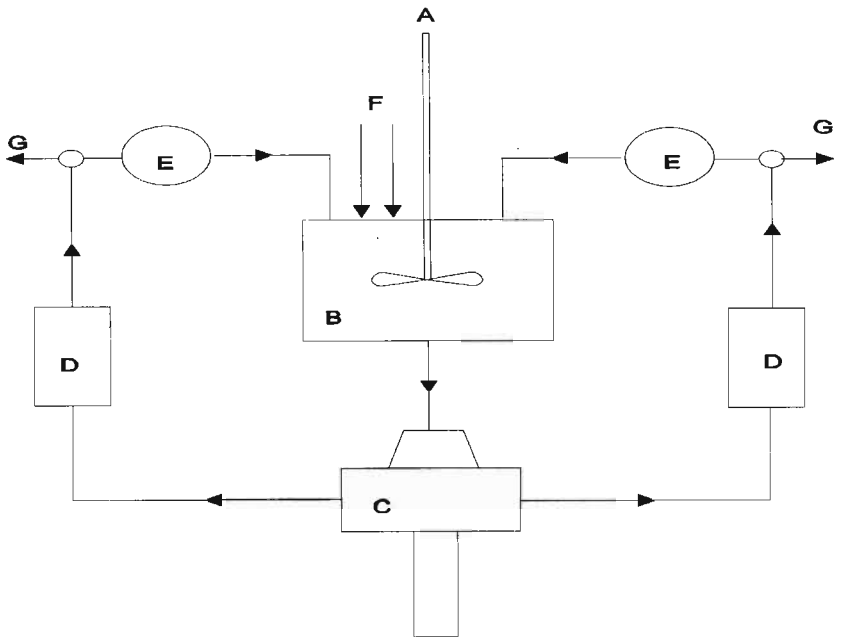

Figure 2.2. Apparatus for determining continuous liquid-liquid equilibria. (A) stirrer (B) mixing chamber (C) centrifuge (D) detector (E) heat control (F) feed (G) sampling point.

2.2.3. Titrimetry :

This technique is based on simple titrations and mass balances.[10,18,19] A third component is added to a binary mixture of known composition until the onset or disappearance of turbidity. The advantage of this technique is that it is cheap and requires very simple equipment. A drawback of this method is that volatile solvents present a problem. It can be overcome by direct injection of the volatile solvent into the liquid mixture, thus minimising vapour space and evaporation. Due to this technique being the most economical it was used in this work.

2.3. Experimental technique used in this work:

The technique used in this work was a modified titration technique described in detail by Letcher *et al.*[18] The binodal curve was determined at 298.2 K by adding to a mixture of known composition, consisting of two components, the third component, using a syringe. The syringe was weighed before and after the addition, to determine the mass of the third component. The tie-line compositions were determined by the refractive-index technique reported by Briggs and Comings[20] and described in detail by Letcher *et al.* [18] The technique for determining tie-line compositions involved the determination of a calibration curve which was obtained by plotting the refractive index (of the solution) versus concentration. This was carried out during the determination of the binodal curve. This calibration curve was used to find the concentration of conjugate phases. Mixtures which involved phase separation were made up and the refractive indices of the conjugate phases were determined. These refractive indices were used to determine the compositions of the conjugate phases from the calibration curves. This method was preferred as it did not involve the use expensive equipment such as a gas-chromatograph.

The precision of the technique is better than 0.01 on a mole fraction basis.

The accuracy of this technique was determined by comparing the liquid-liquid equilibrium data for the binary mixture n-nonane + NMP determined in this work and data published by Malanowski *et al.*[21] The data agreed to within 0.01 mole fraction for this particular set of data.

The Treybal method was used to determine the plait point or critical point.[22] The Treybal method involved plotting the following graphs on the same axes:

$$\frac{x_2}{x_1} \; \textit{versus} \; \frac{x_2}{x_3}$$

and

$$\frac{x_{21}}{x_{11}} \; \textit{versus} \; \frac{x_{23}}{x_{33}}$$

where x_{21} is the mole fraction of component 2 in the alkane-rich phase
x_{11} is the mole fraction of component 1 in the alkane-rich phase
x_{23} is the mole fraction of component 2 in the NMP-rich phase
x_{33} is the mole fraction of component 3 in the NMP-rich phase

and x_1 is the mole fraction of component 1 on the binodal curve
x_2 is the mole fraction of component 2 on the binodal curve
x_3 is the mole fraction of component 3 on the binodal curve.

x_{21}, x_{11}, x_{23} and, x_{33} were determined from tie-line data and x_1, x_2 and x_3 were determined from

binodal curve data. The plait point composition was given by the intercept of the two graphs.

Refractive indices were read at 298.2 K using an ABBE refractometer controlled at a temperature of 298.2 K.

2.3.1. Chemicals :

Details of chemicals used in this work are given in table 2.3. NMP was kept under 4Å molecular sieves and all other chemicals were used without any further treatment.

Table 2.3. Details of chemicals : suppliers, refractive indices and purity.

Compound	Supplier	n^{25}	n^{25}(literature)[23.24]	Purity
NMP	Sigma	1.468	1.4675	>99 %
n-hexane	SAARChem	1.3725	1.3723	99 %
n-nonane	FLUKA	1.4052	1.4031	99.8 %
n-tetradecane	FLUKA	1.4275	1.4269	>99 %
n-hexadecane	ACROS	1.4325	1.4325	99%
toluene	SAARChem	1.494	1.494	99 %
o-xylene	JANSSEN CHIMICA	1.5018	1.5029	99 %
m-xylene	Merck	1.4943	1.4946	99 %
p-xylene	JANSSEN CHIMICA	1.4925	1.4932	>99 %
mesitylene	Merck	1.4965	1.4968	98 %
ethyl benzene	ACROS	1.4928	1.4932	99%

2.3.2. Graphical representation of ternary systems :

The position of a point "O" representing an equilibrium mixture for a ternary liquid system is shown on an equilateral triangle[25] (see figure 2.3.) for a constant temperature and pressure. The pure components are represented by the vertices of the triangle and the edges represent binary mixtures. Ternary points are represented within the triangle. The fixing of temperature and pressure is a condition of the phase rule.

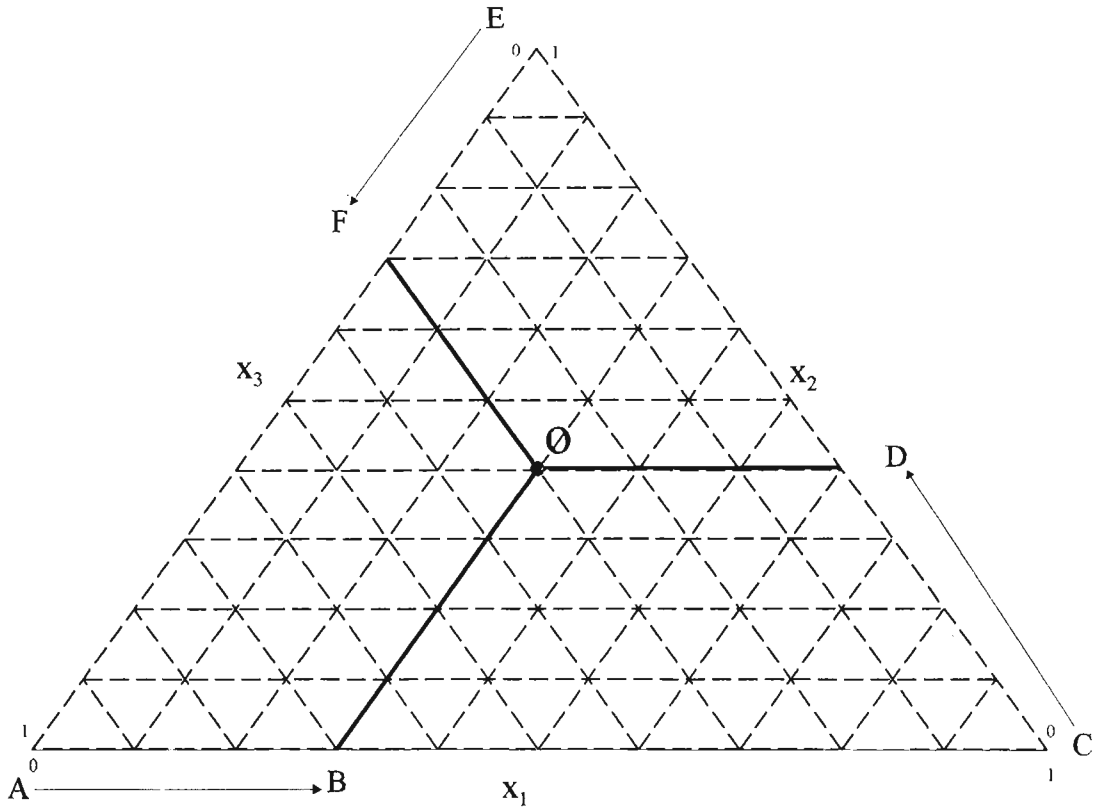

Figure 2.3. Triangular phase diagram depicting a three component mixture.

In figure 2.3 point "O" represents a ternary mixture. The composition of the mixture is determined by taking the distance between the sides of the triangle and lines drawn through point "O" parallel to the sides of the triangle.[25] From the example in figure 2.3 the value of x_1 is given by AB and is equal to 0.3. The value of x_2 is given by CD and is equal to 0.4. The value of x_3 is given by EF and is equal to 0.3.

Ternary liquid-liquid systems have been divided into three types (see figure 2.4) which are dependent on mutual miscibility of the constituents.[10] In a type I system, one pair of constituents are partially miscible in each other, whilst in a type II system two pairs of constituents are partially miscible in each other. A type III system is one in which there are three pairs of partially miscible constituents. In a type III system there exists a point at which three phases are present and the composition of the phases are represented by the three vertices of the inner triangle. Application of the phase rule to such a system shows zero degrees of freedom at constant temperature and pressure; this is called an invariant system. In this work all mixtures are type I.

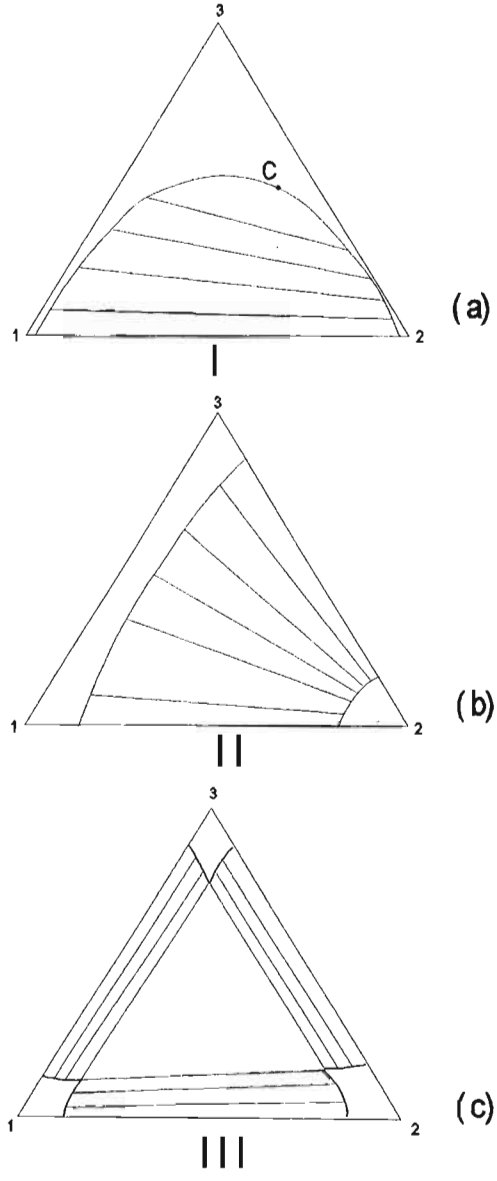

Figure 2.4. Types of ternary mixtures.
(a) type I (b) type II (c) type III.

2.4. Results :

The composition (in mole fractions) of mixtures on the binodal curve at 298.2 K are given in table 2.4 and table 2.5.

Compositions of conjugate mixtures at equilibrium are given in table 2.6 and 2.7. Lines on a phase diagram joining conjugate mixtures at equilibrium are called tie-lines. The composition of the plait points are given in table 2.8 and 2.9.

Phase diagrams showing the binodal curve, tie-lines and plait points are plotted in figures 2.5 to 2.13. The calibration curves used for the determination of the tie-lines are given in figures 2.14 to 2.22.

The Treybal graphs used for the determination of the plait points of the mixtures are given in figures 2.23 to 2.31.

The relative solubility of the aromatic compound in the n-alkane and in NMP has been plotted in figure 2.32 for a variation in the n-alkane chain length, and figure 2.33 for a variation in the aromatic compound.

Composite curves showing the influence of increasing the chain length of the n-alkane and the effect of substitution on the benzene ring on the liquid-liquid equilibria are given in figures 2.34 and 2.35 respectively.

In order to represent the data analytically three methods have been used:

Hlavatý equation:[28]

$$x_2 = A_2 x_A \ln x_A + A_1 x_B \ln x_B + A_3 x_A x_B \qquad (2.1)$$

The β function:[29]

$$x_2 = B_2 (1 - x_A)^{B_1} x_A^{B_3} \qquad (2.2)$$

The log equation:[30]

$$x_2 = C_2 (-\ln x_A)^{C_1} x_A^{C_3} \qquad (2.3)$$

where

$$x_A = (x_1 + \frac{1}{2} x_2 - x_1^o) / (x_{11}^o - x_1^o) \qquad (2.4)$$

and

$$x_B = (x_{11}^{o} - x_1 - \frac{1}{2} x_2) / (x_{11}^{o} - x_1^{o}) \qquad (2.5)$$

and x_1 refers to the mole fraction of the n-alkane, x_2 refers to the mole fraction of the aromatic hydrocarbon and x_{11}^{o} and x_1^{o} are the values of x_1 on the binodal curve which cuts the $x_2 = 0$ axis. These equations summarize the binodal curve data and have been discussed in detail by Letcher and co-workers.[30] The coefficients A_i, B_i and C_i are given in table 2.10 and table 2.11.

Table 2.4. Compositions of points on the binodal curve at 298.2 K for the mixtures: hexadecane (1) + aromatic hydrocarbon (2) + NMP (3). Here $x_3 = 1 - x_2 - x_1$.

x_1	x_2	x_1	x_2	x_1	x_2
Toluene		**m-Xylene**		**Mesitylene**	
0.012	0.000	0.012	0.000	0.012	0.000
0.022	0.106	0.022	0.082	0.023	0.055
0.053	0.289	0.035	0.168	0.027	0.102
0.107	0.359	0.06	0.251	0.051	0.187
0.324	0.396	0.122	0.316	0.057	0.192
0.391	0.368	0.226	0.354	0.109	0.268
0.394	0.363	0.498	0.31	0.11	0.266
0.437	0.348	0.656	0.205	0.187	0.323
0.531	0.309	0.707	0.171	0.202	0.331
0.534	0.308	0.920	0.000	0.295	0.357
0.607	0.247			0.532	0.304
0.71	0.179			0.728	0.163
0.781	0.120			0.831	0.076
0.920	0.000			0.920	0.000
o-Xylene		**p-Xylene**		**Ethyl benzene**	
0.012	0.000	0.012	0.000	0.012	0.000
0.021	0.096	0.021	0.093	0.020	0.097
0.037	0.193	0.038	0.188	0.037	0.192
0.071	0.281	0.073	0.274	0.072	0.279
0.148	0.343	0.156	0.333	0.125	0.327
0.235	0.385	0.268	0.363	0.269	0.365
0.417	0.354	0.420	0.355	0.324	0.370
0.524	0.302	0.543	0.304	0.452	0.335
0.644	0.236	0.662	0.235	0.715	0.203
0.854	0.063	0.732	0.154	0.809	0.105
0.920	0.000	0.920	0.000	0.920	0.000

Table 2.5. Compositions of points on the binodal curve at 298.2 K for the mixtures: n-alkane (1) + toluene (2) + NMP (3). Here $x_3 = 1 - x_2 - x_1$.

x_1	x_2	x_1	x_2
	C_6H_{14}		C_9H_{20}
0.174	0.000	0.079	0.000
0.237	0.058	0.102	0.104
0.282	0.089	0.220	0.166
0.289	0.097	0.290	0.216
0.387	0.127	0.307	0.208
0.434	0.130	0.464	0.208
0.503	0.130	0.645	0.172
0.707	0.100	0.783	0.109
0.785	0.081	0.920	0.000
0.842	0.041		
0.920	0.000		
	$C_{14}H_{30}$		$C_{16}H_{34}$
0.021	0.000	0.012	0.000
0.031	0.098	0.022	0.106
0.052	0.190	0.053	0.289
0.082	0.274	0.107	0.359
0.169	0.333	0.324	0.396
0.299	0.349	0.391	0.368
0.345	0.348	0.394	0.363
0.462	0.310	0.437	0.348
0.593	0.255	0.531	0.309
0.708	0.175	0.534	0.308
0.818	0.095	0.607	0.247
0.920	0.000	0.71	0.179
		0.781	0.120
		0.920	0.000

Table 2.6. Compositions of conjugate solutions at 298.2 K for the mixtures: hexadecane (1) + aromatic hydrocarbon (2) + NMP (3).

x_1'	x_2'	x_1''	x_2''
	Toluene		
0.920	0.000	0.012	0.000
0.635	0.230	0.013	0.050
0.585	0.265	0.015	0.090
0.549	0.290	0.015	0.120
0.540	0.300	0.018	0.150
0.504	0.320	0.021	0.185
0.483	0.335	0.025	0.210
	o-xylene		
0.920	0.000	0.012	0.000
0.875	0.040	0.014	0.038
0.830	0.075	0.017	0.050
0.788	0.110	0.018	0.080
0.730	0.155	0.024	0.125
0.644	0.220	0.033	0.160
0.598	0.245	0.035	0.170
0.485	0.310	0.055	0.230

Table 2.6 continued. Compositions of conjugate solutions at 298.2 K for the mixtures: hexadecane (1) + aromatic hydrocarbon (2) + NMP (3)

x_1'	x_2'	x_1''	x_2''
	m-xylene		
0.920	0.000	0.012	0.000
0.825	0.080	0.013	0.025
0.787	0.112	0.015	0.055
0.758	0.135	0.015	0.060
0.732	0.155	0.017	0.090
0.657	0.210	0.022	0.120
0.595	0.250	0.032	0.173
0.598	0.245	0.035	0.170
0.485	0.310	0.055	0.230
	p-xylene		
0.920	0.000	0.012	0.000
0.851	0.065	0.013	0.035
0.797	0.115	0.017	0.075
0.655	0.230	0.021	0.110
0.605	0.270	0.025	0.120
0.589	0.275	0.025	0.135
0.467	0.340	0.033	0.160
0.390	0.360	0.035	0.180

Table 2.6 continued. Compositions of conjugate solutions at 298.2 K for the mixtures: hexadecane (1) + aromatic hydrocarbon (2) + NMP (3)

x_1'	x_2'	x_1''	x_2''
	mesitylene		
0.920	0.000	0.012	0.000
0.780	0.120	0.016	0.045
0.738	0.155	0.023	0.070
0.656	0.220	0.032	0.115
0.606	0.260	0.047	0.155
0.610	0.250	0.040	0.150
0.468	0.330	0.054	0.180
0.450	0.340	0.050	0.190
0.330	0.350	0.098	0.255
	ethyl benzene		
0.920	0.000	0.012	0.000
0.830	0.095	0.021	0.040
0.809	0.113	0.016	0.068
0.783	0.135	0.017	0.095
0.725	0.180	0.023	0.115
0.702	0.200	0.020	0.145
0.620	0.250	0.033	0.165

Table 2.7. Compositions of conjugate solutions at 298.2 K for the mixture n-alkane (1) + toluene (2) + NMP (3)

x_1'	x_2'	x_1''	x_2''
	C_6H_{14}		
0.919	0.000	0.174	0.000
0.861	0.030	0.209	0.035
0.836	0.045	0.229	0.050
0.834	0.052	0.231	0.058
0.766	0.080	0.318	0.100
0.743	0.085	0.321	0.108
0.719	0.093	0.352	0.117
	C_9H_{20}		
0.931	0.000	0.079	0.000
0.782	0.105	0.136	0.110
0.775	0.110	0.155	0.120
0.755	0.120	0.168	0.135
0.722	0.140	0.185	0.160
0.684	0.153	0.220	0.170
0.620	0.180	0.268	0.205
	$C_{14}H_{30}$		
0.931	0.000	0.021	0.000
0.785	0.120	0.023	0.025
0.747	0.145	0.025	0.040
0.703	0.180	0.037	0.066
0.638	0.225	0.033	0.125
0.593	0.260	0.046	0.175
0.438	0.325	0.068	0.245

Table 2.7 continued. Compositions of conjugate solutions at 298.2 K for the mixture n-alkane (1) + toluene (2) + NMP (3)

x_1'	x_2'	x_1''	x_2''
		$C_{16}H_{34}$	
0.920	0.000	0.012	0.000
0.635	0.230	0.013	0.050
0.585	0.265	0.015	0.090
0.549	0.290	0.015	0.120
0.540	0.300	0.018	0.150
0.504	0.320	0.021	0.185
0.483	0.335	0.025	0.210

Table 2.8. Compositions of plait points at 298.2 K for the mixtures: hexadecane (1) + aromatic hydrocarbon (2) + NMP (3)

x_1	x_2
Toluene	
0.150	0.391
o-xylene	
0.200	0.360
m-xylene	
0.223	0.352
p-xylene	
0.119	0.316
mesitylene	
0.193	0.324
ethyl benzene	
0.190	0.350

Table 2.9. Compositions of plait points at 298.2 K for the mixtures: n-alkane (1) + toluene (2) + NMP (3).

x_1	x_2
C_6H_{14}	
0.565	0.125
C_9H_{20}	
0.457	0.215
$C_{14}H_{30}$	
0.195	0.340
$C_{16}H_{34}$	
0.150	0.391

Table 2.10. Coefficients A, B and C in equations 2.1 to 2.3 respectively for hexadecane(1) + aromatic hydrocarbon(2) + NMP(3) at 298.2 K.

Aromatic hydrocarbon	A_1	A_2	A_3	B_1	B_2	B_3	C_1	C_2	C_3
Toluene	0.12	0.04	1.85	1.07	1.79	1.07	1.03	1.63	1.45
o-xylene	-0.10	0.02	1.49	0.97	1.54	1.02	0.94	1.42	1.37
m-xylene	0.10	0.07	1.73	1.10	1.75	1.09	1.03	1.51	1.45
p-xylene	-0.18	0.00	1.25	0.99	1.58	1.04	0.93	1.41	1.37
mesitylene	-0.10	0.10	1.43	1.03	-1.63	1.12	0.99	1.44	1.46
ethyl benzene	-0.34	-0.15	0.83	0.89	1.41	0.98	0.86	1.29	1.30

Table 2.11. Coefficients A, B and C in equations 2.1 to 2.3 respectively for n-alkane(1) + toluene(2) + NMP(3) at 298.2 K.

n-alkane	A_1	A_2	A_3	B_1	B_2	B_3	C_1	C_2	C_3
n-hexane	-0.02	0.65	1.38	1.08	1.01	1.93	1.07	0.96	2.38
n-nonane	-0.16	0.35	1.15	0.74	0.71	1.00	0.72	0.67	1.28
n-tetradecane	-0.05	0.04	1.42	0.94	1.39	1.02	0.91	1.28	1.36
n-hexadecane	0.12	0.04	1.85	1.07	1.79	1.07	1.03	1.63	1.45

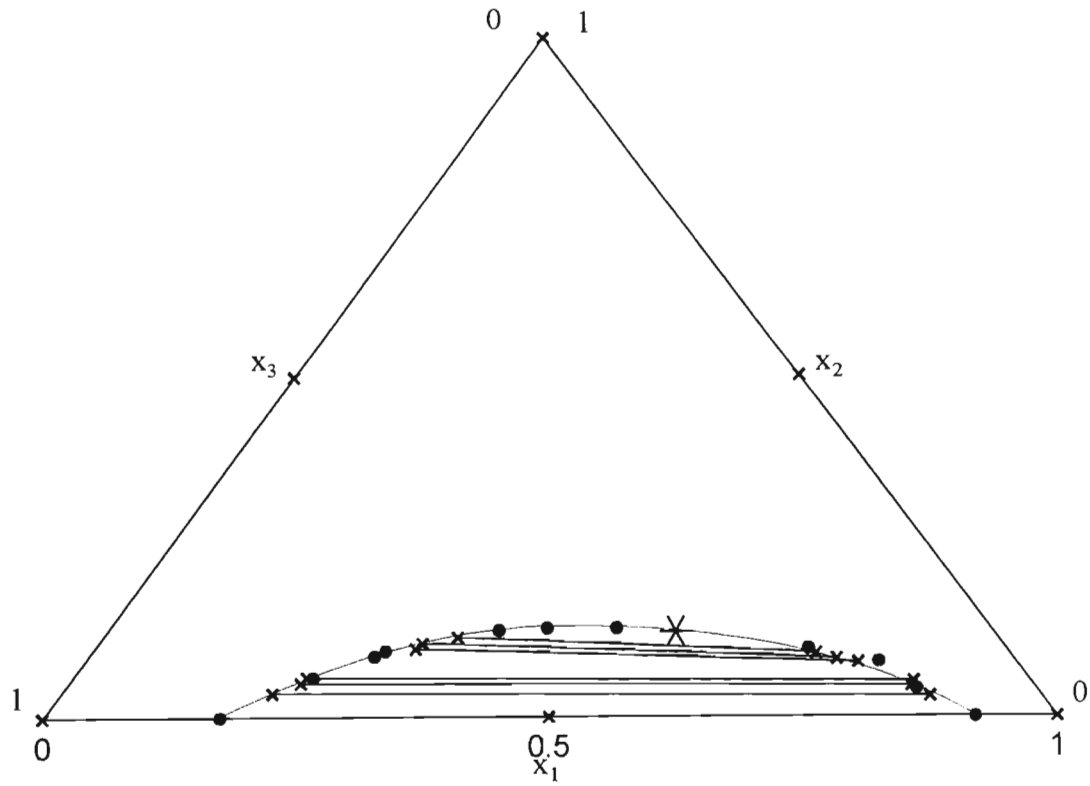

Figure 2.5. Phase diagram for n-hexane (1) + toluene(2) + NMP (3) at 298.2 K

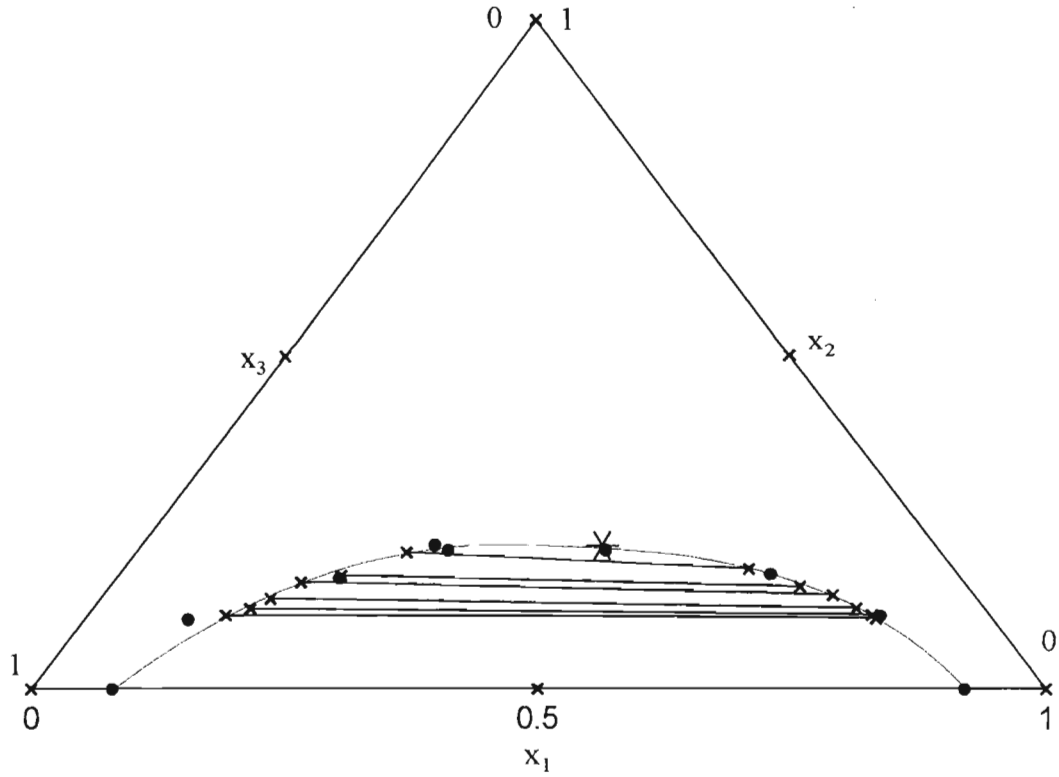

Figure 2.6. Phase diagram for nonane(1) + toluene(2) + NMP(3) at 298.2 K

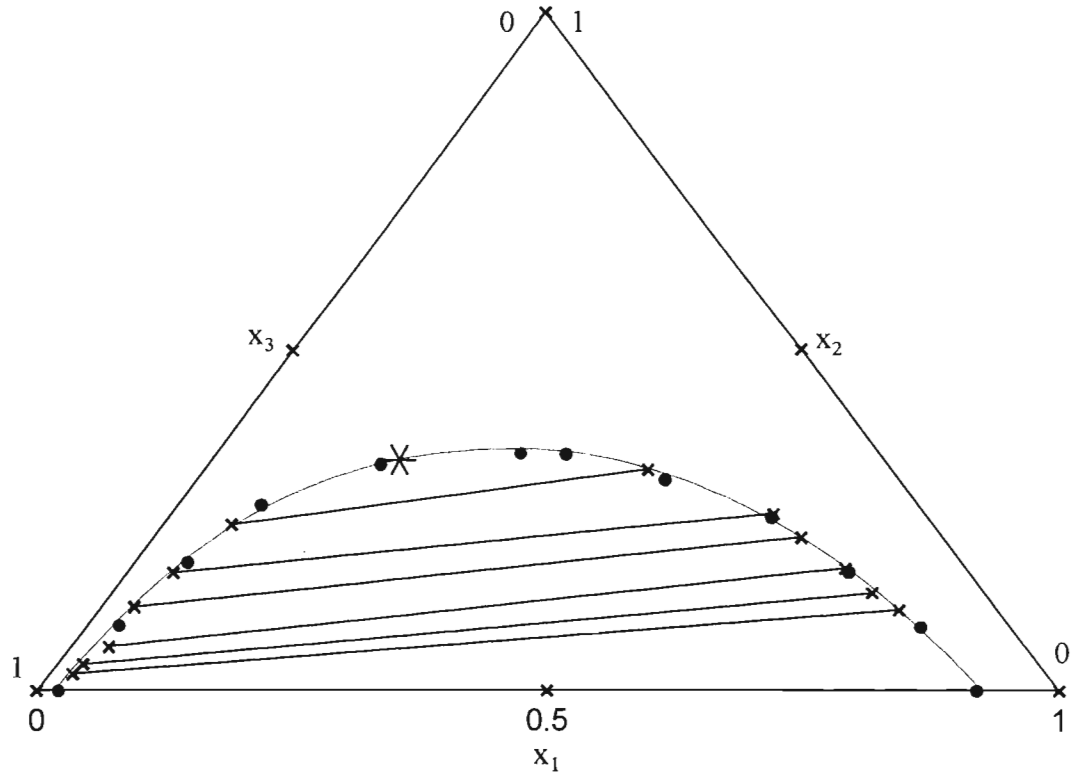

Figure 2.7. Phase diagram for tetradecane(1) + toluene(2) + NMP(3) at 298.2 K

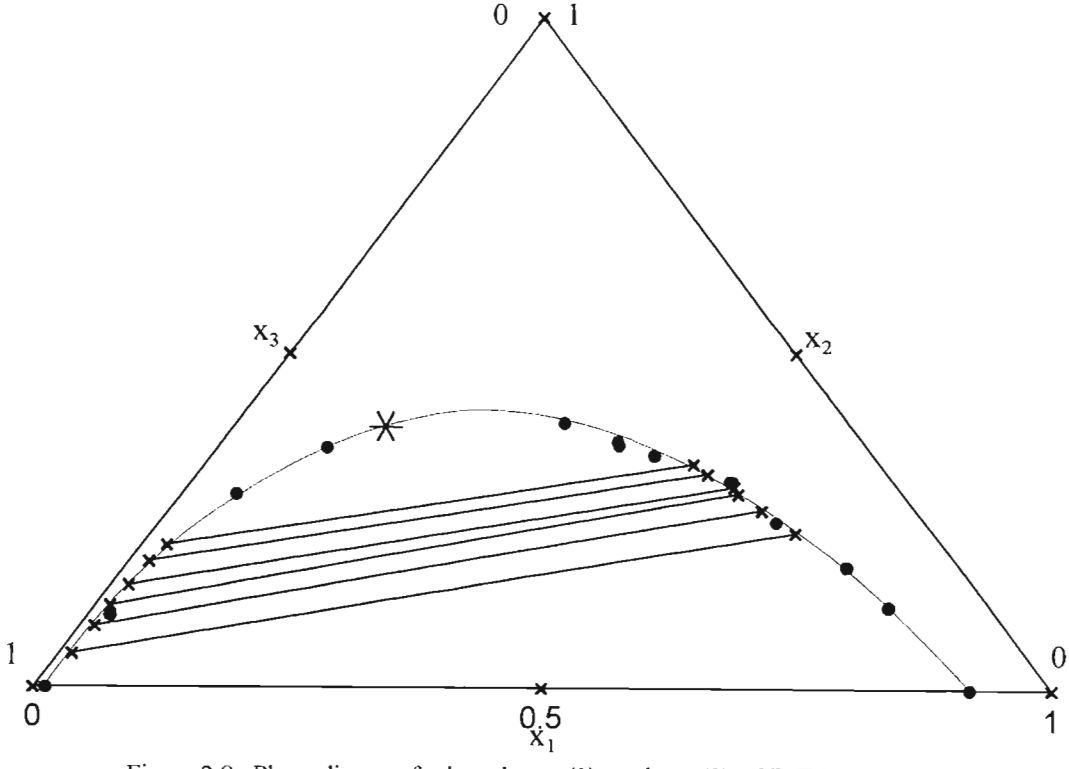

Figure 2.8. Phase diagram for hexadecane(1) + toluene(2) + NMP(3) at 298.2 K

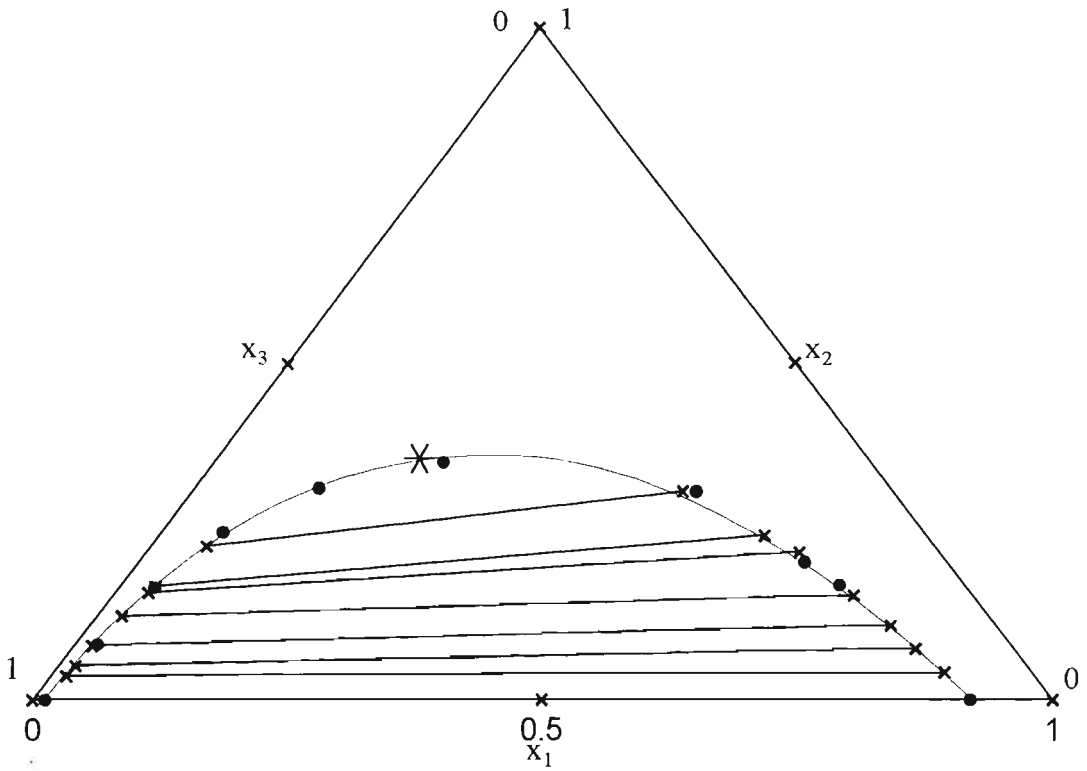

Figure 2.9. Phase diagram for hexadecane(1) + o-xylene(2) + NMP(3) at 298.2 K

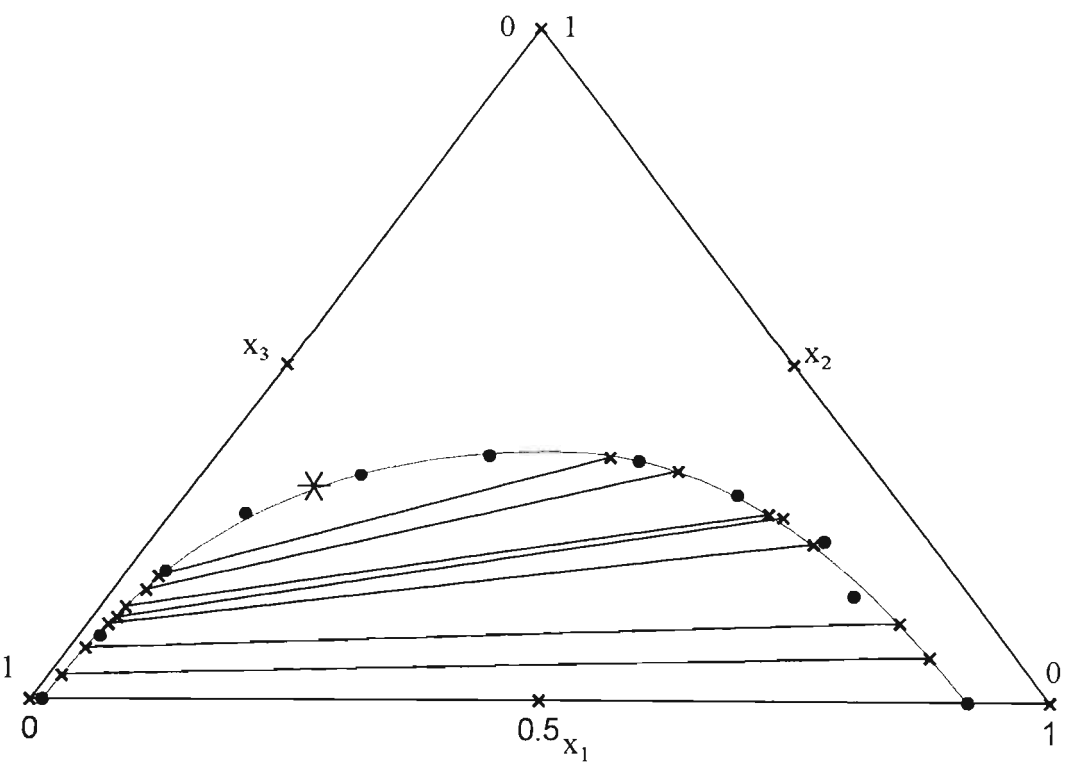

Figure 2.10. Phase diagram for hexadecane(1) + m-xylene(2) + NMP(3) at 298.2 K

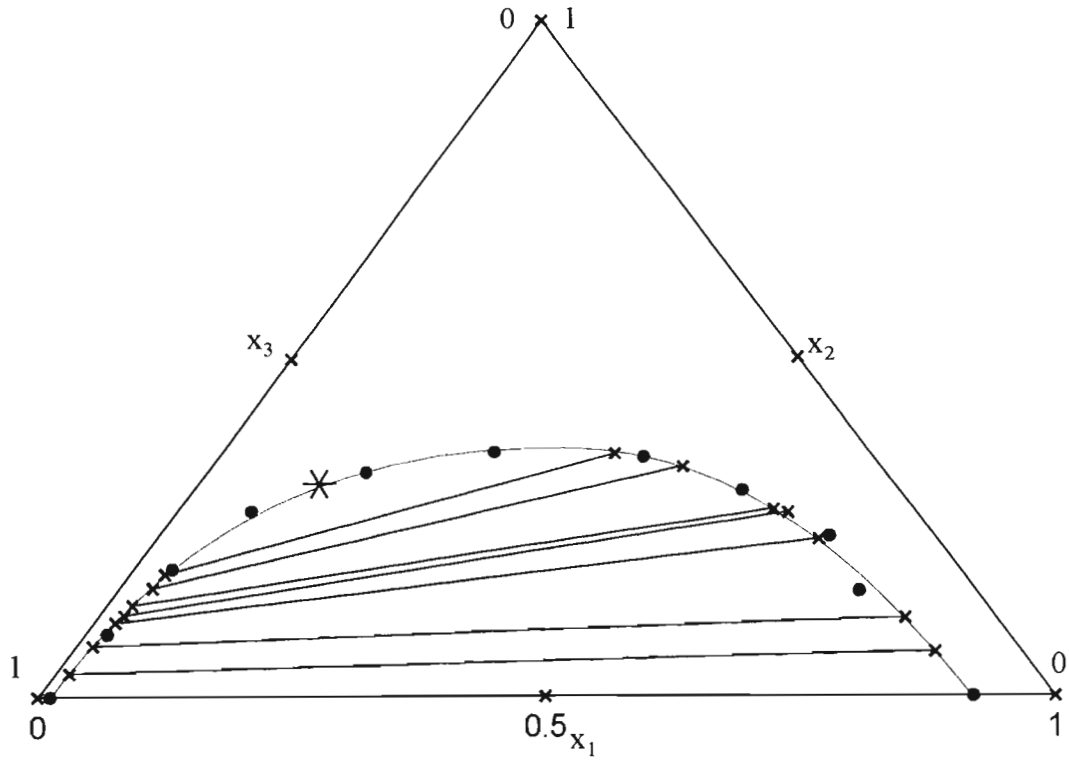

Figure 2.11. Phase diagram for hexadecane(1) + p-xylene(2) + NMP(3) at 298.2 K

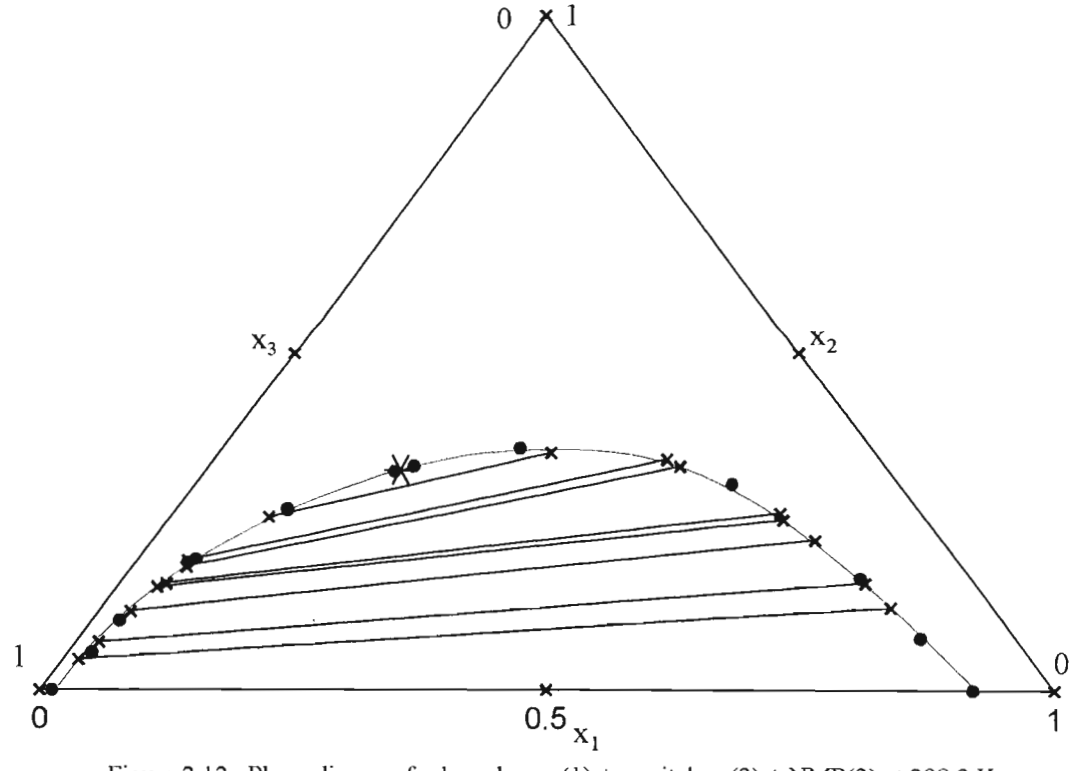

Figure 2.12. Phase diagram for hexadecane(1) + mesitylene(2) + NMP(3) at 298.2 K

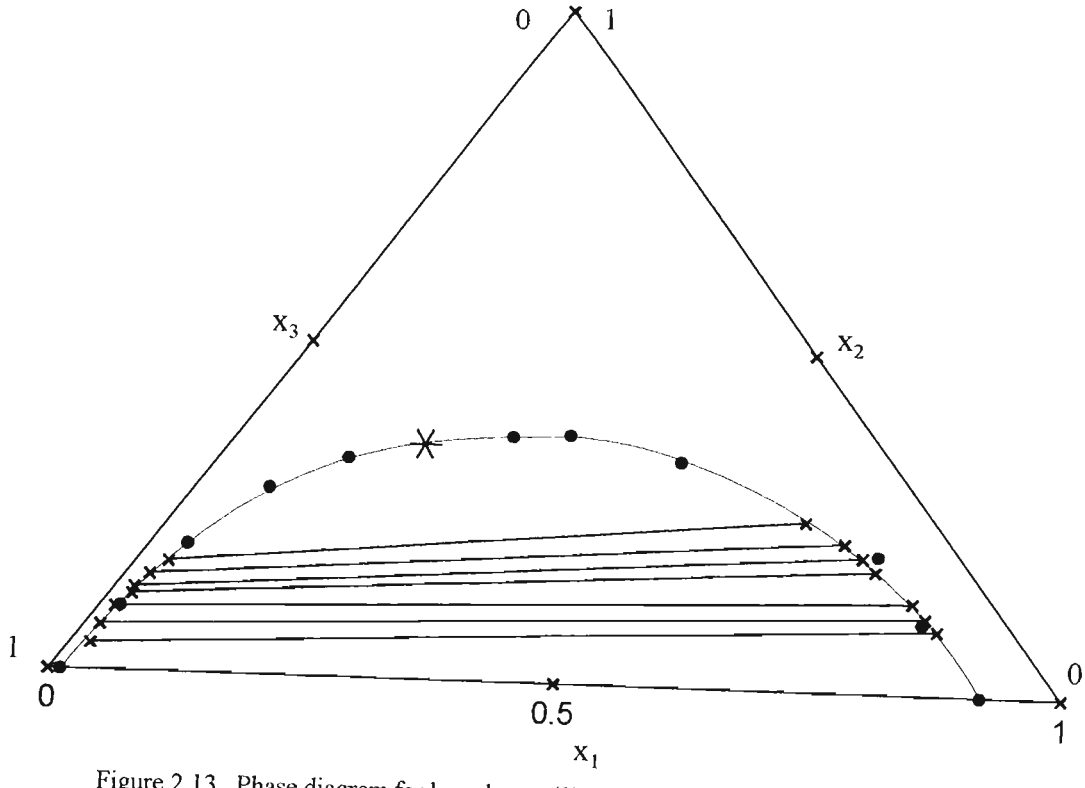

Figure 2.13. Phase diagram for hexadecane(1) + ethyl benzene(2) + NMP(3) at 298.2 K

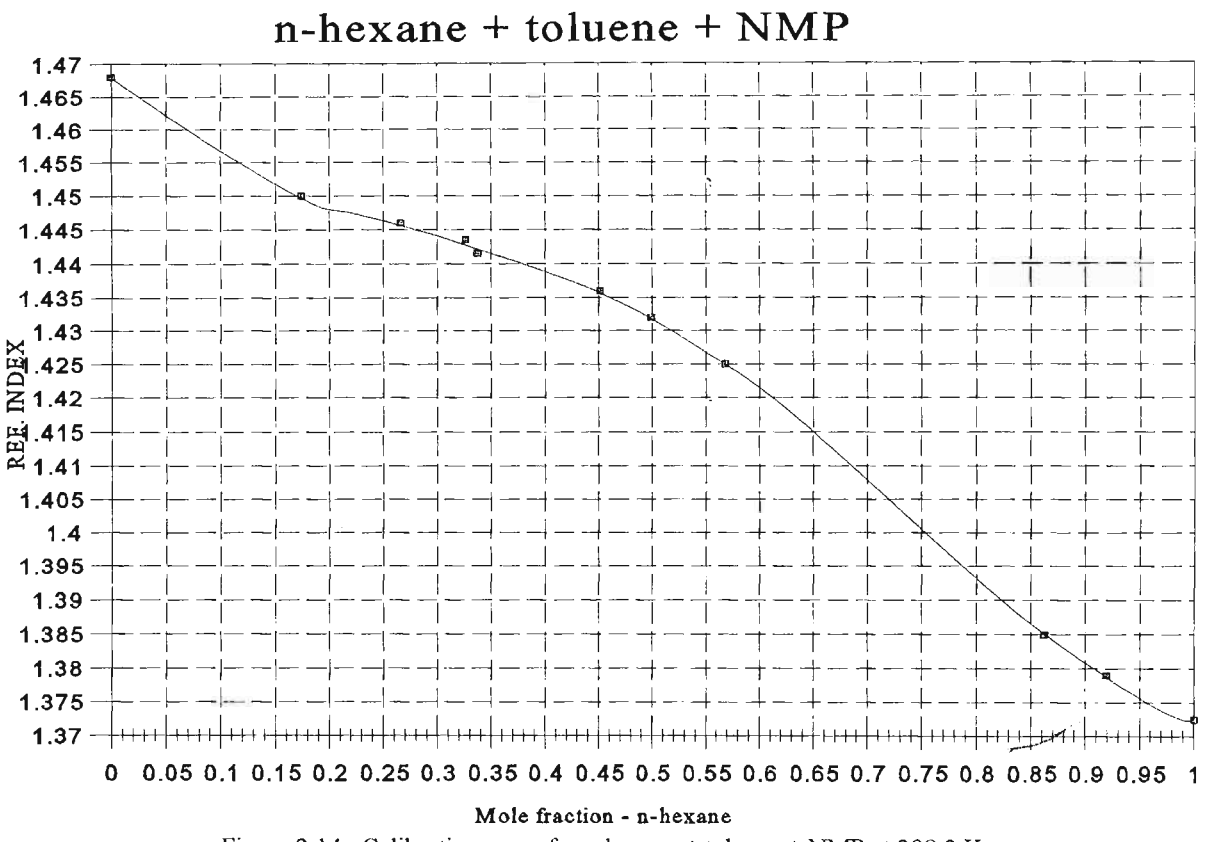

Figure 2.14. Calibration curve for n-hexane + toluene + NMP at 298.2 K

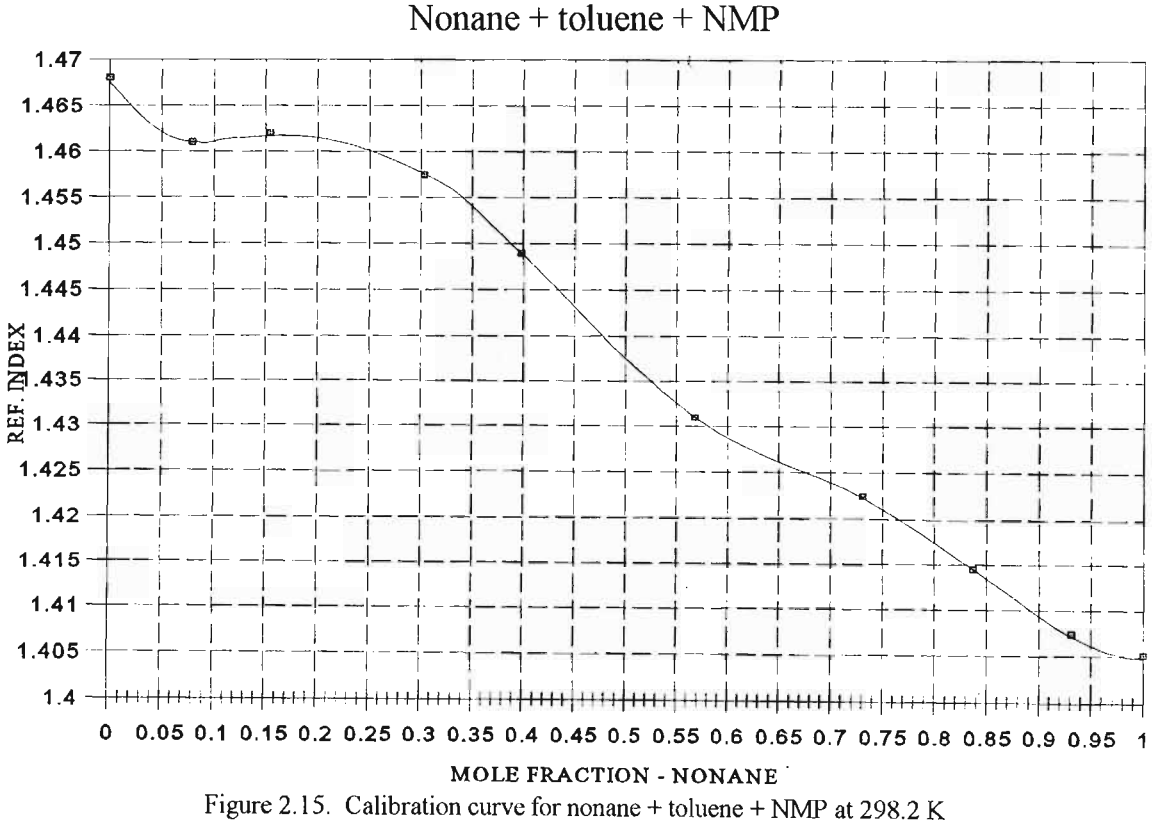

Figure 2.15. Calibration curve for nonane + toluene + NMP at 298.2 K

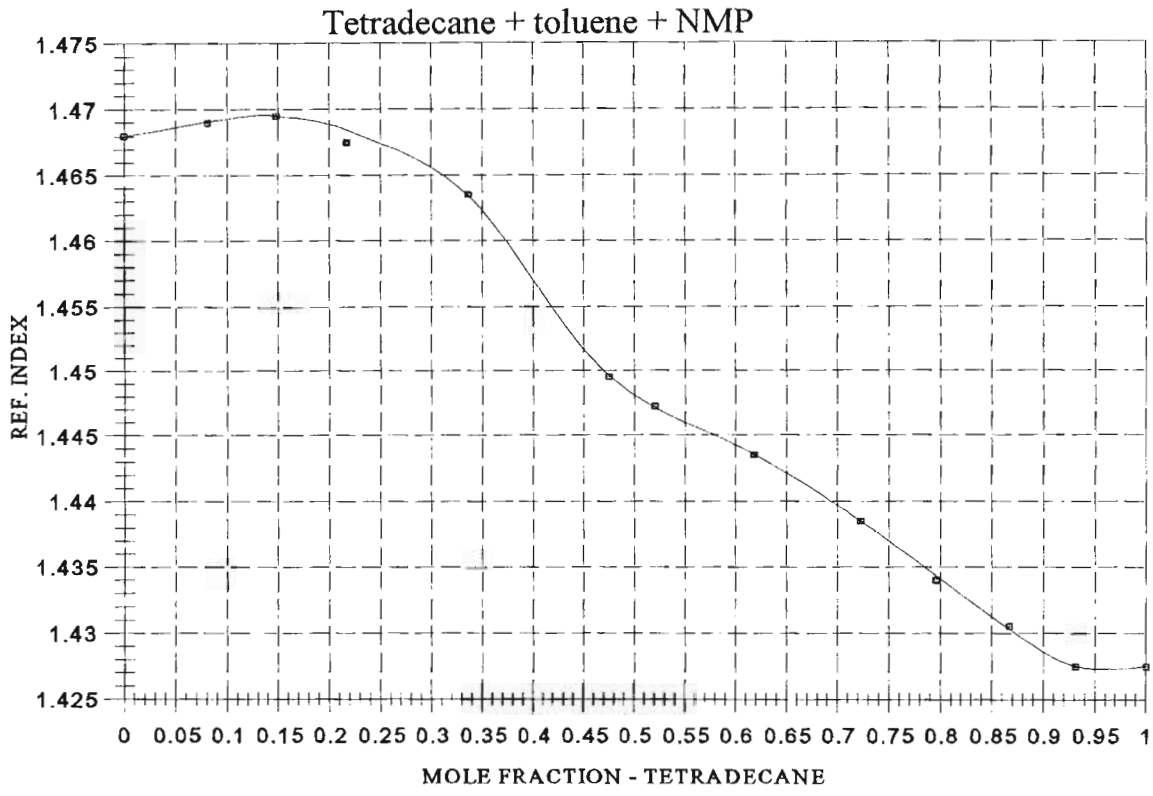

Figure 2.16. Calibration curve for tetradecane + toluene + NMP at 298.2 K

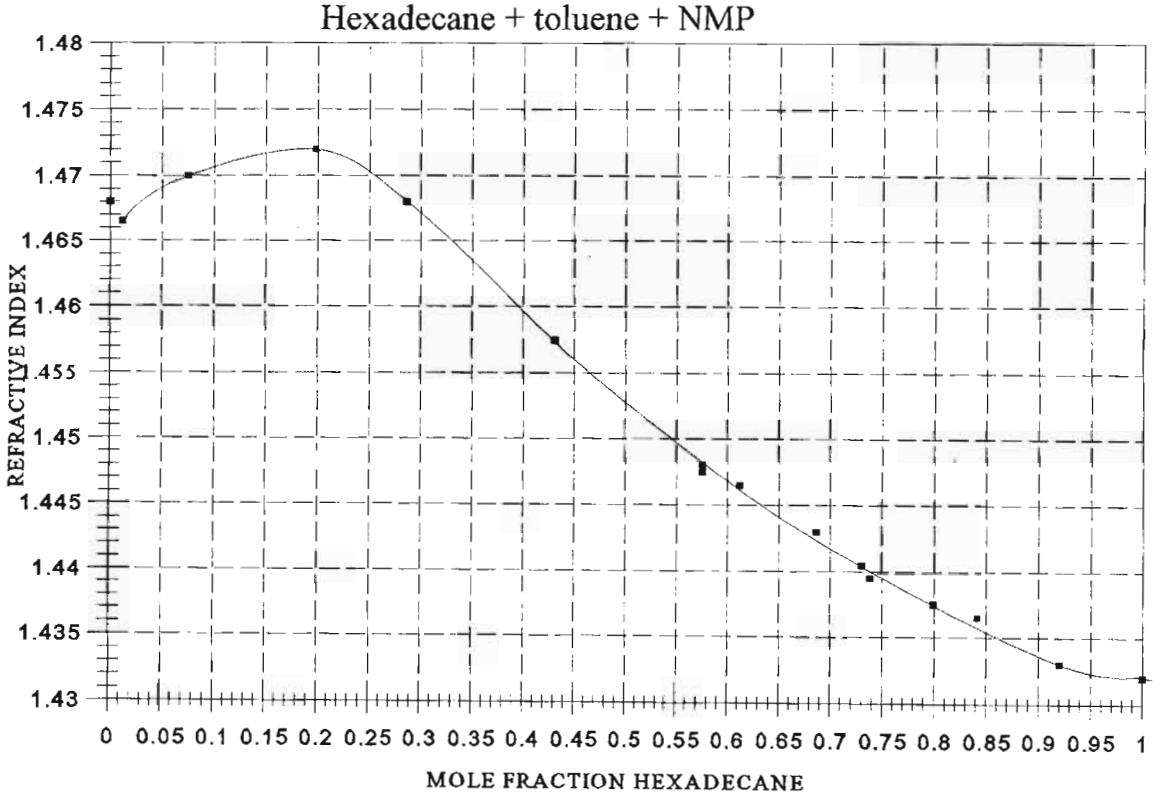

Figure 2.17. Calibration curve for hexadecane + toluene + NMP at 298.2 K

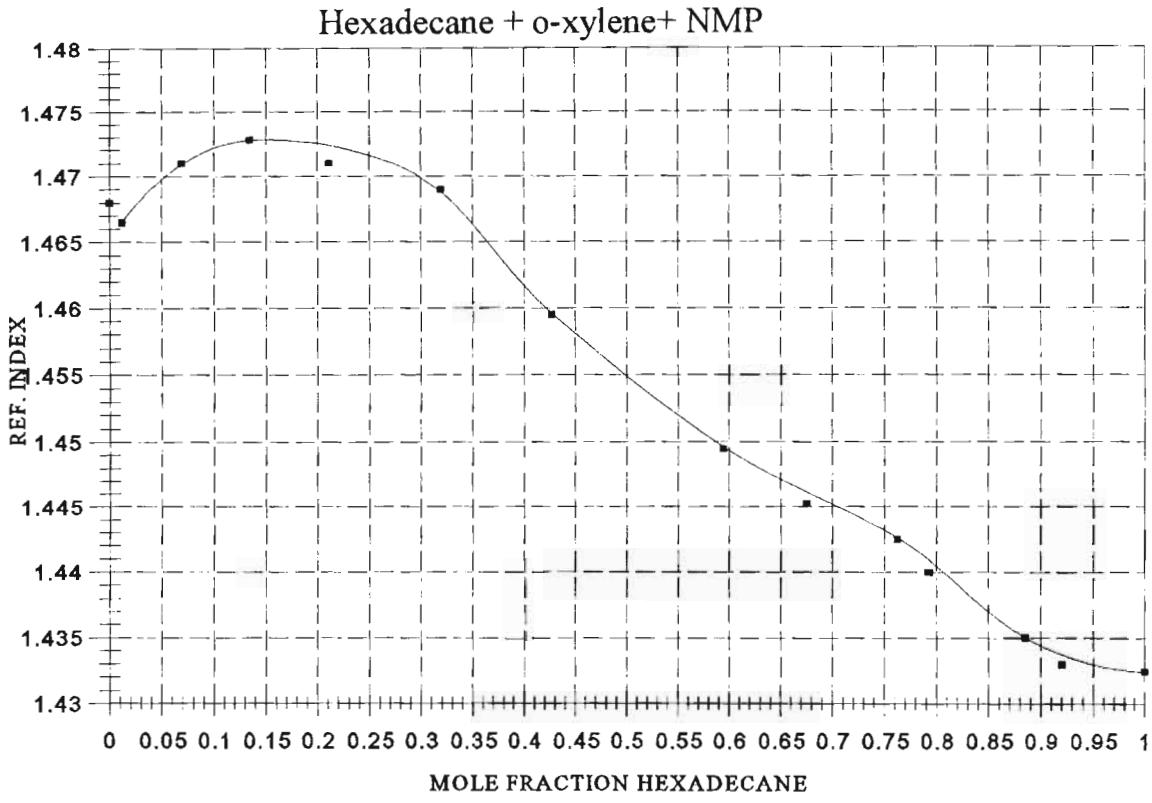

Figure 2.18. Calibration curve for hexadecane + o-xylene + NMP at 298.2 K

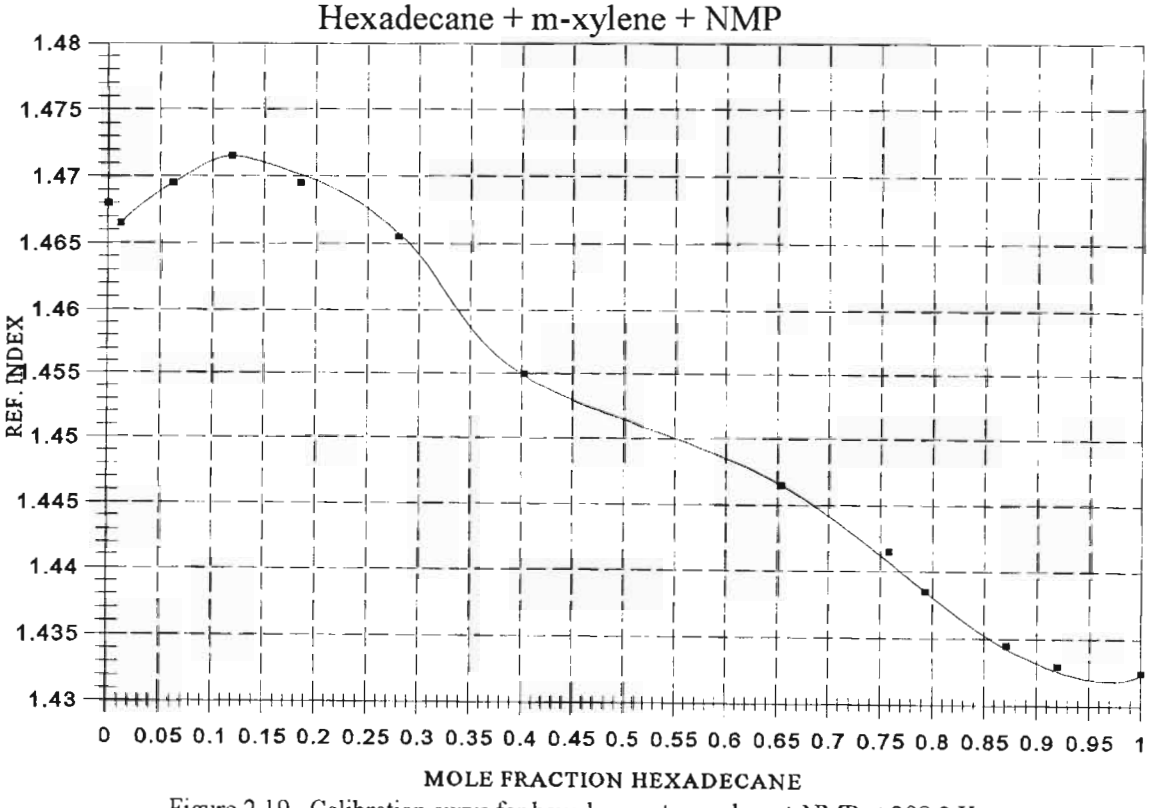

Figure 2.19. Calibration curve for hexadecane + m-xylene + NMP at 298.2 K

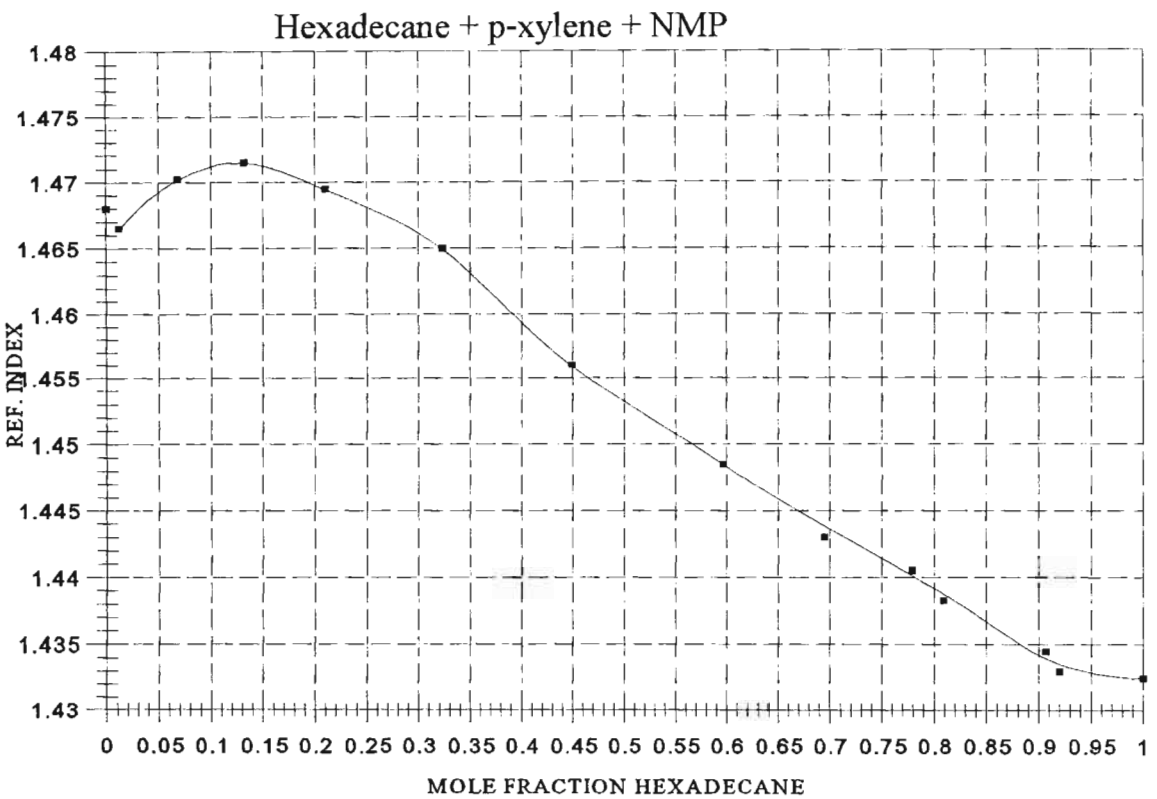

Figure 2.20. Calibration curve for hexadecane + p-xylene + NMP at 298.2 K

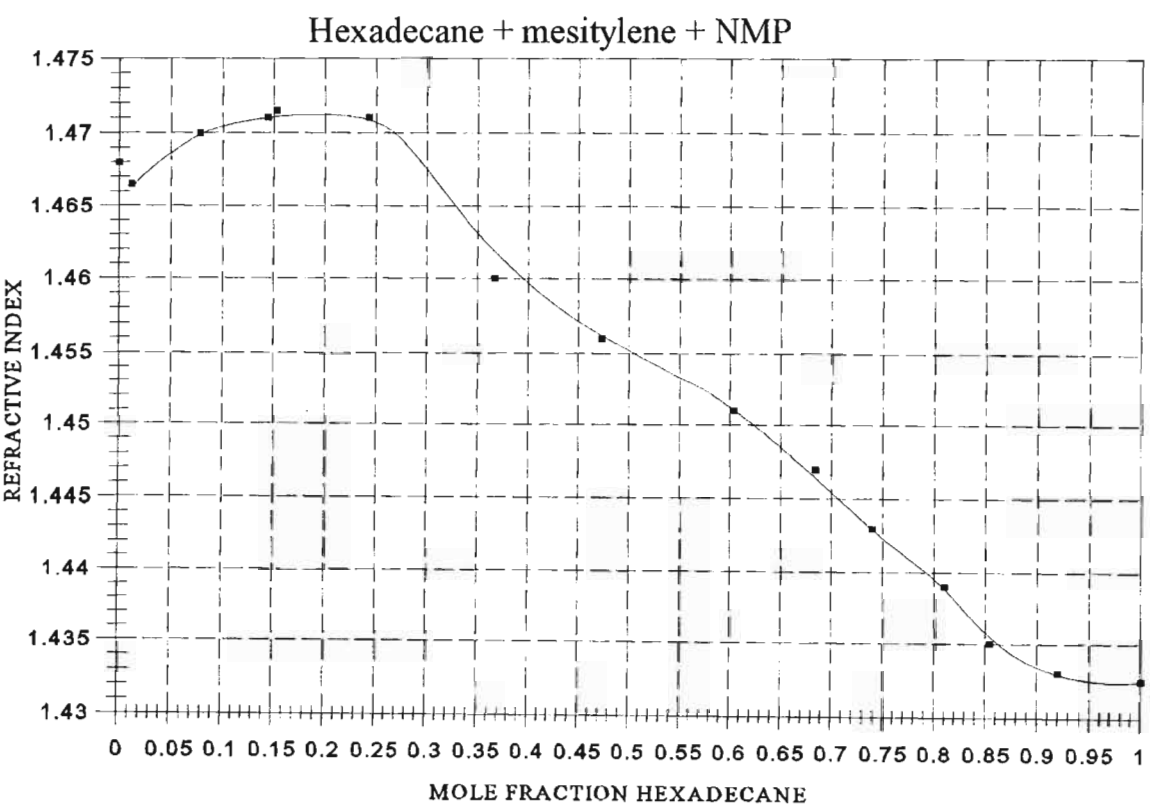

Figure 2.21. Calibration curve for hexadecane + mesitylene + NMP at 298.2 K

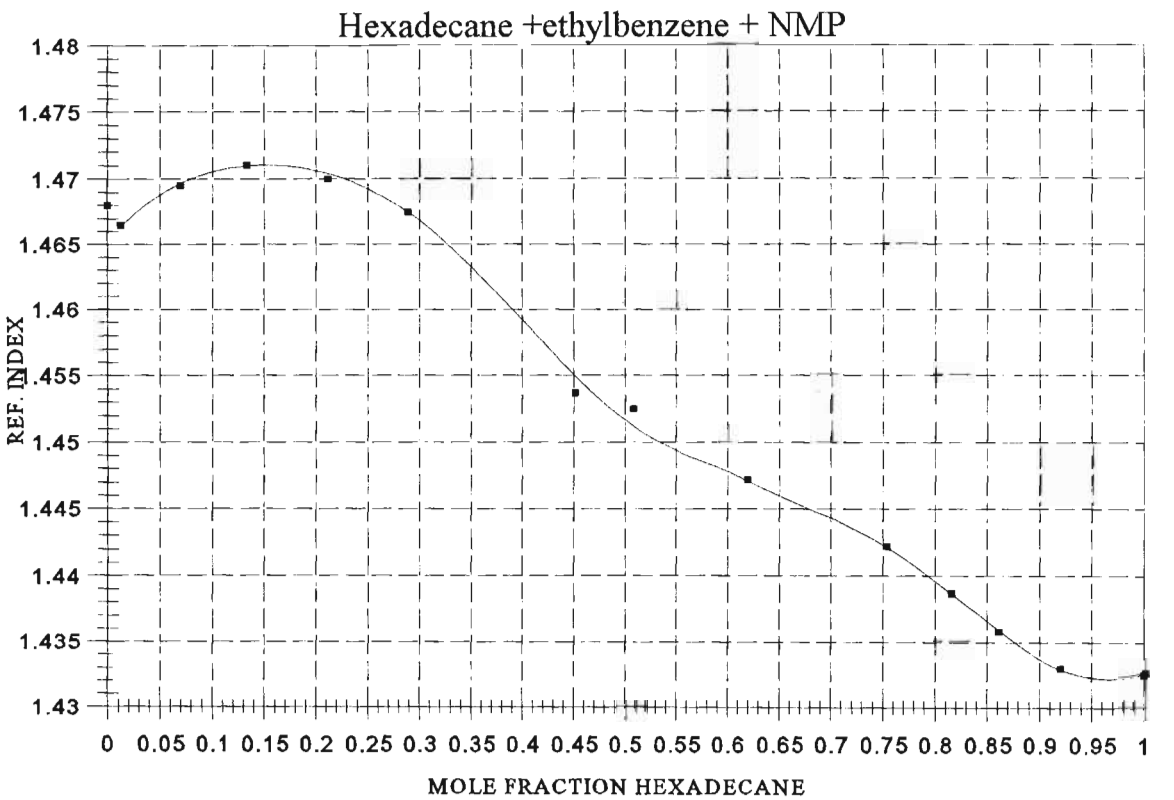

Figure 2.22. Calibration curve for hexadecane + ethyl benzene + NMP at 298.2 K

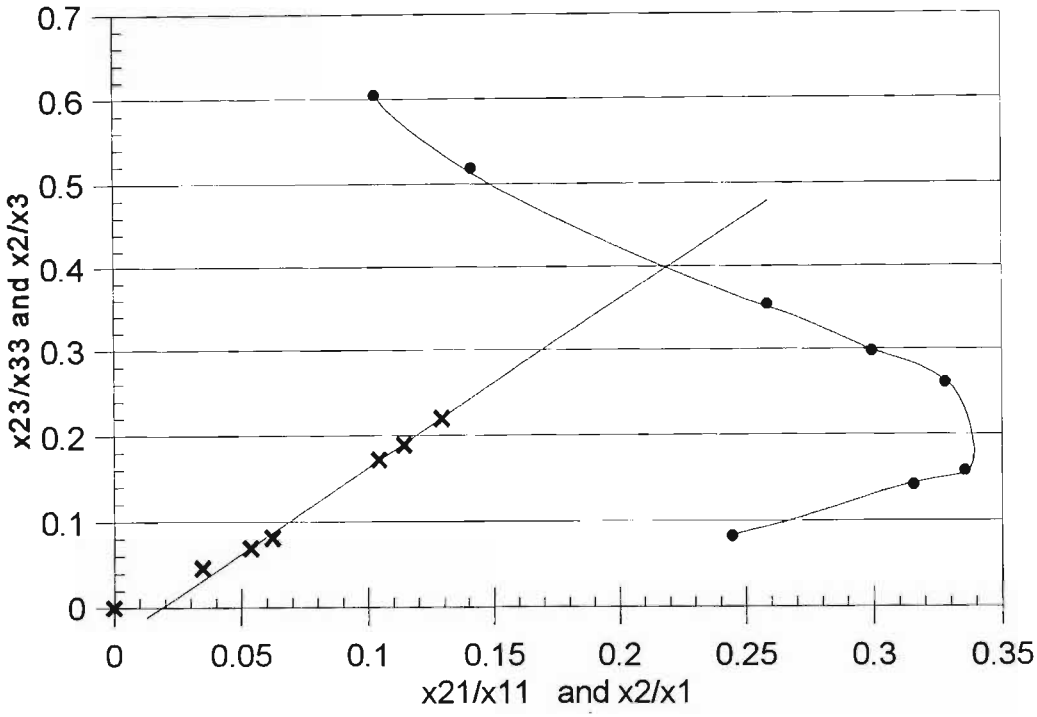

Figure 2.23. Treybal plot for n-hexane+toluene+NMP at 298.2 K

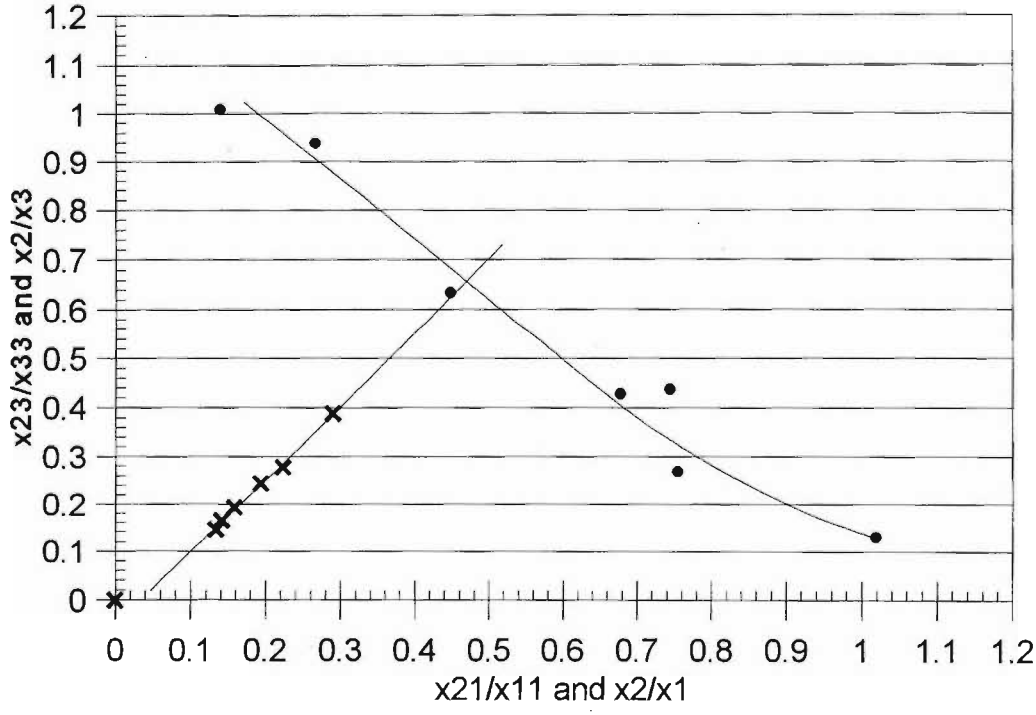

Figure 2.24. Treybal plot for nonane+ toluene+NMP at 298.2 K

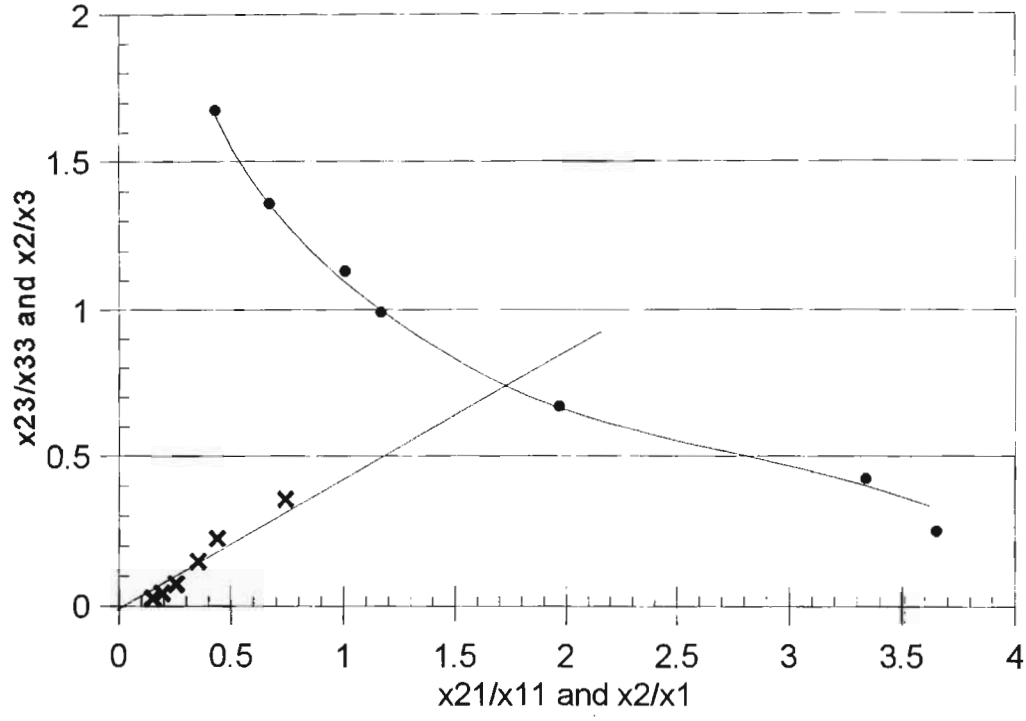

Figure 2.25. Treybal plot for tetradecane+toluene+NMP at 298.2 K

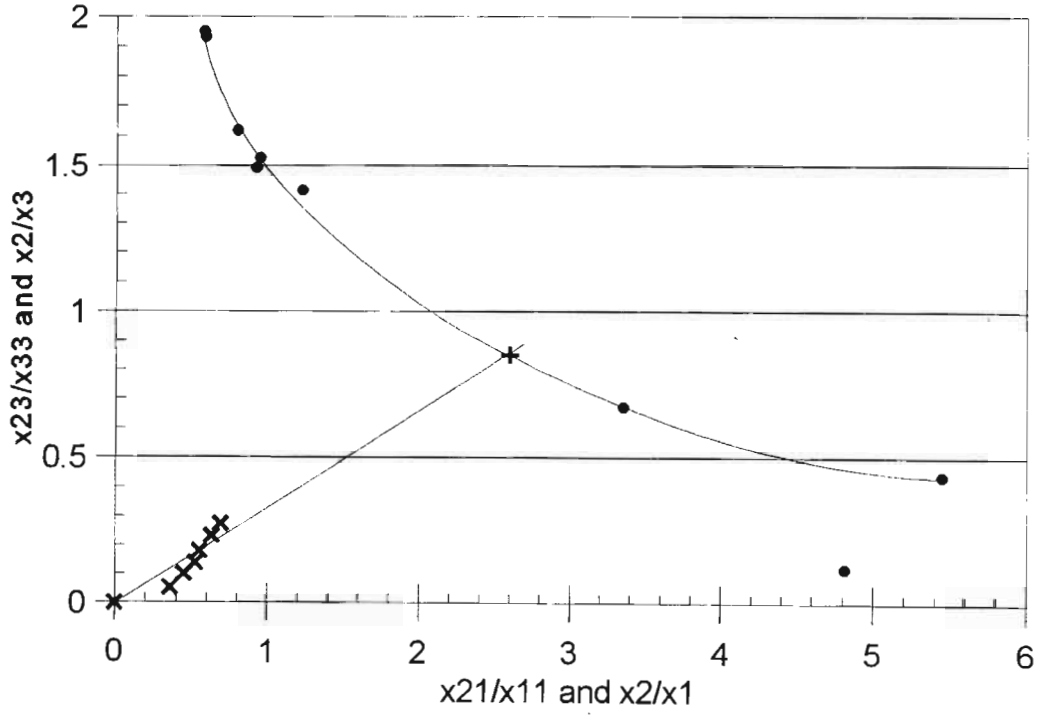

Figure 2.26. Treybal plot for hexadecane+toluene+NMP at 298.2 K

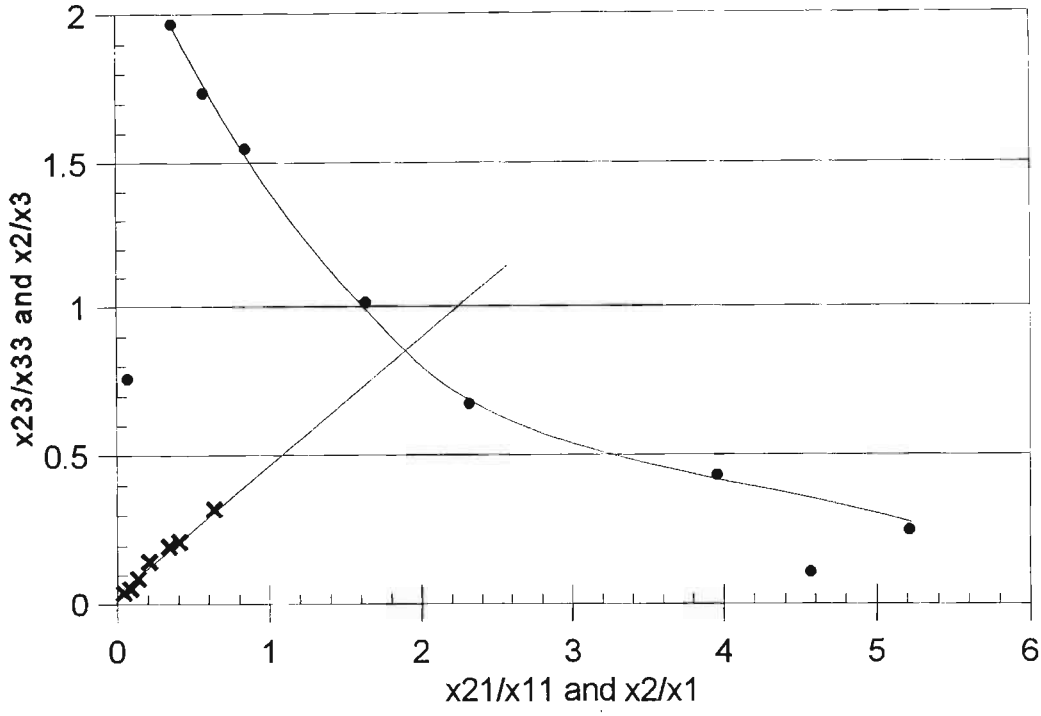

Figure 2.27. Treybal plot for hexadecane+o-xylene+NMP at 298.2 K

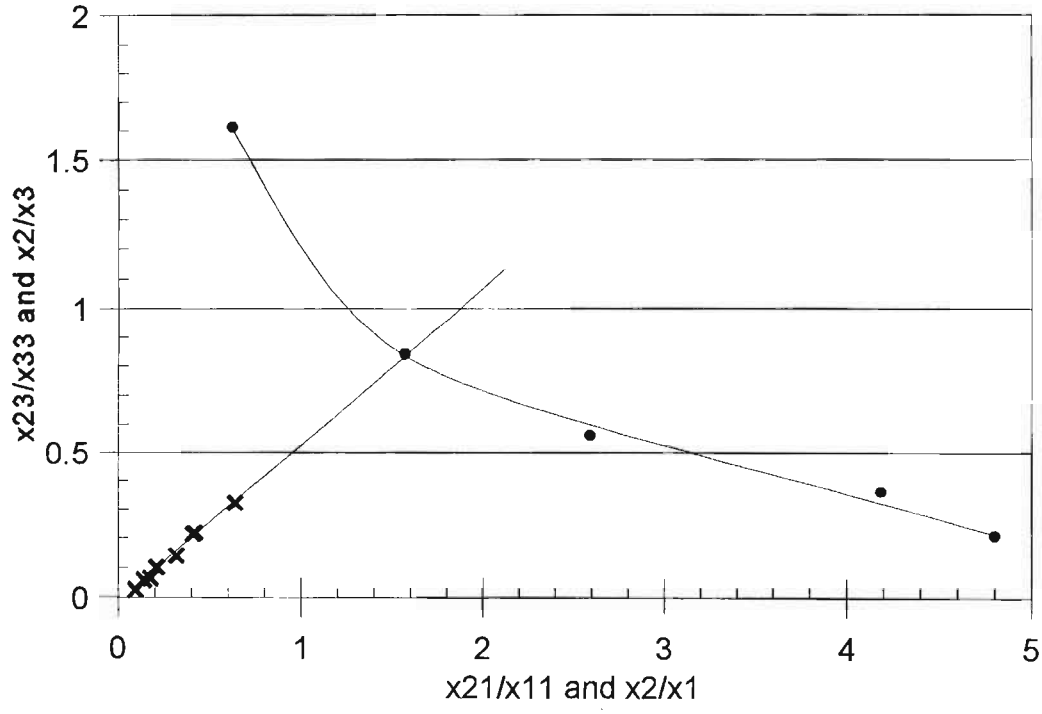

Figure 2.28. Treybal plot for hexadecane+m-xylene+NMP at 298.2 K

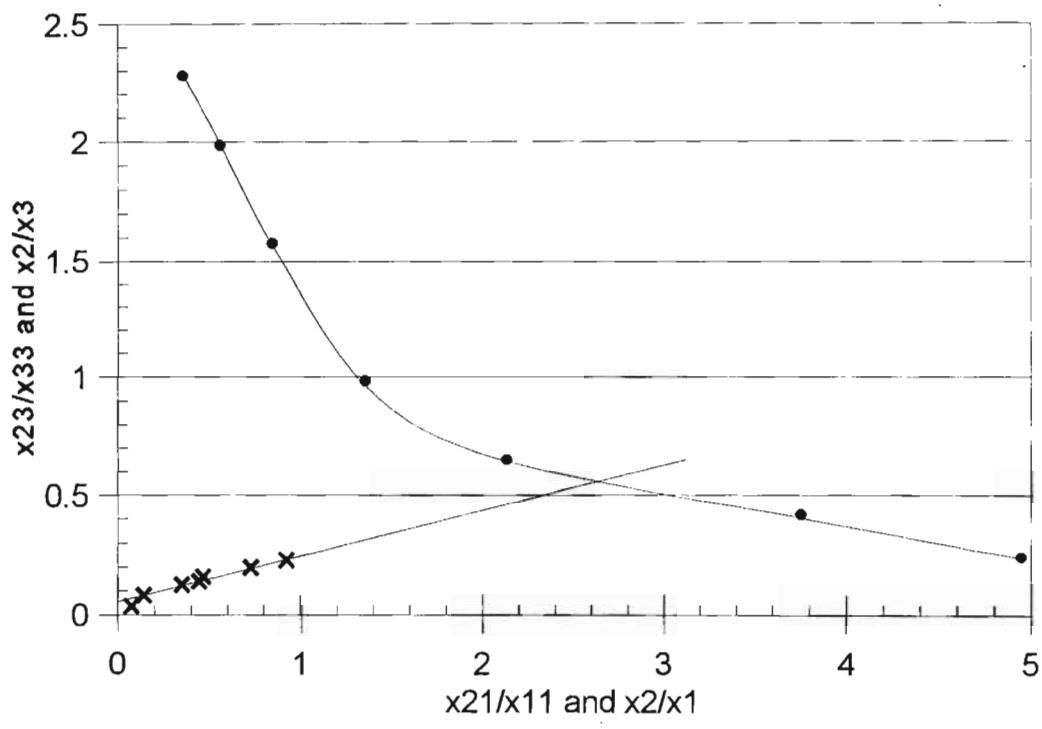

Figure 2.29. Treybal plot for hexadecane+p-xylene+NMP at 298.2 K

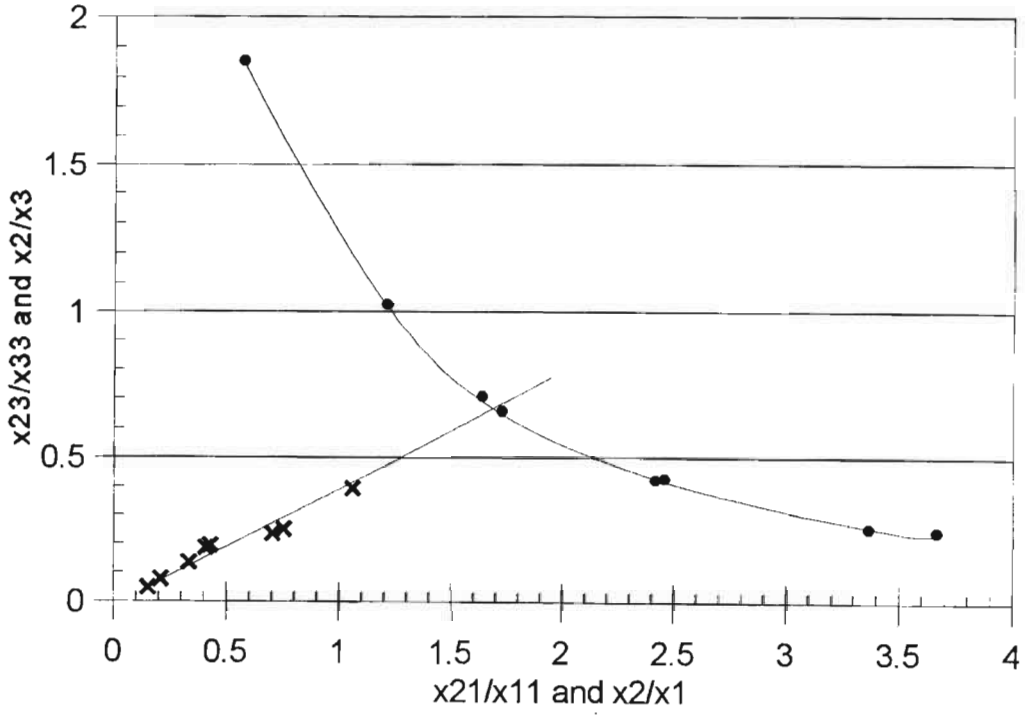

Figure 2.30. Treybal plot for hexadecane+mesitylene+NMP at 298.2 K

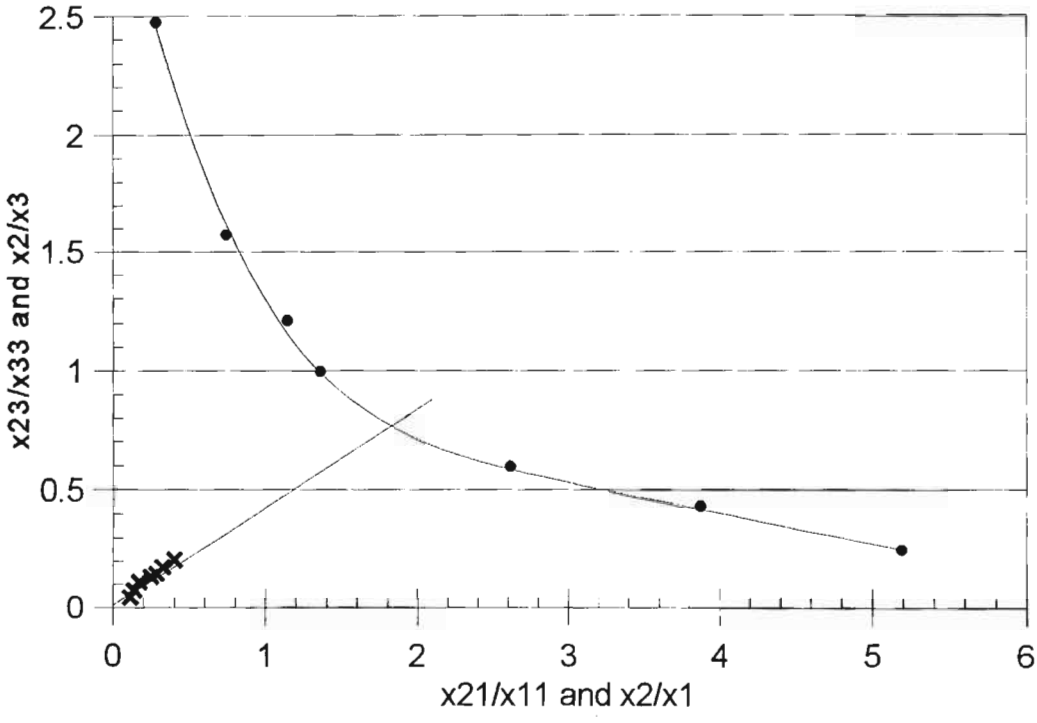

Figure 2.31. Treybal plot for hexadecane+ethyl benzene+NMP at 298.2 K

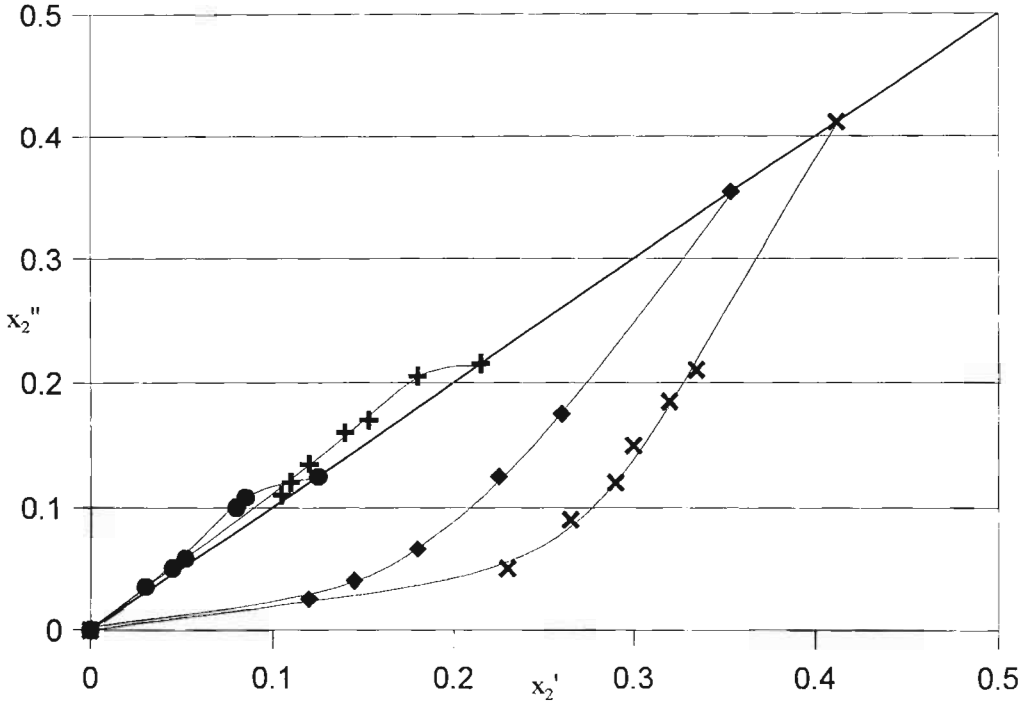

Figure 2.32. Relative solubilities for the mixtures: n-alkane + toluene + NMP at 298.2 K. ● = n-hexane, ✚ = n-nonane, ◆ = n-tetradecane,✖ = n-hexadecane. x_2' = mole fraction of toluene in the alkane rich phase and x_2'' = mole fraction of toluene in the NMP rich phase.

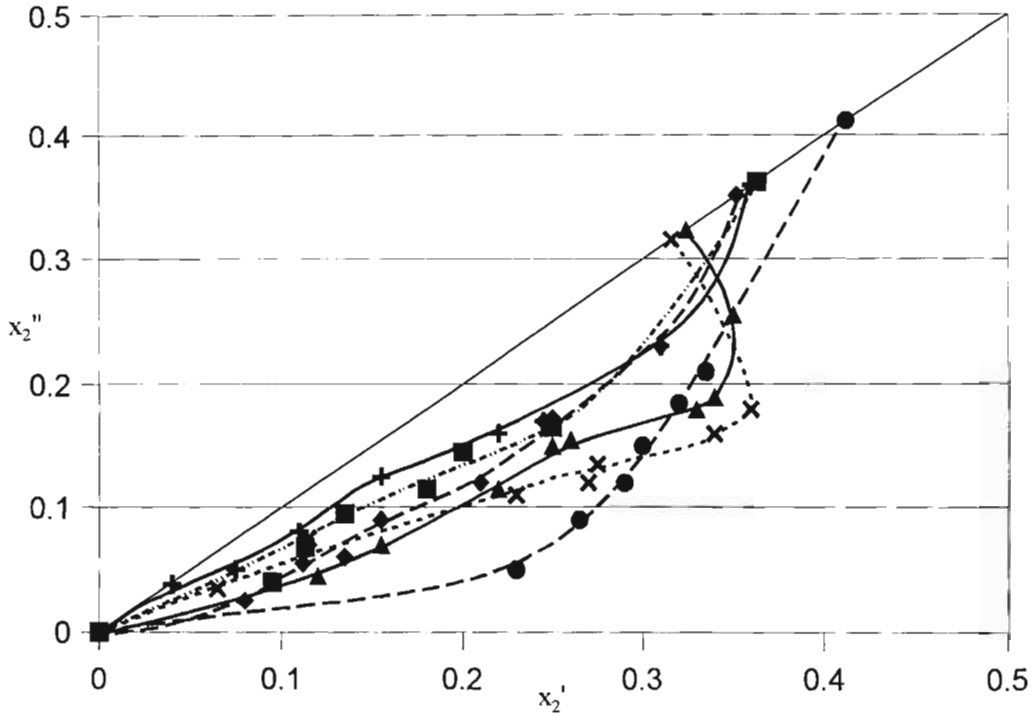

Figure 2.33. Relative solubilities for the mixtures: hexadecane + aromatic hydrocarbon + NMP at 298.2 K. ● = toluene, ✚ = o-xylene, ◆ = m-xylene, ✖ = p-xylene, ▲ = mesitylene and ■ = ethyl benzene. x_2' = the mole fraction of the aromatic compound in the hexadecane rich phase and x_2'' = the mole fraction of the aromatic compound in the NMP rich phase.

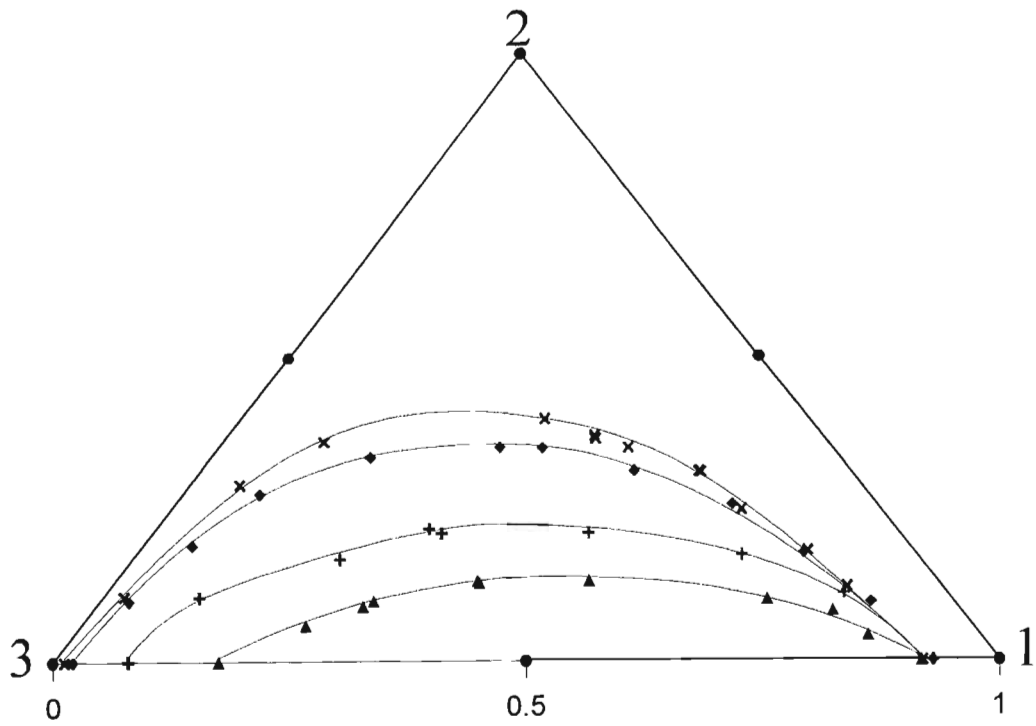

Figure 2.34. Composite plot for the mixtures: alkane (1) + toluene (2) + NMP (3) at 298.2 K. Key: ▲ = n-hexane, ✚ = n-nonane, ◆ = n-tetradecane, ✖ = n-hexadecane.

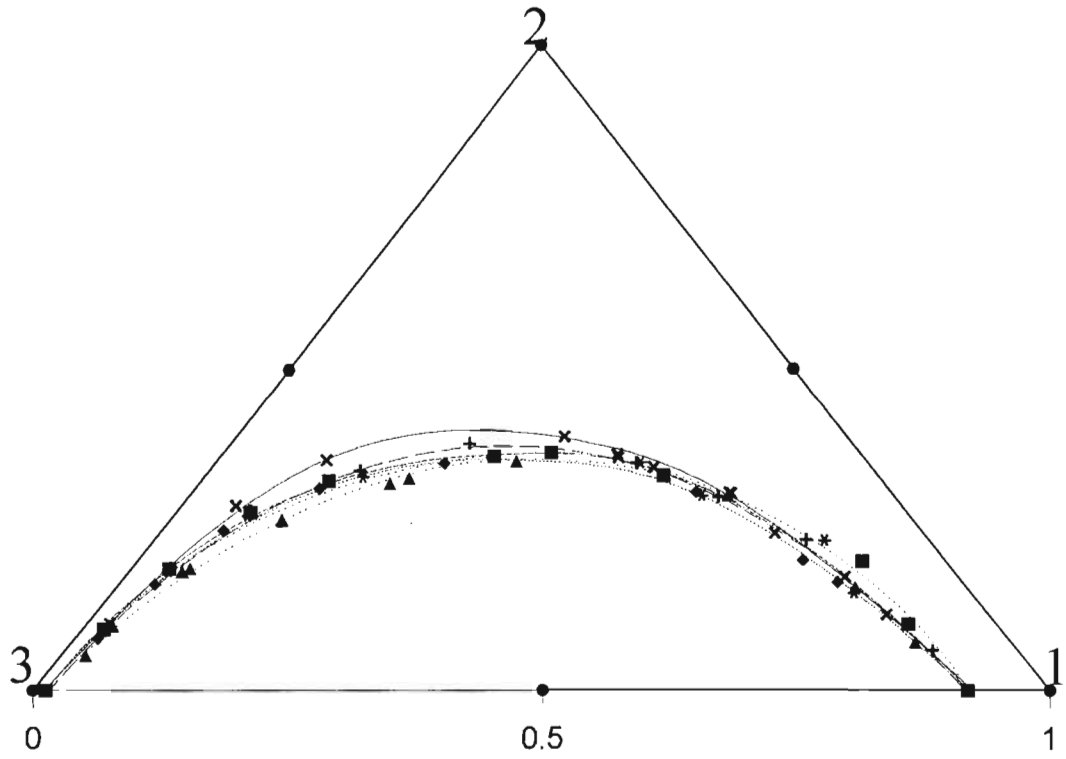

Figure 2.35. Composite plot for the mixtures: hexadecane (1) + aromatic hydrocarbon (2) + NMP (3) at 298.2 K. Key : ✖ = toluene, ✚ = o-xylene, ◆ = m-xylene, ✱ = p-xylene , ▲ = mesitylene, ■ = ethyl benzene.

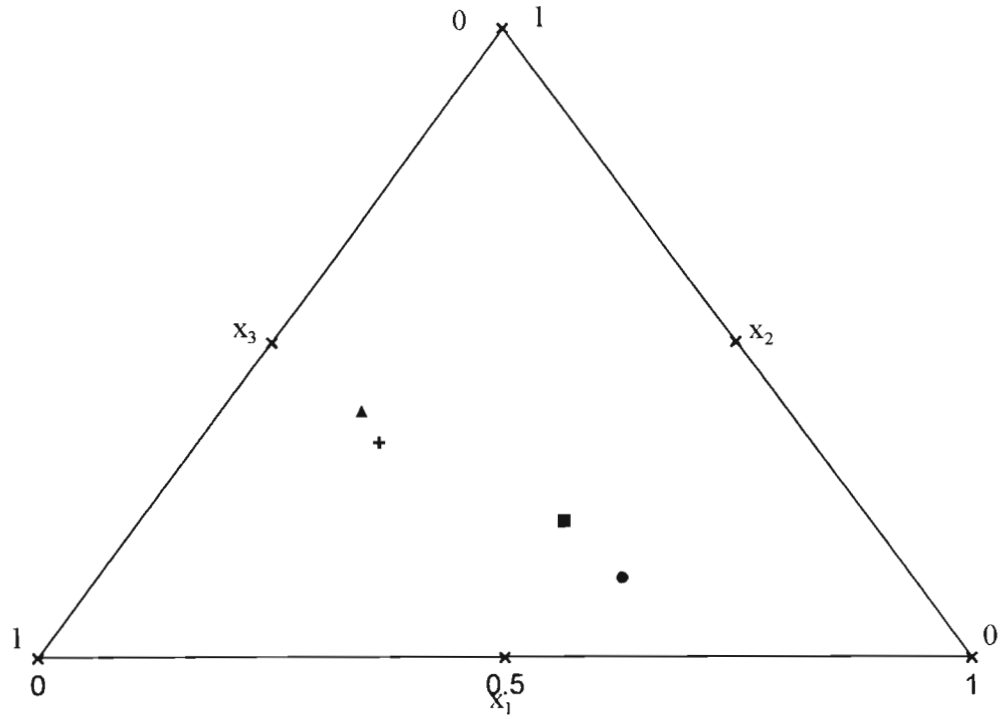

Figure 2.36. Migration of the plait point with change in n-alkane chain length. Key:● = n-hexane, ■ = n-nonane, ✚ = n-tetradecane, ▲ = n-hexadecane.

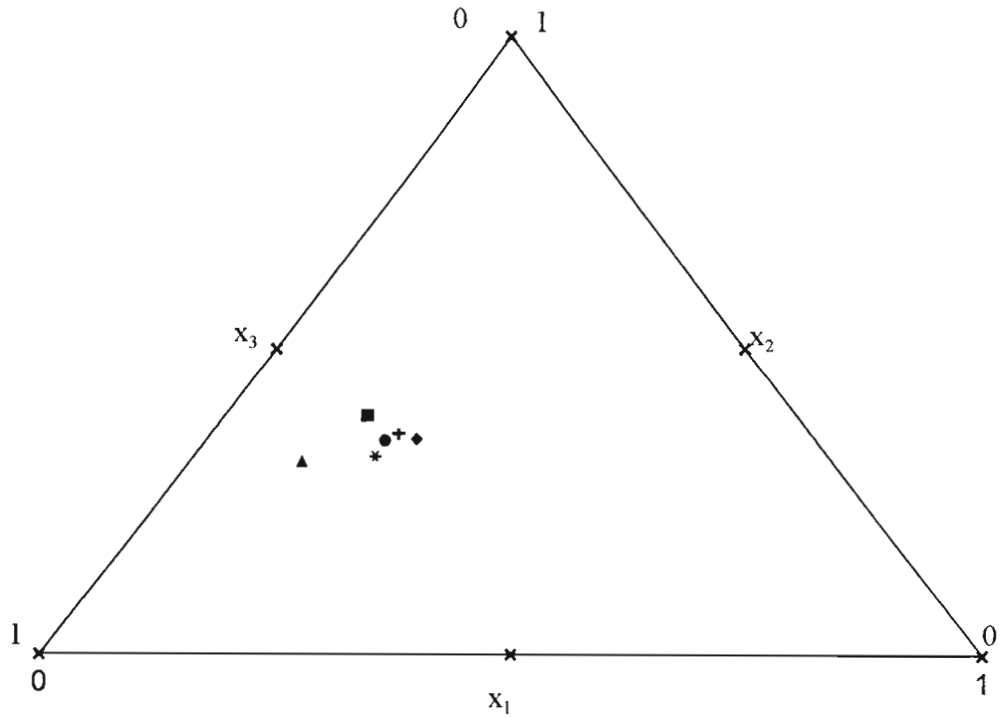

Figure 2.37. Position of plait point for the mixtures: n-hexadecane(1) + an aromatic hydrocarbon(2) + NMP(3). ■ = toluene, ✚ = o-xylene, ◆ = m-xylene, ▲ = p-xylene, ✱ = mesitylene, ● = ethyl benzene.

2.5. Discussion

All the data were measured at a temperature of 298.2 K and a pressure of 1 atmosphere.

2.5.1. Previous work:

2.5.1.1. n-heptane + benzene + NMP:

Fabries *et al.*[14] have presented data for the mixture: n-heptane (1) + benzene (2) + NMP (3) at 298.2 K. This data is plotted in figure 2.38. The slope of the tie-lines show that benzene is more soluble in NMP than in n-heptane. The work has a reported precision of 0.01, which appears to be excellent.

2.5.1.2. n-heptane + toluene + NMP:

The data for the mixture: n-heptane(1) + toluene(2) + NMP(3) at 298.2 K as presented by Ferreira *et al.*[12] is plotted in figure 2.39. The slope of the tie-lines show that toluene is more soluble in NMP than in n-heptane. The precision of this work is reported to be 0.01, which appears to be excellent.

2.5.1.3. n-tetradecane + benzene + NMP:

Data for the mixture: n-tetradecane(1) + benzene(2) + NMP(3) presented by Al-Zayied *et al.*[13] (see figure 2.40) consists of only four tie-lines. This data is considered to be of poor quality as the slopes of the tie-lines are inconsistent.

2.5.1.4. n-tetradecane + toluene + NMP:

Data has been presented by Al-Zayied *et al.*[13] for the mixture: n-tetradecane(1) + toluene(2) + NMP(3) at 298.2 K which is compared to the data from this work in figure 2.41. As can be seen the literature data is meagre and consists of only three tie-lines. This data is in poor agreement with the data presented here, with a maximum difference on the order of 0.18 mole fraction. This data is considered to be of poor quality, due to the unusual shape of the binodal curve. The shape of this binodal curve is inconsistent with the shapes of the binodal curves presented by Fabries *et al.*[14] and Ferreira *et al.*[12] for systems of the same type.

2.5.1.5. n-tetradecane + xylene + NMP:

Al-Zayied *et al.*[13] have presented data for the mixture: n-tetradecane(1) + xylene(2) + NMP(3) at 298.2 K which is plotted in figure 2.42. The data is very limited and consists of only two tie-lines. This data cannot be compared to our work as the xylene used by Al-Zayied *et al.*[13] is presumably a mixture of o-xylene, m-xylene and p-xylene and in this work o-xylene, m-xylene and p-xylene have been treated separately.

2.5.1.6. n-tetradecane + ethyl benzene + NMP:

Al-Zayied *et al.*[13] have also presented data for the mixture: n-tetradecane + ethyl benzene + NMP which consists of data for only three tie-lines. This data is plotted in figure 2.43. The binodal curve has an unusual shape hence, this data is considered to be of poor quality. The shape of this binodal curve is inconsistent with the shapes of the binodal curves presented by Fabries *et al.*[14] and Ferreira *et al.*[12] for systems of the same type.

2.5.2. This work:

The aim of this work is to obtain a better overall picture of the tie-lines and binodal curves for the ternary mixtures: an n-alkane + an aromatic hydrocarbon + NMP. This information is not available in the literature (see section 2.5.1). The work reported in this thesis gives a complete set of binodal curves and tie-lines and allows a discussion of (a) (see section 2.5.2.1) the effect that the alkane chain length has on the liquid-liquid equilibria of mixtures of the type, n-alkane + toluene + NMP, where the n-alkane was one of n-hexane or n-nonane or n-tetradecane or n-hexadecane, and (b) (see section 2.5.2.2) the effect that substitution on the benzene ring has on the liquid-liquid equilibria of mixtures of the type, n-hexadecane + an aromatic hydrocarbon + NMP, where an aromatic hydrocarbon is one of toluene or o-xylene or m-xylene or p-xylene or mesitylene or ethyl benzene.

2.5.2.1. n-Alkane + toluene + NMP:

The increase in chain length of the n-alkane (see figure 2.34) causes an increase in the area defining the two-phase region. This is expected as an increase in chain length (from C_6 to C_{16}) increases the hydrophobic nature of the n-alkane and, thus, reduces the solubility of the nonpolar n-alkane in the polar NMP.

The value of x_1 decreases at $x_2 = 0$ (from 0.174 for n-hexane to 0.020 for n-hexadecane) for high NMP concentrations, when the chain length of the n-alkane increases (from C_6 to C_{16}). This is expected as an increase in chain length (from C_6 to C_{16}) of the n-alkane results in an increase in the hydrophobic nature of the n-alkane, which manifests itself as a reduction of the interaction between the hydrophobic n-alkane and the polar NMP. The value of x_1 remains fixed (0.92 ± 0.01) at $x_2 = 0$ for low NMP concentrations when the chain length of the n-alkane increases (from C_6 to C_{16}). This is expected, because at low NMP concentrations the interactions between NMP and the n-alkane are minimal, hence, any reduction in the interaction between NMP and the n-alkane, due to an increase in hydrophobic nature of the n-alkane, with an increase chain length will not have a significant effect on the liquid-liquid equilibria. The two points discussed in this paragraph is confirmed by data reported in the literature for binary mixtures of the type an n-alkane + NMP.[21]

The slopes of the tie-lines in figure 2.5 and figure 2.6 and the relative solubility plot shown in figure 2.32 indicate that toluene is more soluble in NMP than it is in n-hexane and n-nonane. The slopes of the tie-lines in figure 2.7 and figure 2.8 and the relative solubility plot shown in figure 2.32 show that toluene is more soluble in n-tetradecane and n-hexadecane than it is in NMP.

The migration of the plait point with a change in n-alkane chain length is shown in figure 2.36. An increase in the chain length of the n-alkane causes the plait point to migrate from the alkane-rich region to the NMP-rich region.

The data predicted from this work for the mixture n-heptane + toluene + NMP compares well with the data reported by Ferreira *et al.*[12] (see figure 2.39). The data for the mixture: n-

heptane + toluene was predicted by interpolation from data for the mixtures: n-hexane + toluene + NMP and n-nonane + toluene + NMP. There is a minor discrepancy in the composition of the binary mixture n-heptane + NMP. The data presented in this work is believed to be correct, as repeated analysis of this mixture were carried out and the results presented here are consistent with binary data.[21]

2.5.2.2. Hexadecane + aromatic hydrocarbon + NMP:

The influence of methyl substitution on the benzene ring (see figure 2.35) on the liquid-liquid equilibria for mixtures of the type n-hexadecane + an aromatic hydrocarbon + NMP is very small, however the area of the two phase region is greatest for toluene and is smallest for mesitylene. The small decrease in the two phase area is expected as an increase in methyl substitution on the benzene ring increases the steric bulk of the molecule and this would reduce the interaction between the aromatic hydrocarbon and the n-alkane as well as the interaction between the aromatic hydrocarbon and NMP. The reduced association between NMP and the aromatic hydrocarbon is consistent with the excess molar enthalpy data and excess molar volume data presented later. The excess molar enthalpy and excess molar volume results are accounted for by taking into account a reduced association between NMP and the aromatic hydrocarbon.

The general order for the area under the curve defining the two phase region is:

toluene > o-xylene > p-xylene ≈ m-xylene ≈ ethyl benzene > mesitylene.

The position of the plait point is random within a small area as can be seen in figure 2.37. This indicates that methyl substitution on the benzene ring does not have as major an effect on the liquid-liquid equilibria as an increase in the chain length of the n-alkane has.

The slope of the tie-lines (see figures 2.8 to 2.13) for mixtures of the type n-hexadecane + an aromatic hydrocarbon + NMP and the relative solubility plot in figure 2.33 do not show any specific pattern with regards to solubility. This implies that methyl substitution does not have a major affect on the relative solubility of the aromatic hydrocarbon in the n-alkane or in NMP.

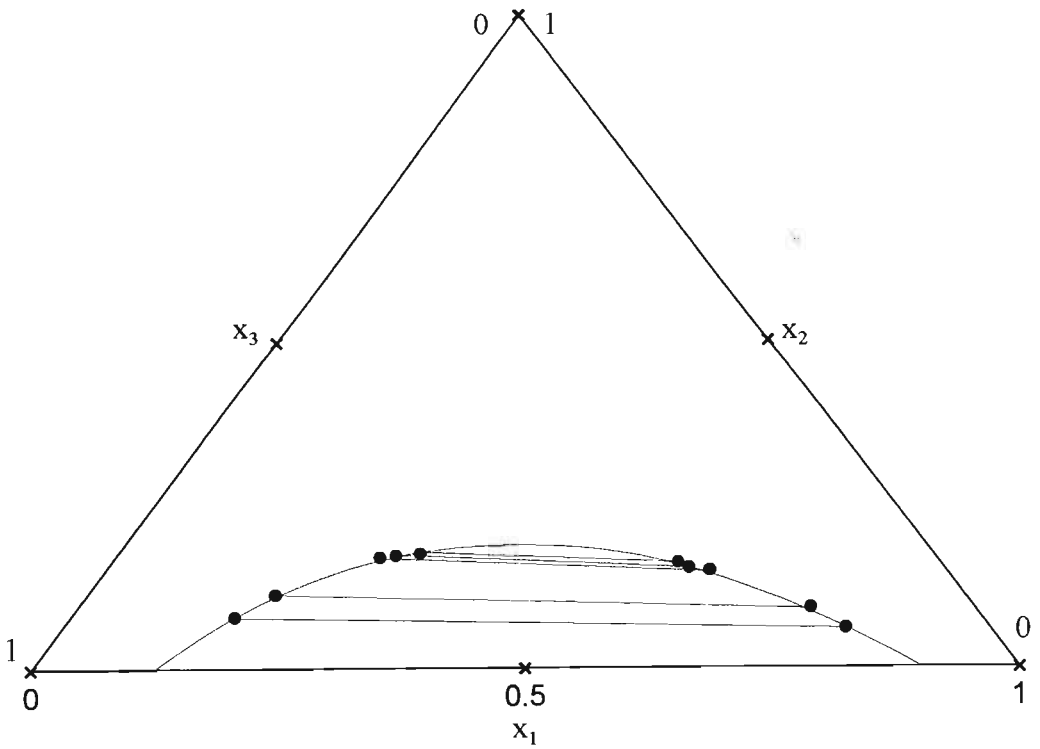

Figure 2.38. Phase diagram for n-heptane (1) + benzene (2) + NMP (3) at 298.2 K. Determined from literature data presented by Fabries *et al*[14]

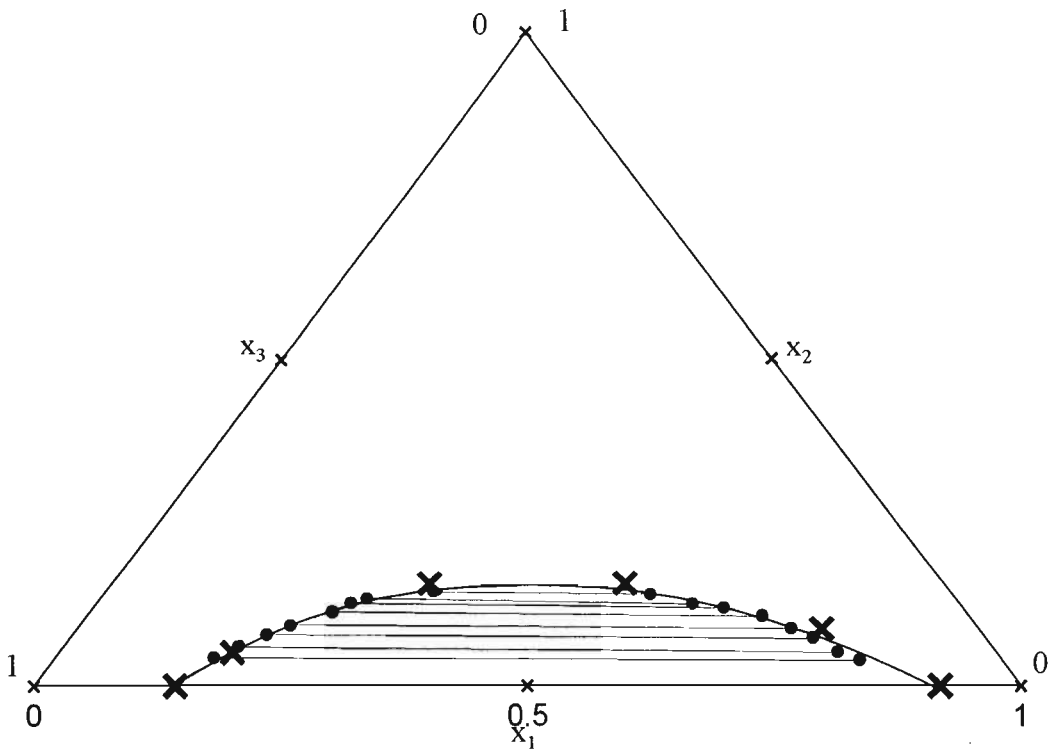

Figure 2.39. Phase diagram for n-heptane(1) + toluene (2) + NMP (3) at 298.2 K. Key : ● = Ferreira *et al.*[12], ✖ = predicted from this work.

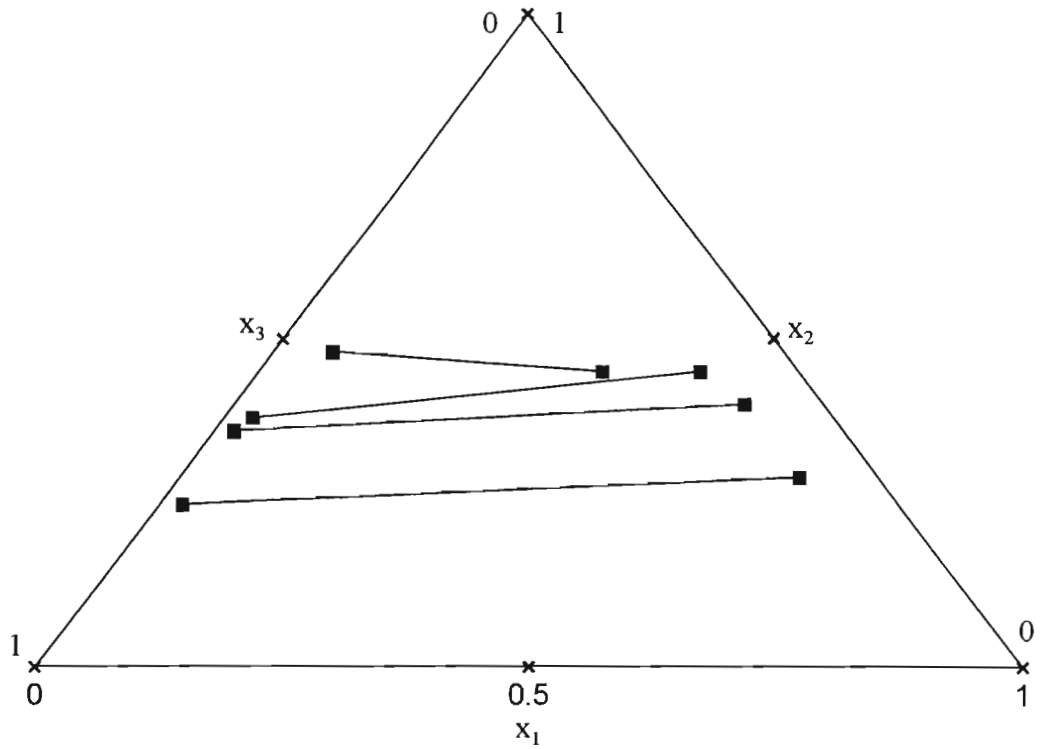

Figure 2.40. Phase diagram for tetradecane (1) + benzene (2) +NMP at 298.2 K based on the work by Al-Zayied *et al.*[13]

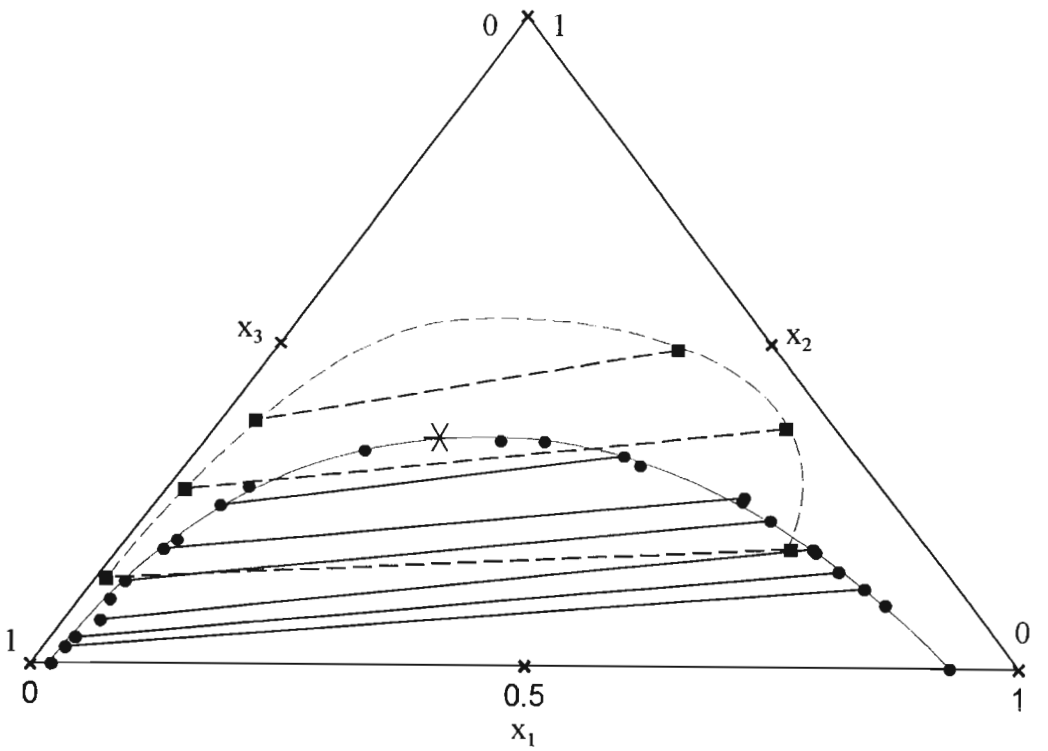

Figure 2.41. Phase diagram for tetradecane(1) + toluene (2) + NMP (3) at 298.2 K.
Key : ● = this work, ■ = Al-Zayied *et al.*[13]

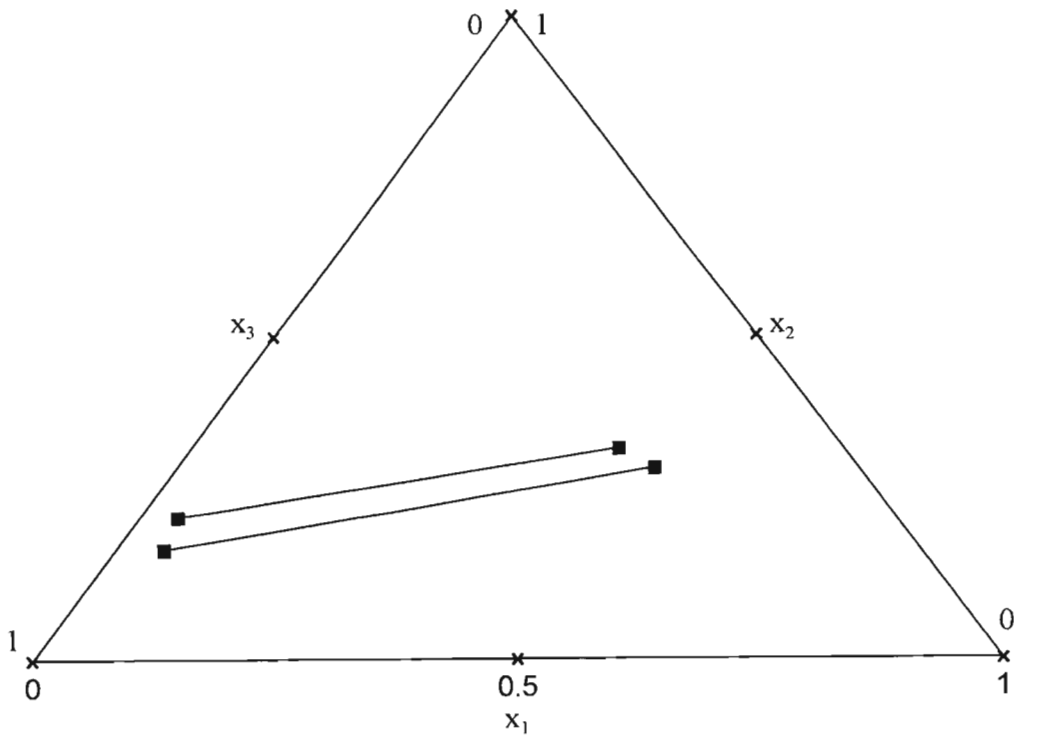

Figure 2.42. Phase diagram for n-tetradecane(1) + xylene (2) + NMP(3) at 298.2 K based on the work by Al-Zayied *et al.*[13]

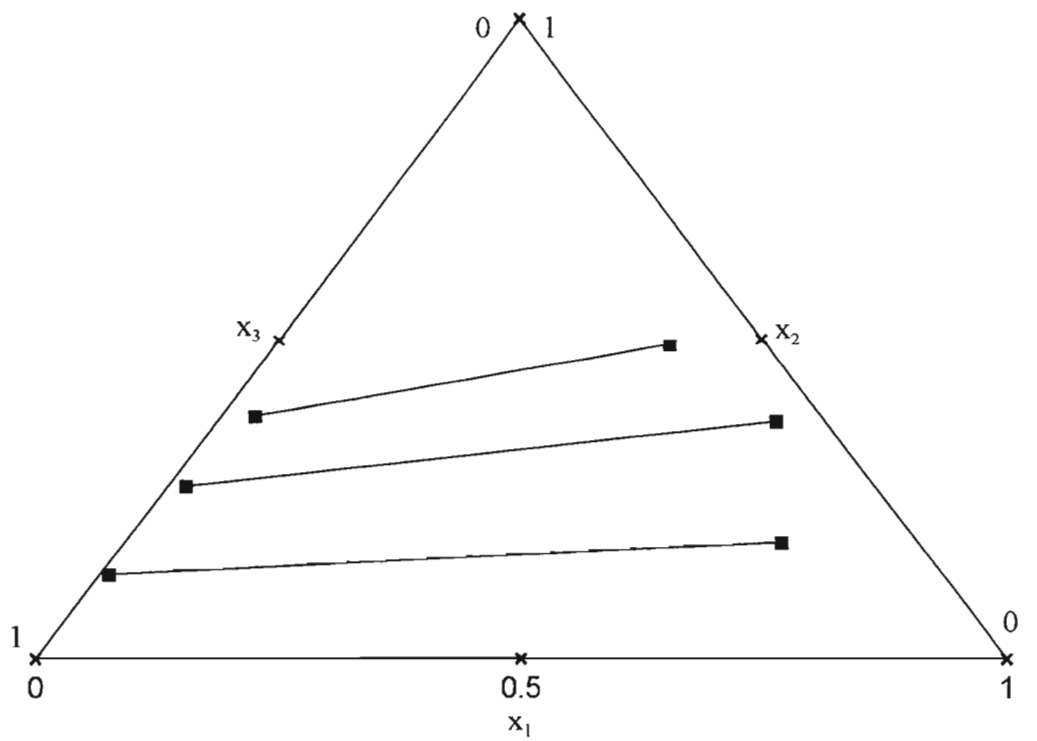

Figure 2.43. Phase diagram for n-tetradecane (1) + ethyl benzene (2) + NMP (3) at 298.2 K based on the work by Al-Zayied *et al.*[13]

Chapter 3
Infinite dilution activity coefficients

3.1. Introduction

This chapter is devoted to the activity coefficients at infinite dilution (γ^{∞}) of mixtures in which N-methyl-2-pyrrolidone (NMP) is the solvent. This work was carried out in order to better understand the interaction of NMP with compounds such as n-alkanes, cycloalkanes, 1-alkenes and ethers. The results found in the literature (see table 3.1) for the mixtures investigated here are not consistent which is the motivation for this work. Another reason for this work was to extend the literature data to include data for the solutes: cyclopentane, cycloheptane, 1-heptene, 1-octene, diethyl ether and diisopropyl ether.

The activity coefficient, γ, describes the deviation of a real solution from the limiting-law behaviour of Raoult's law and is defined by the following equation:[26]

$$\mu_A = \mu_A^* + RT\ln x_A + RT\ln \gamma_A \qquad (3.1)$$

where μ_A is the chemical potential of A,
μ_A^* is the chemical potential of A in the standard state,
x_A is the mole fraction of A and
γ_A is the activity coefficient of A.

The standard state in this case is pure liquid A which implies that the ideal solution obeys Raoult's Law. The activity coefficient at $x_A = 0$ is termed the activity coefficient at infinite dilution, γ_A^{∞} (see figure 3.1). The convention used here is: $\gamma_A \to 1$ as $x_A \to 1$.

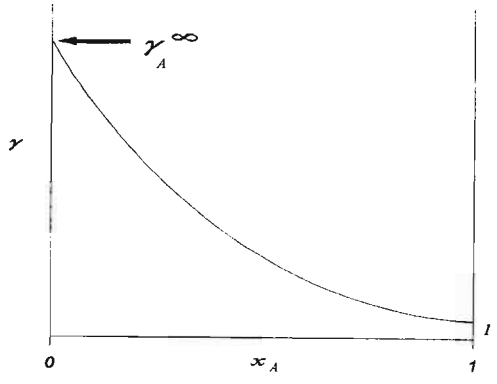

Figure 3.1. Typical graph of γ versus x_A

Table 3.1. Available literature data for the activity coefficients at infinite dilution at 298.15 K for the solutes investigated in this work where NMP is the solvent.

Solute	γ_{13}^{∞}	Literature reference	Technique
n-pentane	13.80	31	GLCI
n-hexane	12.90	32	GLCI
	23.00	33	GLCI
	14.77	34	GLCN
	14.30	35	GLCI
	20.96	36	GLCI
	13.57	37	DILU
	12.50	38	GLCN
	13.00	39	GLCN
	13.47	40	DILU
n-heptane	19.10	14	GLCN
	28.00	33	GLCI
	26.72	36	GLCI
	15.10	32	GLCI
	18.54	34	GLCR
	16.30	41	DILU
n-octane	33.60	36	GLCI
	17.60	32	GLCI
	20.95	42	STAT
cyclohexane	9.09	34	GLCR
	8.80	35	GLCI
	13.44	36	GLCI
	8.50	32	GLCI
	11.88	43	GLCN
	11.00	33	GLCI
1-hexene	6.70	39	GLCN

γ_{13}^{∞} is the activity coefficient at infinite dilution of compound 1 in compound 3.

KEY: GLCN = Gas liquid chromatography without a specification of gas phase correction.
GLCI = Gas liquid chromatography without gas phase correction.
GLCR = Gas liquid chromatography with gas phase correction.
DILU = Dilution techniques.
STAT = Static method.

Activity coefficients at infinite dilution, γ^{∞}, are theoretically and practically important.[44] From the solute point of view infinite dilution represents the state of maximum nonideality because at this concentration the solute molecule is surrounded by a maximum number of solvent molecules.[44] The infinitely dilute state is important in the development of mixing theories because at this concentration solute-solute interactions can be ignored.[45]

Activity coefficients are vital in the calculation of vapour-liquid equilibria[46] which are important to the proper design of separation processes.[11] Activity coefficients at infinite dilution for the solute and the solvent, together with equations for the excess Gibbs functions, derived from mixing theories can be used to predict equilibria over complete composition ranges, even though experimental data points for γ may be limited. Schreiber and Eckert have shown; that if accurate values of γ^{∞} of the solute and solvent are known, then it is possible to predict vapour-liquid equilibria over entire composition ranges with good accuracy.[47] The value of knowing the phase equilibria is that they allow for the calculation of separation factors which indicate the lowest amount of solvent that could be used and the suitability of the solvent for a particular separation.[48] Phase equilibria are also important in determining the efficiencies of separation processes.[48]

In this chapter a list of the available experimental techniques are given together with a list of the more popular methods for predicting γ^{∞} from theory. This is followed by a summary of the gas-liquid chromatography method and details of the experimental procedure used here. In this work, γ^{∞} for the mixtures given in table 3.2 are determined at 298.15 K. The data presented here not only extend the available literature data, but also improve on the existing data, by taking into account gas phase imperfections.

Table 3.2. Systems for which activity coefficients at infinite dilution are determined in this work.

stationary phase	solute
NMP	n-pentane
NMP	n-hexane
NMP	n-heptane
NMP	n-octane
NMP	c-pentane
NMP	c-hexane
NMP	c-heptane
NMP	1-hexene
NMP	1-heptene
NMP	1-octene
NMP	diethyl ether
NMP	diisopropyl ether

3.2. Experimental techniques for the determination of infinite dilution activity coefficients:

There are various techniques for the experimental determination of activity coefficients at infinite dilution . These are listed below. The techniques are described in detail in the references.

i. Gas-liquid chromatography, [49]
ii. Differential ebulliometry, [50]
iii. Dew-point method, [51]
iv. Headspace chromatography, [52]
v. Differential pressure, [53]
vi. Gas stripping[54] and
vii. Inverse solubility.[49]

The two preferred techniques are gas-liquid chromatography which is described in detail by Letcher[49] and ebulliometry described in detail by Eckert and coworkers.[55] These two techniques complement each other as gas-liquid chromatography works well for low volatility solvents and ebulliometry works well with volatile solvents.[11]

3.3. Theoretical prediction of infinite dilution activity coefficients using models:

Three of the most popular models used to predict infinite dilution activity coefficients are listed below:

3.3.1. Modified separation of cohesive energy density (MOSCED)

This method based on the regular solution theory was proposed by Thomas and Eckert[56] for the calculation of infinite dilution activity coefficients from pure component parameters only. A comprehensive review of this method is given by Malanowski and Anderko[45] as well as by Reid and Prausnitz.[48]

A summary of the equation used in this model is given below:

$$\ln\gamma_i^{\infty} = \frac{v_i}{RT}\left[(\lambda_j-\lambda_i)^2 + \frac{q_j^2 q_i^2 (\tau_j-\tau_i)^2}{\psi_j} + \frac{(\alpha_j-\alpha_i)(\beta_j-\beta_i)}{\xi_j}\right] + d_{12} \qquad (3.2)$$

where i and j represent the two liquids (that is the solute and solvent),
v_i is liquid molar volume at 20 °C of i,
λ is the dispersion parameter,

q is the induction parameter,
τ is the polar parameter,
α is the acidity parameter,
β is the basicity parameter,
ψ is the parameter that accounts for the difference in polarity between i and j and
ξ is the parameter that accounts for the degree of hydrogen bonding..

These parameters: α, β, τ, λ, ψ, ξ, q and v are given in reference 48 and d_{12} is the Flory-Huggins combinatorial term which accounts for the difference in size and is calculated using the following equation:

$$d_{12} = \ln\left(\frac{v_2}{v_1}\right)^{aa} + 1 - \left(\frac{v_2}{v_1}\right)^{aa} \qquad (3.3)$$

where aa is a parameter available in the literature.[48]

The parameters α, β, τ, ψ, ξ and aa are temperature dependent.

3.3.2. Analytical solution of groups (ASOG)

Deal and Wilson[57, 58] proposed this method following the work of Redlich, Derr, Pierotti and Papadopoulous.[59, 60] The basic idea is that there are fewer functional groups than there are compounds hence parameters determined for functional groups allowed the calculation of activity coefficients for any mixture. A molecule is analysed for all the functional groups and each functional group contributes to the infinite dilution activity coefficient. A detailed account of ASOG is given by Malanowski and Anderko[45] as well as Reid and Prausnitz.[48]

The functional equation is given below:

$$\ln\gamma_i = \ln\gamma_i^S + \ln\gamma_i^G \qquad (3.4)$$

where S and G designate size and group respectively.

The size activity, γ_i^S, depends only on the number of groups of a particular size in the various molecules that constitute the mixture.

$$\ln\gamma_i^S = 1 - \mathbb{R}_i + \ln\mathbb{R}_i \qquad (3.5)$$

here $\mathbb{R}_i = \dfrac{s_i}{\sum s_j x_j}$

where s_i = size fraction of component i in the mixture.

γ_i^G is the group activity and describes the contribution made by functional groups.

3.3.3. Universal quasi-chemical functional group activity coefficient (UNIFAC)

UNIFAC is another functional group contribution method developed by Fredenslund *et al.* [61] It is based on the UNIQUAC model proposed by Abrams and Prausnitz.[62] Of the three models listed in this thesis UNIFAC is the preferred one as it is more universal and various modifications have been made to improve accuracy for vapour-liquid equilibria and liquid-liquid equilibria.[63, 64,65,66] The UNIFAC approach is the most widely used method today for the simulation of phase equilibria.[45]

The functional equation for this model is:

$$\ln \gamma_i = \ln \gamma_i^C + \ln \gamma_i^R \tag{3.6}$$

where $\ln \gamma_i^C$ (the combinatorial term) and $\ln \gamma_i^R$ (the residual term) are defined as follows:

$$\ln \gamma_i^C = \ln \frac{\Phi_i}{x_i} + \frac{z}{2} q_i \ln \frac{\theta_i}{\Phi_i} + \ell_i \frac{q_i}{x_i} \Sigma x_j \ell_j \tag{3.7}$$

and

$$\ln \gamma_i^R = q_i \left[1 - \ln \left(\Sigma \theta_j \tau_{ji} \right) - \Sigma\Sigma \left(\frac{\theta_j \tau_{ij}}{\Sigma \theta_k \tau_{kj}} \right) \right] \tag{3.8}$$

where

$$\ell_i = \frac{z}{2} (r_i - q_i) - (r_i - 1) \tag{3.9}$$

and

$$\theta_i = \frac{q_i x_i}{\Sigma q_j x_j} \quad , \quad \Phi_i = \frac{\tau_i x_i}{\Sigma r_j x_j} \quad , \quad \tau_{ji} = \exp\left(-\frac{u_{ij} - u_{ii}}{RT} \right) \qquad z = 10$$

Where x_i = mole fraction of component i, θ_i is the area fraction, Φ_i is the segment fraction which is similar to the volume fraction, r_i is the molecular van der Waals volume, q_i is the molecular surface area and τ_{ij} are adjustable parameters.

3.4. Experimental:

3.4.1. Gas-liquid chromatography:

Gas-liquid chromatography, described in detail by Letcher,[49] was used in this work to determine the activity coefficients at infinite dilution.

The idea of using gas-liquid chromatography to determine activity coefficients was proposed by Martin and Synge in 1941.[67] The result of their work was the following relationship between the retention volume, V_R, the partition coefficient, K, the gas holdup volume, V_G, and the solvent volume, V_3.[a]

$$V_R = V_G + KV_3 \tag{3.10}$$

Work by Martin and James [68] in 1952 and later by Martin [69] in 1956 led Porter *et al.*[70] in 1956 to relate the activity coefficient at infinite dilution, γ^{∞}, to the net retention volume, V_N by the following equation:

$$V_N = \frac{n_3 RT}{\gamma_{13}^{\infty} p_1^o} \tag{3.11}$$

where n_3 = the number of moles of the solvent,
p_i^o = the solute vapour pressure,
T = the temperature of the experiment and
γ_{13}^{∞} = the activity coefficient at infinite dilution of compound 1 in compound 3 according to the format is used in the literature.[49]

The net retention volume is related to the outlet flow rate, U_o, by the following equation:

$$V_N = J_3^2 \, U_o(t_r - t_G) \tag{3.12}$$

---

[a] In this work subscripts 1, 2 and 3 represent the solute, carrier gas and the solvent respectively.

where U_o = the outlet flow rate,
t_r = the retention time of solute and
t_G = time taken for an unretained gas to pass through the column.

J_3^2 is the correction factor proposed by Martin and James[68] resulting from the pressure drop along the column and is given below:

$$J_3^2 = \frac{3[(p_i/p_o)^2 - 1]}{2[(p_i/p_o)^3 - 1]} \tag{3.13}$$

where p_i = the inlet pressure and
p_o = the outlet pressure.

Work by Everett and Stoddard[71] taking into account solute-vapour and solute-carrier gas imperfections and later work by Cruickshank *et al.*[72] accounting for solubility of the carrier gas in the stationary liquid resulted in the equation below:

$$\ln\gamma_{13}^{\infty} = \ln\left(\frac{n_3 RT}{V_N p_1^o}\right) - \frac{(B_{11} - V_1^o)p_1^o}{RT} + \frac{(2B_{12} - V_1^{\infty})J_3^2 p_o}{RT} \tag{3.14}$$

where B_{11} is the virial coefficient for the solute, B_{12} is the mixed virial coefficient, V_1^{∞} is the molar volume of component 1 at infinite dilution and V_1^o is the molar volume of the pure solute. This is the equation used to determine the activity coefficients at infinite dilution in this work.

3.4.2. Experimental Details:

Calculation of the activity coefficients at infinite dilution from equation 3.14 requires the experimental determination of the following values:

i. The retention time of air which represents the time an unretained gas takes to pass through the column, t_G,
ii. the outlet pressure, p_o, which is equal to atmospheric pressure,
iii. the number of moles of solvent, n_3,
iv. the flow rate, U_o,
v. the inlet pressure, p_i, and
vi. the solute retention time, t_r.

3.4.2.1. Apparatus:

The experimental details of the apparatus is shown in figure 3.2.

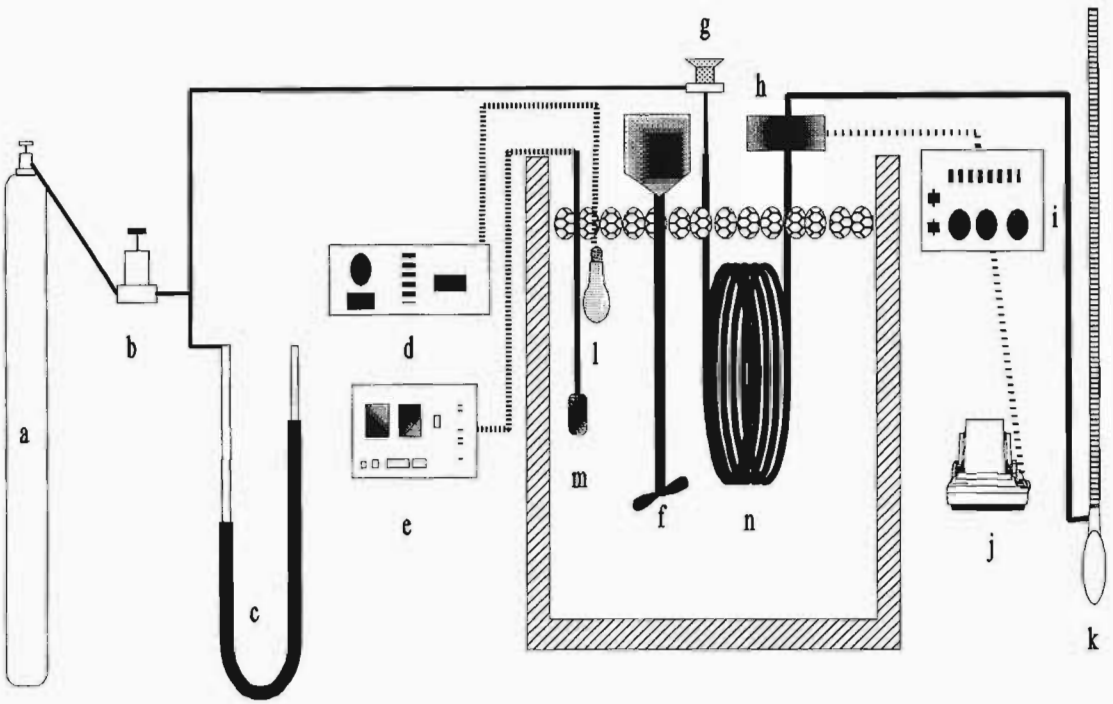

Figure 3.2. Apparatus for the determination of γ^{∞}. a. Helium cylinder, b. Precision pressure control, c. mercury manometer, d. Tronac temperature controller, e. Hewlett-Packard quartz thermometer, f. stirrer, g. sample injection port, h. Thermal conductivity detector, i. Gow-mac bridge, j. plotter, k. soap film flow meter, l. globe (heating element), m. thermometer probe, n. Column containing the solvent and celite.

3.4.2.2. Determination of the inlet pressure, p_i:

The inlet pressure is determined by use of the mercury manometer. The total inlet pressure is equal to the difference in height of the mercury levels plus the atmospheric pressure, p_o, which is accurate to within 0.05 mmHg.

3.4.2.3. Determination of the flow rate, U_o:

The flow rate is determined by use of the soap film flow meter which is accurate to within 0.01 $cm^3\ s^{-1}$.

3.4.2.4. Determination of the retention times, t_G and t_r:

The retention time determined from a chromatogram is accurate to 0.1 s over a period of 40 to 600 seconds. A typical chromatogram is shown below in figure 3.3. Here the unretained gas is air. The retention time is determined at the intersection of the tangents to the sides of the peak.[49]

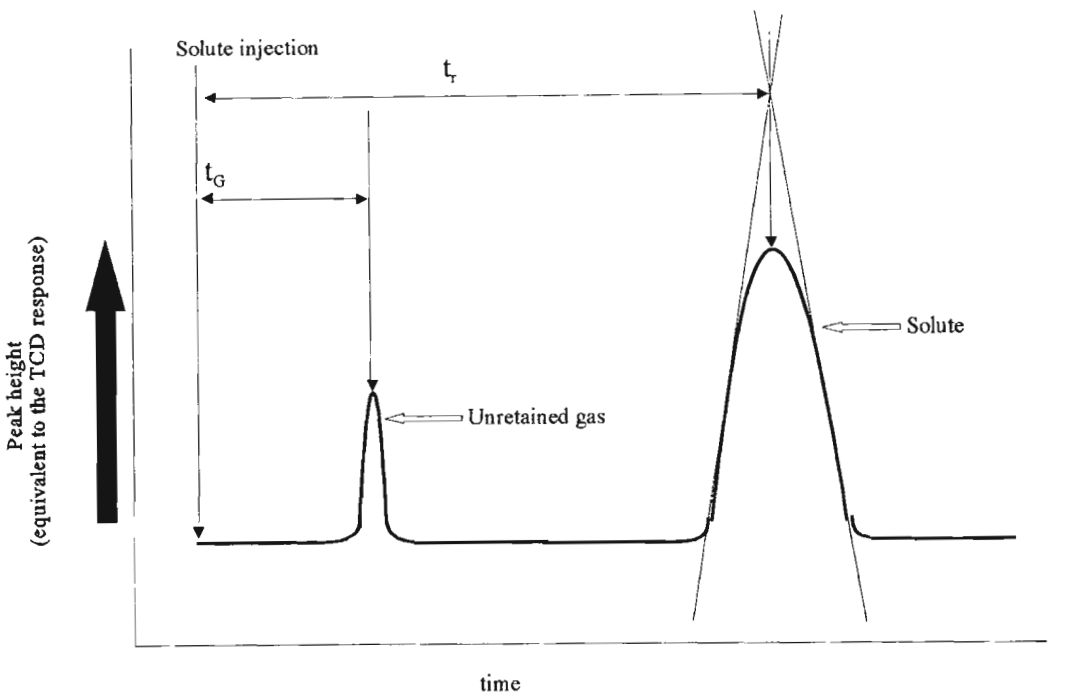

Figure 3.3. Typical chromatogram showing the detector response versus time.
t_G = time taken for an unretained gas (air) to pass through the column, t_r = retention time of the solute.

3.4.2.5. Determination of n_3 :

The determination of the number of moles of the solvent, n_3, requires high accuracy and extreme caution. The solvent was carefully weighed and added to celite, which was also carefully weighed. Diethyl ether was added to distribute the solvent evenly over the celite.

The diethyl ether was removed using a rotary evaporator and the celite-solvent mixture was reweighed to ensure that all the ether was removed. The amount of celite-solvent mixture added to the column was carefully determined. From this the value of n_3 was determined to within 0.001 moles.

3.4.2.6. Chemicals:

The chemicals used in this work and their respective suppliers are shown in table 3.3. NMP was dried using 4Å molecular sieves.

Table 3.3. List of chemical and suppliers.

Chemical	Supplier	Purity
N-methyl-2-pyrrolidone	Sigma	> 99 %
n-pentane	SAARChem	99 %
n-hexane	SAARChem	99 %
n-heptane	SAARChem	99 %
n-octane	EGA-Chemie	99 %
c-pentane	MERCK	99 %
c-hexane	SAARChem	99 %
c-heptane	SAARChem	99 %
1-hexene	JANSSEN	99 %
1-heptene	Sigma	> 99 %
1-octene	Riedel-de-Haen	98 %
Diethyl ether	ACE	99 %
diisopropyl ether	ACROS	> 99 %

3.5. Results:

The γ_{13} results were calculated using equation 3.14 where the molar volume at infinite dilution, V_1^{∞}, was approximated to the molar volume of the pure solute, V_1^{o}. There was no loss of accuracy. Actual experimental data are given in appendix A.

The virial coefficients, B_{11}, were calculated using the equation developed by McGlashan and Potter: [73]

$$\frac{B_{11}}{V_c} = 0.43 - 0.886\left(\frac{T_c}{T}\right) - 0.694\left(\frac{T_c}{T}\right)^2 - 0.0375(n-1)\left(\frac{T_c}{T}\right)^{4.5} \qquad (3.15)$$

where T_c is the critical temperature, n is the number of carbon atoms and V_c is the critical molar volume. Equation 3.15 was also used for the determination of the mixed virial coefficient where the value of T_c, V_c and n are determined as follows, based on the mixing rules of Hudson and McCoubrey [74].

$$T_{c,12} = 128(T_{c,11} \cdot T_{c,22})^{\frac{1}{2}} (I_{c,11} \cdot I_{c,22})^{\frac{1}{2}} V_{c,11} V_{c,22} / I_{c,12} \qquad (3.16)$$

and

$$V_{c,12} = \left(V_{c,11}^{1/3} + V_{c,22}^{1/3}\right)^3 / 8 \qquad (3.17)$$

where

$$I_{c,12} = (I_{11} + I_{22})\left(V_{c,11}^{1/3} + V_{c,22}^{1/3}\right)^6 \qquad (3.18)$$

and

$$n_{12} = (n_1 + n_2) \qquad (3.19)$$

Where n_i is equal to the numbers of carbon atoms for the organic compounds and is 1.0 for helium. I is the ionization energy.

The vapour pressures which were used in equation 3.14 were calculated using the Antoine equation:

$$\log_{10} p^{o} = A - \frac{B}{C + t} \tag{3.20}$$

where A,B and C are obtained from the literature (see table 3.5), and t is the temperature in degrees celsius.

Ionization energies, critical volumes, critical temperatures and n are given in table 3.4. Antoine constants and vapour pressures at 298.15 K are given in table 3.5.

Activity coefficients at infinite dilution at 298.15 K are shown in table 3.6.

Table 3.4. Ionization energies [75], critical volumes [23], critical temperatures[23] and n at 298.15 K.

solute	ionization energy in eV	critical volume in cm^3/mol	critical temperature in K	n
n-pentane	10.35	313.0	469.69	5
n-hexane	10.13	370.0	507.50	6
n-heptane	9.97	426.4	540.30	7
n-octane	9.82	480.0	568.83	8
c-pentane	10.56	260.0	511.61	5
c-hexane	9.89	309.7	553.50	6
c-heptane	9.97	359.0	359.00	7
1-hexene	9.48	353.6	353.60	6
1-heptene	9.44	412.6	412.60	7
1-octene	9.43	471.5	471.50	8
diethyl ether	9.51	280.0	466.70	4
diisopropyl ether	9.27	386.0	500.00	6
helium	54.42	57.0	5.19	1

Table 3.5. Constants [23] for the Antoine equation and Vapour pressures at 298.15 K

Solute	*A*	*B*	*C*	units	Vapour pressure (for the units see the preceding column)	Vapour pressure in Pa
n-pentane	6.85296	1064.84	232.012	mmHg	512.6337	68345.54
n-hexane	6.87601	1171.17	224.408	mmHg	151.4295	20188.93
n-heptane	6.89677	1264.90	216.544	mmHg	45.7133	6094.61
n-octane	6.91868	1351.99	209.155	mmHg	13.9563	1860.68
c-pentane	6.92094	1142.20	233.463	mmHg	317.4964	42329.37
c-hexane	6.83917	1200.31	222.504	mmHg	97.6138	13014.10
c-heptane	6.83840	1322.22	215.297	mmHg	2.6750	2889.76
1-hexene	3.98260	1148.62	225.340	Bar	0.2479	24794.77
1-heptene	4.02677	1258.34	219.300	Bar	0.0752	7515.74
1-octene	4.05985	1355.46	213.050	Bar	0.0232	2321.86
diethyl ether	6.05115	1062.41	228.183	kPa	71.6045	71604.47
diisopropyl ether	5.97678	1143.07	219.340	kPa	19.8872	19887.19

Table 3.6. Results obtained in this work for activity coefficients at infinite dilution at 298.15 K where NMP is the solvent

Solute	γ_{13}^{∞}
n-pentane	14.0
n-hexane	15.4
n-heptane	18.1
n-octane	19.2
c-pentane	6.5
c-hexane	8.1
c-heptane	9.1
1-hexene	6.8
1-heptene	8.2
1-octene	13.5
diethyl ether	3.3
diisopropyl ether	5.3

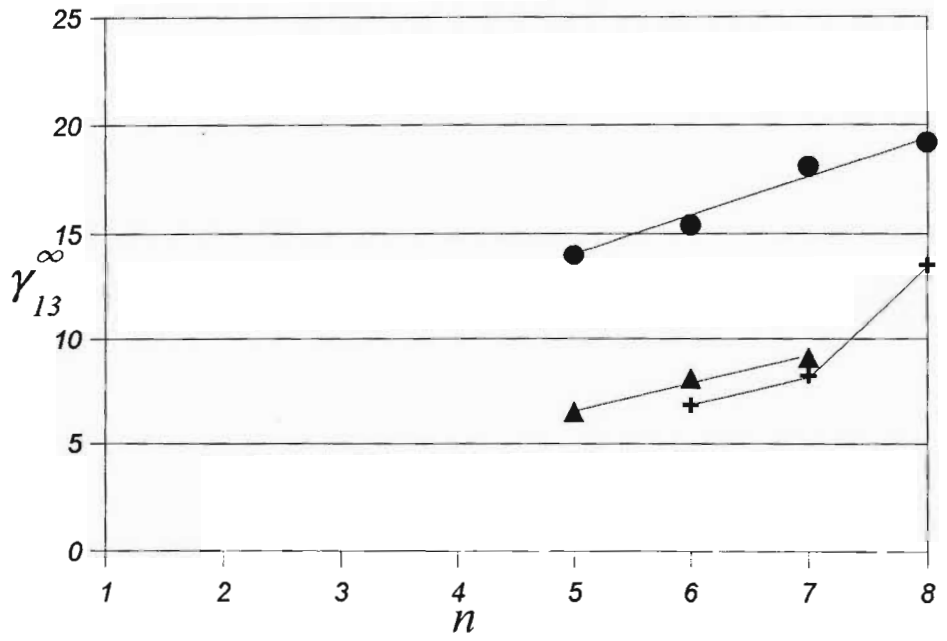

Figure 3.4. Graph of activity coefficient at infinite dilution versus the number of carbon atoms. Key: ● = n-alkane, ▲ = cycloalkane, ✚ = 1-alkene.

3.6. Discussion:

3.6.1. Previous work:

3.6.1.1. n-Alkanes + NMP:

The literature values for γ_{13}^{∞} for the n-alkanes in NMP are given in table 3.1 and plotted in figure 3.5. The γ_{13}^{∞} values range from 11.80 for n-pentane to 33.60 for n-octane. γ_{13}^{∞} increases as the carbon-chain length of the alkane increases. This indicates that as the carbon-chain length of the n-alkane increases then the deviation from ideality of the mixture increases. Unfortunately, the literature presents a large range of γ_{13}^{∞} values for a particular n-alkane as can be seen in figure 3.5. A range of precision for γ_{13}^{∞} of 0.02 to 0.05 was reported in the literature.

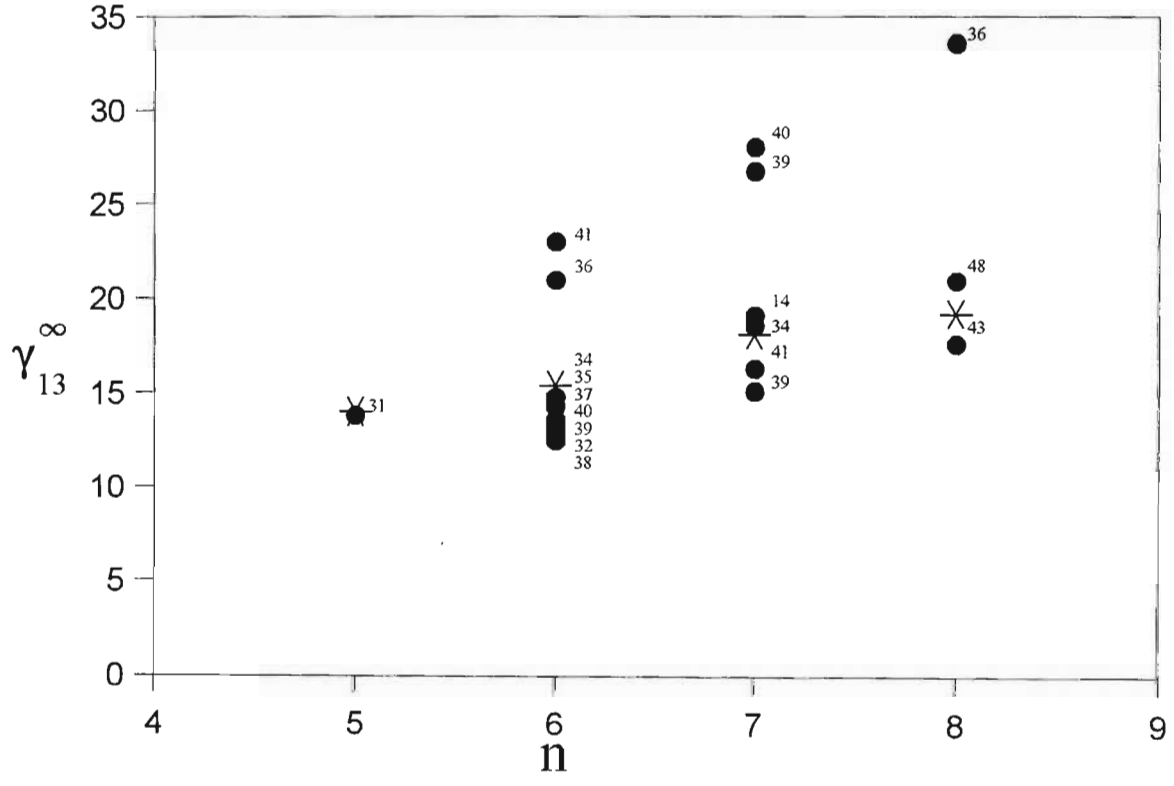

Figure 3.5. Plot of γ_{13}^{∞} versus *n* for the n-alkanes. Key : ✳ = this work, ● = literature.

3.6.1.2. Cycloalkanes + NMP:

The only γ_{13}^{∞} values for these systems available in the literature are for cyclohexane which range from 8.50 to 13.44. The available data is plotted in figure 3.6. A range of precision for γ_{13}^{∞} of 0.02 to 0.05 was reported in the literature.

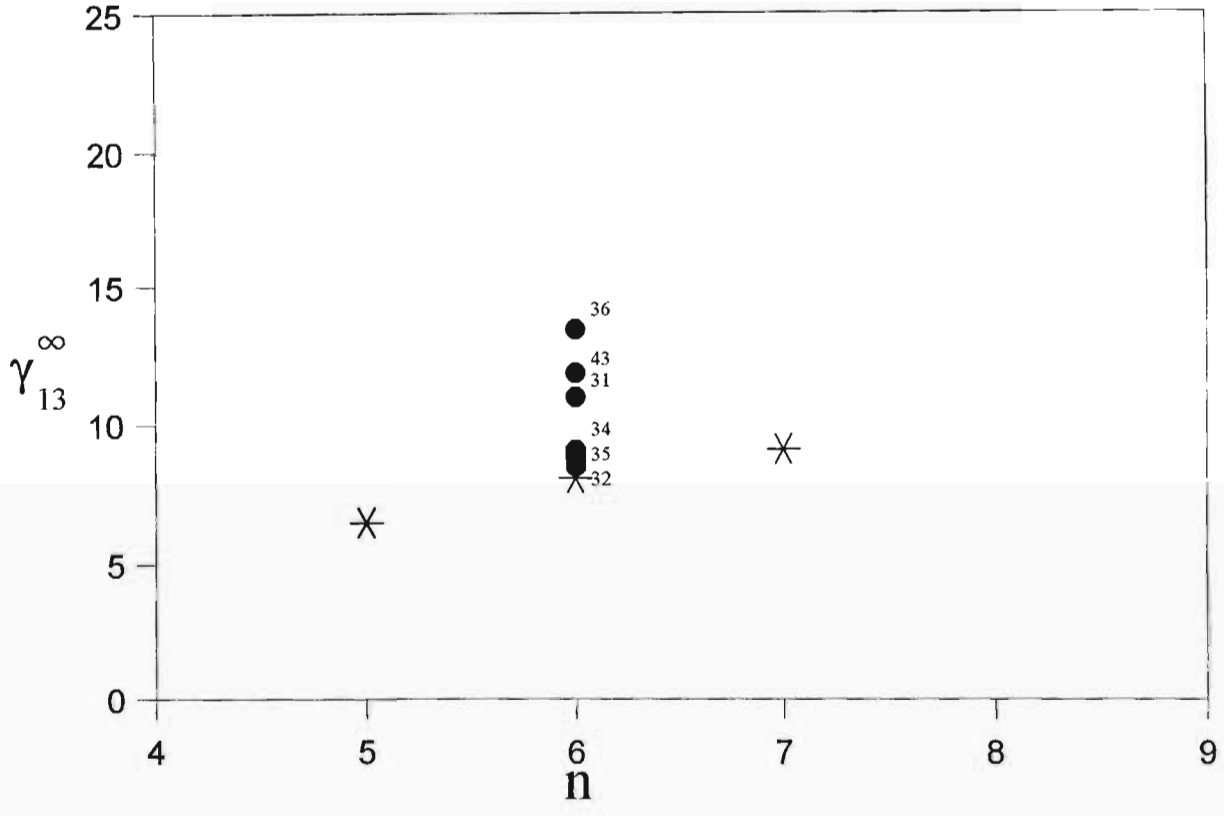

Figure 3.6. Plot of versus *n* for the cycloalkanes. Key :✳ = this work, ● = literature.

3.6.1.3. 1-Alkenes + NMP:

The γ_{13}^{∞} for the 1-alkenes in NMP is limited to a single data point presented for 1-hexene.[39] A γ_{13}^{∞} value equal to 6.70 was determined using gas-liquid chromatography. However, no gas-phase correction was quoted in this work. A precision equal to 0.01 was reported in the literature.

3.6.2. This work:

The γ_{13}^{∞} results obtained in this work for the solutes in NMP are given in table 3.6. The precision of this work is estimated to be 0.1.

3.6.2.1. n-Alkanes:

The activity coefficients at infinite dilution for the n-alkanes in NMP at 298.15 K range from 14.0 for n-pentane to 19.2 for n-octane. γ_{13}^{∞} for the n-alkanes in NMP increases with an increase in the carbon-chain length of the n-alkane (see figure 3.4). The increase in γ_{13}^{∞} as the carbon-chain length of the n-alkane increases indicates that the deviation from ideality for mixtures of this type increases as the carbon-chain length of the n-alkane increases. This is consistent with the data presented in chapter two on the liquid-liquid equilibria for mixtures of the type: an n-alkane + toluene + NMP, where an increase in the area defining the two phase region with an increase in carbon-chain length was observed. An increase in the area defining the two phase region indicates a greater deviation from ideality. The data presented here lie within the range of values reported in the literature (see figure 3.5).

3.6.2.2. Cycloalkanes:

New γ_{13}^{∞} data is presented in table 3.6 for cyclopentane and cycloheptane in NMP. This data is plotted in figure 3.4. The cycloalkanes have lower activity coefficients than the corresponding n-alkanes ranging from 6.5 for cyclopentane to 9.1 for cycloheptane. As in the case of the n-alkanes γ_{13}^{∞} increases with an increase in the carbon-chain length. The increase in γ_{13}^{∞} with an increase in carbon carbon-chain length is greater for the n-alkanes than it is for the cycloalkanes as can be seen from the slopes in figure 3.4. The high γ_{13}^{∞} values for the n-alkanes and the cycloalkanes is reflected in the fact that the n-alkanes and cycloalkanes do not mix with NMP at finite concentrations. γ_{13}^{∞} for cyclohexane in NMP obtained in this work is in good agreement with the data presented by Vernier *et al.*[35], Kikic *et al.*[34] and Park *et al.*[42] (see figure 3.6).

3.6.2.3. 1-Alkenes:

New γ_{13}^{∞} data is presented for 1-heptene and 1-octene in table 3.6. The data is plotted in figure 3.4. The value of γ_{13}^{∞} for the 1-alkenes in NMP range from 6.8 for 1-hexene to 13.5 for 1-octene and as with the n-alkanes and the cycloalkanes γ_{13}^{∞} increases with an increase in the carbon carbon-chain length. The values of γ_{13}^{∞} for a given 1-alkene are lower than those for the corresponding n-alkane and cycloalkane. This is probably due to the presence of the π-electrons on the 1-alkene, which interact with the polar NMP and result in an association between the polar NMP and the 1-alkene. The γ_{13}^{∞} data presented here for 1-hexene in NMP is within 0.1 of the value presented by Masalsccky *et al.*[39]

3.6.2.4. Ethers:

There are no γ_{13}^{∞} data available in the literature, for ethers in NMP, hence the data presented

here is new. The ethers have low γ_{13}^{∞} values 3.3 for diethylether and 5.3 for diisopropyl ether. The γ_{13}^{∞} values for the ethers are lower than the γ_{13}^{∞} values for the n-alkanes, the cycloalkanes or the 1-alkenes. This indicates that mixtures of NMP and the ethers behave more ideally than mixtures of NMP and n-alkanes or cycloalkanes or 1-alkenes. The low γ_{13}^{∞} is reflected in the fact that NMP is soluble in these ethers over the whole composition range. This is probably due to the oxygen atom with two lone pairs which would result in an interaction between the ether and polar NMP molecule.

Chapter 4
Excess molar enthalpies of mixing

4.1. Introduction

In this chapter the basic principles of calorimetry are given together with a listing of the techniques available for the determination of excess molar enthalpies of mixing. This is followed by a brief description of the work carried out and the results obtained in this work.

Of all the mixtures discussed in this thesis only those of the type NMP + an aromatic hydrocarbon (where the aromatic hydrocarbon refers to benzene or toluene or o-xylene or m-xylene or p-xylene or mesitylene or ethyl benzene) are miscible over the whole composition range hence, only these mixtures have been used to determine the excess molar enthalpy of mixing (H_m^E). The only available data for mixtures of the above type are presented by Gustin and Renon[76] for the mixture NMP + benzene and by Shcherbina *et al.*[77] for the mixture NMP + o-xylene. New data is presented for toluene, m-xylene, p-xylene, mesitylene and ethyl benzene.

Any reaction, physical or chemical, is accompanied by a net production or absorption of heat. In the case of mixing, the heat produced or absorbed is called the enthalpy of mixing, ΔH_{mix}.

Prausnitz[78] defines an excess function as follows: "Excess functions are thermodynamic properties of solutions which are in excess of those of an ideal (or ideal dilute) solution at the same conditions of temperature, pressure and composition." Because the enthalpy change of mixing for an ideal liquid mixture is zero, the excess molar enthalpy is the enthalpy of mixing.

$$H_m^E = \Delta H_{mix} \tag{4.1}$$

H_m^E is related to the excess molar Gibbs function, G_m^E, by the Gibbs-Helmholtz equation:

$$(H_m^E)_{x_1} = \left(\frac{\partial(G_m^E/T)}{\partial(1/T)}\right)_{x_1,p} \tag{4.2}$$

The determination of H_m^E from the variation of G_m^E with temperature is not practical because of magnification of the errors inherent in the measurement of G_m^E. However the equation can be used to test the reliability of G_m^E data.

4.1.1. Calorimetry:

Excess molar enthalpies are measured using calorimeters. There are three basic types of calorimetry namely:

a. Adiabatic calorimetry[79]
b. Isothermal Displacement Calorimetry[80]
c. Flow Calorimetry [81, 82, 83, 84, 85, 86]

The most recent review of calorimetry is by Marsh and O' Hare[79] which covers calorimetry up to 1995. Brief reviews of the above techniques are given by Govender [87] and by Mercer-Chalmers.[88] Calorimetry of solutions and mixtures has been comprehensively reviewed by McGlashan[89] who covered work up to 1961. Shorter reviews by Marsh, [90,91,92] Becker, [93] and again by McGlashan [94] are also available.

The most important aspects of accurate enthalpy measurement relate to (a) minimizing the vapour space,[95, 96] (b) maintaining excellent temperature sensing and control[79] and (c) achieving good mixing.[79]

4.2. Experimental:

Flow microcalorimetry [79, 97, 98] was used in this work, and all determinations were carried out at 298.15 K. As it was easier and less time consuming than the other techniques.

4.2.1. Apparatus:

In this work a thermometric 2277 thermal activity monitor [99] was used to determine the excess molar enthalpies. The thermometric 2277 thermal activity monitor is described in greater detail by Govender.[87] The principle behind this technique is that when two components are mixed together isothermally, the heat required to maintain an isothermal condition is regarded as the heat of mixing. When heat is added, the enthalpy is positive. To add heat, a known current is passed through a heater of known resistance which allows calculation of the heat (see figure 4.1. for a simple diagram of the apparatus). When heat is given off by the mixing process (a negative enthalpy) a calibration is required. The calibration involves determining the amount of heat which must be added to the system to produce the same positive, heating effect as the mixing process. This process is no longer isothermal. Mixing of the two liquids takes place in a gold mixing cell designed to ensure proper mixing.

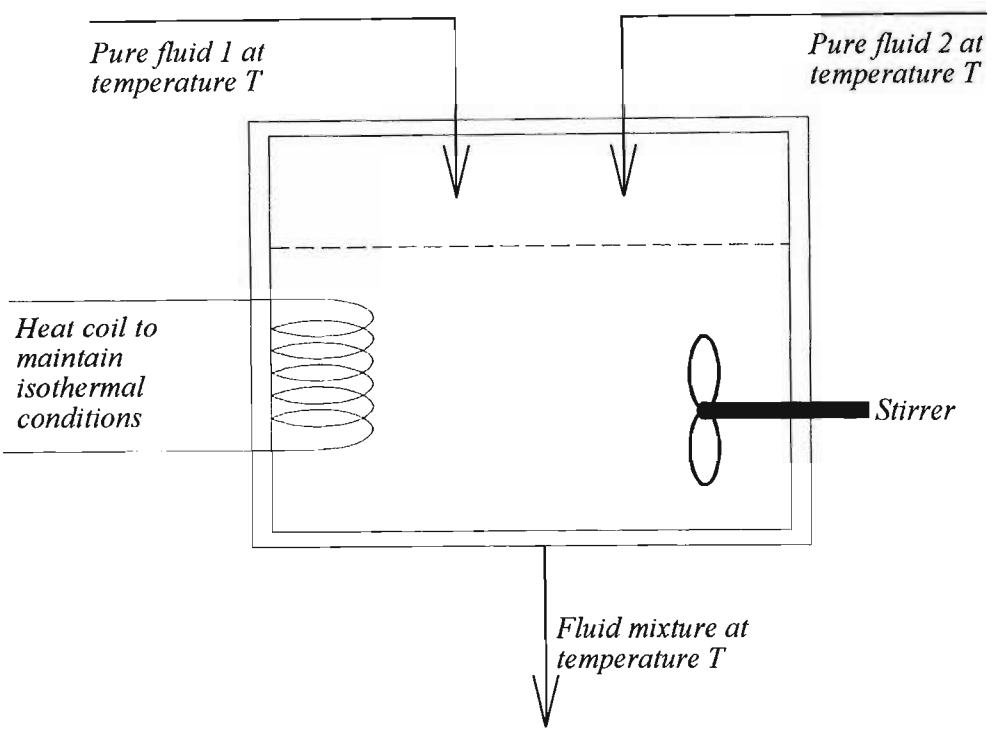

Figure 4.1. Schematic diagram of an isothermal flow calorimeter.

The system is equipped with two Eldex variable-speed piston pumps which allows control of the liquid flow rates in the range of 0.05 to 3 cm^3 min^{-1}.

The thermal activity monitor uses the principle of heat leakage or heat flow where heat produced in a vessel flows away to establish equilibrium between the vessel and its surroundings. The two components are allowed to come together and mix in a 22 carat gold mixing cell (see figure 4.2.). The mixing cell is sandwiched between two Peltier thermopile sensors which are in contact with a metal heat sink (see figure 4.3.). This results in the flow of heat to or from the mixing cell through the Peltier elements. The Peltier elements respond to any temperature gradient, down to one millionth of a degree Kelvin. These sensors act as detectors that convert the heat energy to a voltage signal that is proportional to the heat flow. Results are presented as energy per unit time (that is, in watts).

The calorimeter is calibrated by passing a known current through precision heaters of known resistance while the liquid[a] is flowing through both tubes. These heaters are in intimate contact with the mixing cell and closely simulate the actual reaction. This ensures an accurate calibration of the detectors.

[a]The liquid is a mixture of the two solvents.

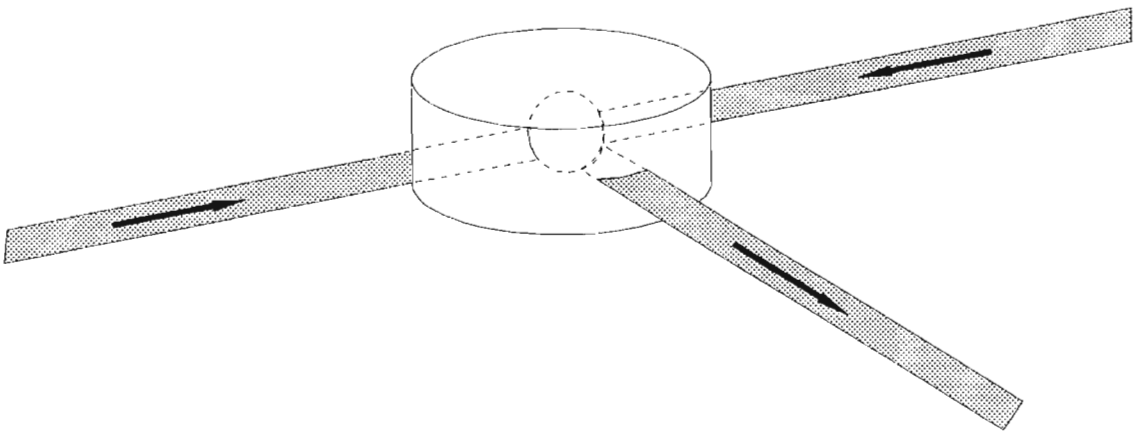

Figure 4.2. Flow measuring cell which allows mixing of the two components.

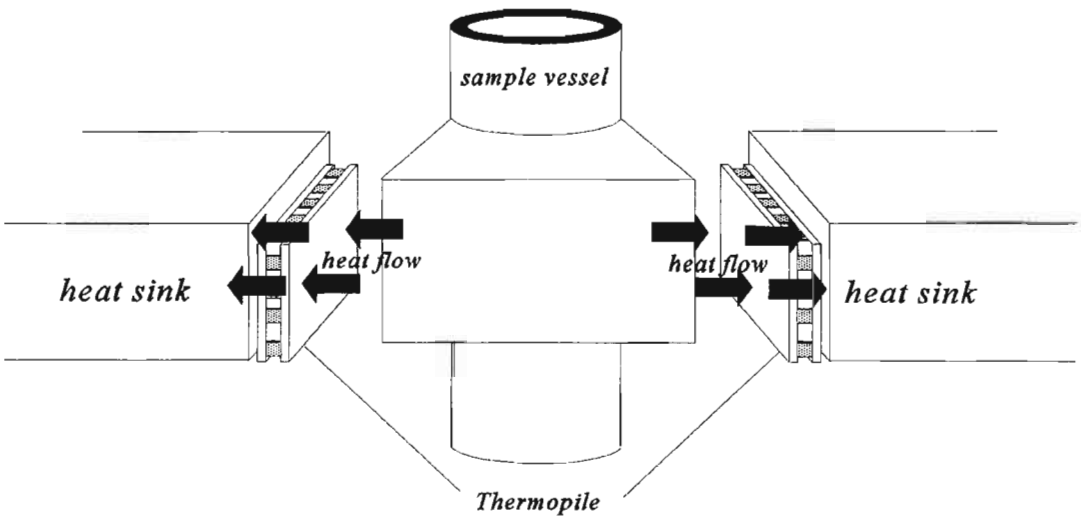

Figure 4.3. Representation of the heat flow system used in the Thermometric 2277 thermal activity monitor.

4.2.2. Experimental procedure:

Each experimental run consists of two steps: first, a calibration and second, the actual determination of the excess molar enthalpy.

4.2.2.1. Calibration:

The calibration not only sets the detectors for correct output, but also accounts for frictional effects. A calibration is specific to each flow rate. Once the flow rates are set, a mixture of the solvents is pumped through both inlet lines until a steady output reading is obtained. This reading corresponds to a reading of zero. The instrument is adjusted until a reading of zero is obtained.

The next step in the procedure is to apply a known, steady current through the calibration heater until a steady reading is obtained. Given the following relationship between the heat flow per unit time; that is, power, P, and the current injected, I, one is able to calibrate the instrument:

$$P = I^2R \tag{4.3.}$$

where R is the resistance of the calibration heater, which is known.

4.2.2.2. Determination:

Both the components are pumped through the system and, as soon as the output stabilizes, the reading (P), in watts, is recorded. The molar flow rate is determined by accurately weighing the solvents before and after the determination. The entire run is timed to within 1 second over a period of about 15 minutes.

The molar flow rate (F) is calculated as follows:

$$F = \frac{(n_1+n_2)}{t} \tag{4.4}$$

where n_1 and n_2 are the number of moles of components 1 and 2 respectively and t is equal to the time in seconds.

The excess molar enthalpy at a particular mole fraction is calculated using the following relationship[b] and is accurate to within 2 J mol^{-1}.

$$H_m^E = \frac{P}{F} \tag{4.5}$$

The mole fractions are easily calculated from the numbers of moles, n_1 and n_2 which are determined by weighing the solvents before and after the determination. The mole fractions are accurate to within 0.001.

4.2.3. Chemicals:

The chemicals used, the suppliers and purity are listed in table 4.1.

Table 4.1. Details of chemicals: purity and suppliers.

Compound	Supplier	Purity
NMP	Sigma	>99 %
toluene	SAARChem	99 %
o-xylene	JANSSEN CHIMICA	99 %
m-xylene	Merck	99 %
p-xylene	JANSSEN CHIMICA	>99 %
mesitylene	Merck	98 %
ethyl benzene	ACROS	99%

All chemicals were used without further purification. NMP was kept under molecular sieves; as it is hygroscopic.

[b] P is given in watts. 1 W = 1 J s^{-1} . F is given in mol s^{-1} and hence H_m^E is in units of J mol^{-1}.

4.3. Results:

The raw data used for the calculations of the mole fractions and H_m^E are given in Appendix B. The excess molar enthalpies for the mixtures NMP(1) + an aromatic hydrocarbon(2) over the entire composition range are given in table 4.2 and are plotted against composition in figure 4.4. The composition is expressed in mole fraction NMP, x_1.

The Redlich-Kister smoothing function[100] was fitted to the H_m^E data:

$$H_m^E = x(1-x)\sum_{r=0}^{n} A_r(1-2x)^r \qquad (4.6)$$

by the method of unweighted least squares. The coefficients A_r given in table 4.3. were determined using the commercial STATGRAPHICS package.

Table 4.2. Excess molar enthalpies for mixtures of the type NMP (1) + an aromatic hydrocarbon(2) at 298.15 K.

x_1	H_m^E	x_1	H_m^E	x_1	H_m^E	x_1	H_m^E
Benzene		Toluene		o-xylene		m-xylene	
0.210	-365.11	0.216	-184.25	0.226	-41.21	0.211	50.25
0.223	-387.13	0.298	-262.09	0.234	-40.76	0.217	50.02
0.312	-469.03	0.353	-299.46	0.391	-90.28	0.234	47.50
0.415	-533.00	0.435	-320.28	0.415	-90.68	0.253	49.08
0.452	-540.53	0.522	-315.53	0.446	-102.76	0.254	45.22
0.469	-544.12	0.534	-311.11	0.497	-111.49	0.324	36.11
0.484	-546.40	0.610	-287.09	0.553	-120.44	0.354	32.68
0.514	-540.11	0.656	-272.25	0.561	-121.60	0.408	25.90
0.658	-471.37	0.739	-234.59	0.621	-120.16	0.466	9.53
0.693	-443.05			0.692	-121.88	0.621	-1.77
0.761	-358.65			0.720	-121.92	0.710	-5.95
0.844	-237.25			0.828	-98.19	0.740	-8.92
						0.767	-8.47
						0.790	-9.14
						0.828	-10.74

Table 4.2. continued: Excess molar enthalpies for mixtures of the type NMP (1) + an aromatic hydrocarbon (2) at 298.15 K.

x_1	H_m^E	x_1	H_m^E	x_1	H_m^E
p-xylene		mesitylene		ethyl benzene	
0.256	-8.42	0.200	237.15	0.157	-19.30
0.258	-8.36	0.325	319.10	0.291	-39.33
0.377	-39.22	0.414	336.77	0.398	-60.57
0.393	-44.60	0.484	336.44	0.462	-69.82
0.402	-41.60	0.526	327.14	0.511	-70.97
0.447	-54.85	0.537	327.43	0.522	-70.48
0.482	-57.76	0.559	319.47	0.551	-70.87
0.515	-61.93	0.583	314.29	0.560	-70.55
0.539	-64.17	0.621	302.23	0.595	-70.38
0.586	-67.53	0.652	291.84	0.611	-69.31
0.605	-68.79	0.687	278.66	0.660	-64.82
0.639	-65.94	0.748	245.52	0.725	-56.44
0.680	-69.12	0.887	128.24	0.791	-46.82
0.686	-66.71			0.881	-24.73
0.706	-65.65				
0.725	-63.13				
0.826	-47.64				
0.882	-38.30				

Table 4.3. Coefficients A_r and the standard deviation, σ, for mixtures of the type NMP (1) + an aromatic hydrocarbon (2) at 298.15 K.

Aromatic hydrocarbon	A_0	A_1	A_2	A_3	σ
benzene	-2178.36	-90.25	319.91	-489.55	2.67
toluene	-1279.15	-302.95	295.79	1437.12	1.61
o-xylene	-446.88	325.90	43.64	171.35	2.38
m-xylene	38.33	250.81	255.90	182.29	2.03
p-xylene	-243.34	244.62	253.30	173.30	1.53
mesitylene	1334.33	302.20	249.11	-549.12	1.66
ethyl benzene	-278.91	106.45	178.50	-39.04	1.63

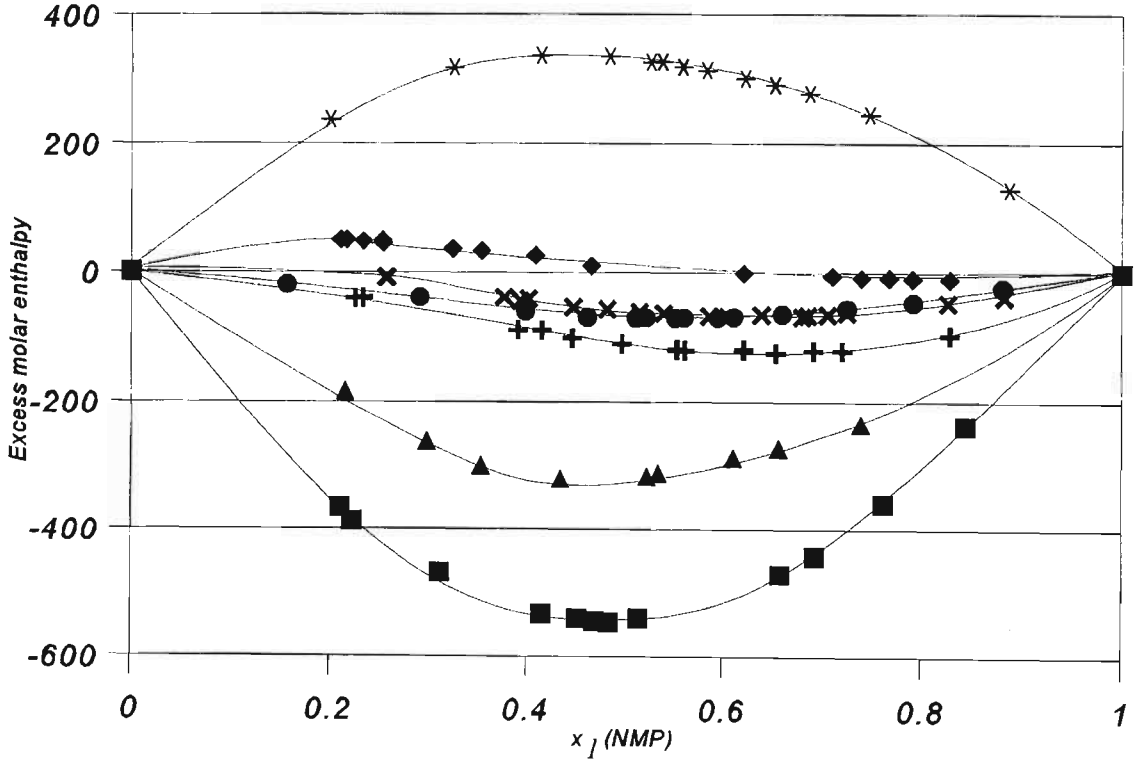

Figure 4.4. Composite plot of excess molar enthalpy versus x_1 at 298.15 K for the mixture NMP (1) + an aromatic hydrocarbon (2). Where : ■ = benzene, ▲ = toluene, ✚ = o-xylene, ◆ = m-xylene, ✖ = p-xylene, ✱ = mesitylene, ● = ethyl benzene.

4.4. Discussion:

4.4.1. Previous work:

Excess enthalpy data for only two systems of the type NMP + an aromatic hydrocarbon are available in the literature: (a) NMP + benzene reported by Gustin and Renon [76] and (b) NMP +o-xylene reported by Shcherbina *et al.* [77]

The H_m^E data reported by Gustin and Renon [76] for the mixture NMP + benzene is plotted in figure 4.5. The data shows that H_m^E is exothermic over the entire composition range. The data reported by Gustin and Renon [76] is in reasonably good agreement with data of this work (within 37 $J\,mol^{-1}$ in the worst case).

The data reported by Shcherbina *et al.* [77] shows that H_m^E for the mixture NMP + o-xylene is endothermic for low concentrations of NMP and is endothermic at higher concentrations of NMP. The meagre data which consists of only four data points was not in agreement with the data produced in this work (see figure 4.6).

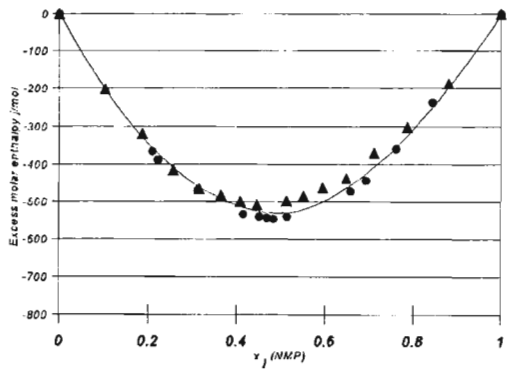

Figure 4.5. Comparison of literature data versus data from this work for the mixture NMP (1) + benzene (2) at 298.15 K.
Key: ● = this work, ▲ = Gustin and Renon.[76]

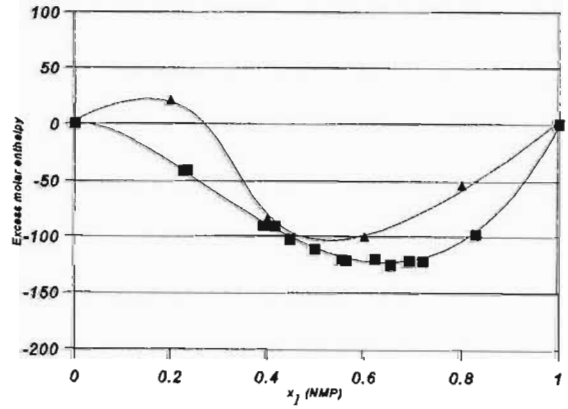

Figure 4.6. Comparison of literature data versus data from this work for the mixture NMP + o-xylene at 298.15 K.
Key : ■ = this work , ▲ = Shcherbina *et al.* [77]

4.4.2. This work:

This work presents new data for mixtures of the type NMP + an aromatic hydrocarbon where the aromatic hydrocarbon is toluene or m-xylene or p-xylene or mesitylene or ethyl benzene. The new data describes the effect that substitution on the benzene ring has on H_m^E for the mixtures.

The data presented in this work show that H_m^E is reasonably exothermic for benzene ($H_{m,\min}^E \approx -546\ J\ mol^{-1}$) and toluene ($H_{m,\min}^E \approx -320\ J\ mol^{-1}$) and is reasonably endothermic for mesitylene ($H_{m,\max}^E \approx 336\ J\ mol^{-1}$). H_m^E for o-xylene ($H_{m,\min}^E \approx -121\ J\ mol^{-1}$), p-xylene ($H_{m,\min}^E \approx -70\ J\ mol^{-1}$) and ethyl benzene ($H_{m,\min}^E \approx -71\ J\ mol^{-1}$) are mildly exothermic while H_m^E for the mixture NMP + m-xylene ranges from mildly endothermic at low concentrations of NMP to mildly exothermic for high concentrations of NMP.

The enthalpy of mixing can be considered to be a result of three main effects: (a) the dissociation of NMP on mixing, which is an endothermic effect (b) the dissociation of the aromatic moiety on mixing, which is also an endothermic effect and (c) the association of NMP with the polarizable aromatic compound, which is an exothermic effect.

Of all the results presented here (see figure 4.4) the exothermic effect is greatest for the mixture NMP + benzene. This exothermic effect is no doubt due to the association mentioned in the previous paragraph. This association appears not to be as strong for the substituted aromatics. This is probably due to steric hindrance of the substituted groups(see figure 4.7). For the mixture NMP + mesitylene, the endothermic effect outweighs the exothermic effect. This is, no doubt, due to the increased steric effect caused by increased methyl substitution on the benzene moiety (see figure 4.7) resulting in a decreased association of NMP with mesitylene. H_m^E for the mixtures xylene + NMP (where xylene refers to o-xylene or m-xylene or p-xylene) is between the H_m^E for the mixtures NMP + benzene and NMP + mesitylene. This is to be expected if the above idea regarding association is correct.

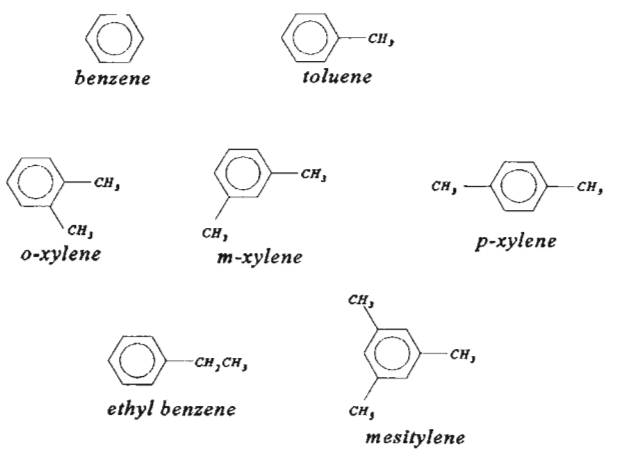

Figure 4.7. Structures of the aromatic compounds used in this work.

Chapter 5
Excess molar volumes of mixing

5.1. Introduction:

In this chapter, a brief definition of the excess molar volume, V_m^E, is given together with a concise summary of the available techniques used in measuring V_m^E. This is followed by the results and a discussion on the V_m^E results obtained for the mixtures, N-methyl-2-pyrrolidone (NMP) + an aromatic hydrocarbon, where the aromatic hydrocarbon is one of benzene or toluene or o-xylene or m-xylene or p-xylene or mesitylene or ethyl benzene.

V_m^E measurements on the mixtures (NMP + an aromatic hydrocarbon) at 298.15 K have been carried out by Al-Mashhadani *et al.*[101] using densitometry and by Liu *et al.* [102] using dilatometry, where an aromatic hydrocarbon refers to benzene or toluene or o-xylene or m-xylene or p-xylene or ethyl benzene or mesitylene. Kanbour *et al.*[103] have also measured the V_m^E for mixtures of NMP and an aromatic hydrocarbon where the aromatic hydrocarbons were benzene or toluene. The work presented here, was carried out to test the reliability of the method used here, and to compare the work done here with the precision dilatometric work done by Liu *et al.*[102] and the work done by Al-Mashhadani *et al.*[101]

The excess molar volume is defined by the following equation:[26]

$$V_m^E = V_{(mixture)} - [x_A V_A^o + (1-x_A) V_B^o] \qquad (5.1)$$

where V_{mixture} is the actual volume per mole of mixture
and V_A^o is the molar volume of pure A and V_B^o is the molar volume of pure B,
and x_A is the mole fraction of component A.

V_m^E is also related to the excess Gibbs function by the following relationship:

$$V_m^E = \left(\frac{\partial G^E}{\partial P}\right)_{x,T} \qquad (5.2)$$

This equation (5.2) is useful in relating V_m^E to other thermodynamic functions but will not be discussed in this work.

V_m^E is a function of many properties which include (a) the packing of the dissimilar molecules (which includes steric factors), (b) the relative sizes of the molecules of the components and (d) the interactions between the different species. It is impossible to single out any one of

these factors from V_m^E data.

5.2. Techniques for the determination of excess molar volumes:

Excess molar volumes can be determined from density measurements or from direct dilatometric measurements. Comprehensive reviews of these techniques have been published by Battino,[104] Letcher,[105] Handa and Benson [106] and Stokes and Marsh.[107,91,92]

In dilatometric determinations the change in volume is measured directly on mixing the two components. The most sophisticated direct volume measuring equipment was designed by McGlashan and Kumaran.[108] For detailed reviews of this technique refer to Govender [87] and Mercer-Chalmers [88]. The precision of this technique is better than 0.003 $cm^3\ mol^{-1}$.

Density measurements can be performed by pycnometry [109, 110, 111] which has a precision between 0.01 and 0.02 $cm^3\ mol^{-1}$ or by using densitometers.[112] In this work a mechanical oscillating densitometer was used. The precision is of the order of 0.005 to 0.01 $cm^3\ mol^{-1}$. This method was used as it is simple and is cheaper.

5.2.1. Temperature control:

Density measurements are extremely sensitive to temperature changes as can be seen by the following error analysis:

Molar volume, V, is defined as:

$$V = \frac{M}{\rho} \tag{5.3}$$

where M is the molar mass and ρ is the density.

The error, dV, can be determined by differentiation of this equation:

$$dV = \frac{d(M/\rho)}{dM}.dM + \frac{d(M/\rho)}{d\rho}.d\rho \tag{5.4}$$

$$\therefore \quad dV = \frac{1}{\rho}.dM + M.\frac{d(1/\rho)}{d\rho}.d\rho \tag{5.5}$$

Assuming that the changes are finite, equation 5.5 becomes :

$$\Delta V' = \frac{\Delta M}{\rho} - \frac{M}{\rho^2}\Delta\rho \qquad (5.6)$$

where $\Delta V'$ is the error in V resulting from an error in the molar mass of ΔM and an error in density of $\Delta\rho$. Assuming that the molar masses are well known $\frac{\Delta M}{\rho} = 0$. The resultant equation for the change in volume is:

$$\Delta V' = -\frac{M}{\rho^2}.\Delta\rho \qquad (5.7)$$

The negative sign in equation 5.7 is eliminated as the error is given by the magnitude of this equation.[113]

From equation 5.1 it can be seen that the V_m^E is made up of two terms; that is, the volume of the ideal solution and the volume of the mixture hence the error is doubled. Therefore the error in V_m^E, ΔV, is:

$$\Delta V \approx 2 \times \Delta V' = 2 \times \frac{M}{\rho^2} . \Delta\rho \qquad (5.8)$$

In the following calculation, the error in ΔV is calculated for an error in density, ρ, resulting solely from a temperature change. For the simple calculation below, the density and the molar masses are averaged for the ideal solution and the mixture of benzene + NMP:

$$\rho_{avg} = \rho_{benzene} + \rho_{NMP} \qquad (5.9)$$

$$M_{avg} = M_{benzene} + M_{NMP} \qquad (5.10)$$

Based on the following densities[23] of benzene at different temperatures, $\Delta\rho$ can be calculated for an error in temperature of 1 °C :

$\rho^{25} = 0.87901$ g cm $^{-3}$
$\rho^{20} = 0.87370$ g cm $^{-3}$

Thus an error in temperature of 1 °C will result in an error in ρ of 0.00106 g cm^{-3}, through linear interpolation. (ie. $\Delta\rho = 0.00106$ g cm^{-3}).

$\rho_{NMP} = 1.0259$

Therefore

$\rho_{avg} = (0.8737 + 1.0259)/2 = 0.9498$ g cm^{-3}

$M_{avg} = (78.11 + 99.13)/2 = 88.62$ g mol^{-1}

Therefore ΔV per 1 °C is:

$$\Delta V \approx 2 \times \frac{88.62}{(0.9498)^2} \times 0.00106 = 0.2083$$

Therefore an error in temperature of 0.01°C will result in an error in the volume of 0.002 cm^3.

Thus, if the temperature is controlled only to within 0.01 °C and there is no other error (for example, in x_1) then the error in ΔV would be 0.002 cm^{-3} mol^{-1}. To ensure that temperature is not an important factor in the final error in V_m^E (that is, less than 0.002 cm^{-3} mol^{-1}) the temperature must be controlled to better than 0.01 °C and preferably to better than 0.005 °C.

5.3. Experimental:

5.3.1. Apparatus:

In this work an Anton Paar vibrating-tube densitometer[a] model DMA 601 was used to determine the densities. The density is determined by measuring the period of oscillation of a hollow tube that contains the sample. This period is related to the density by the following equation:[88]

$$\rho = A + B\tau^2 \qquad (5.11)$$

where ρ is the density,
A and B are constants specific to the instrument and operating temperatures and
τ is the period of oscillation.

The constants are obtained by determining the period for two compounds of known density. In this work air, and pure water were used to calibrate the instrument.

A schematic layout of the apparatus is given in figure 5.1.

---

[a] For a description of mechanical oscillating densitometers refer to Govender[87] and Mercer-Chalmers.[88]

5.3.1.1. Temperature control:

The Anton Paar DMA 601 densitometer has an integral temperature control associated with it which controls the temperature to within 0.001 °C. To ensure that the temperature control was efficient, the temperature was measured using a Hewlett-Packard quartz thermometer (see figure 5.1). The Hewlett-Packard quartz thermometer is capable of detecting the temperature to within 0.0001 °C. Polystyrene balls placed in the waterbath prevented temperature fluctuations due to evaporation.

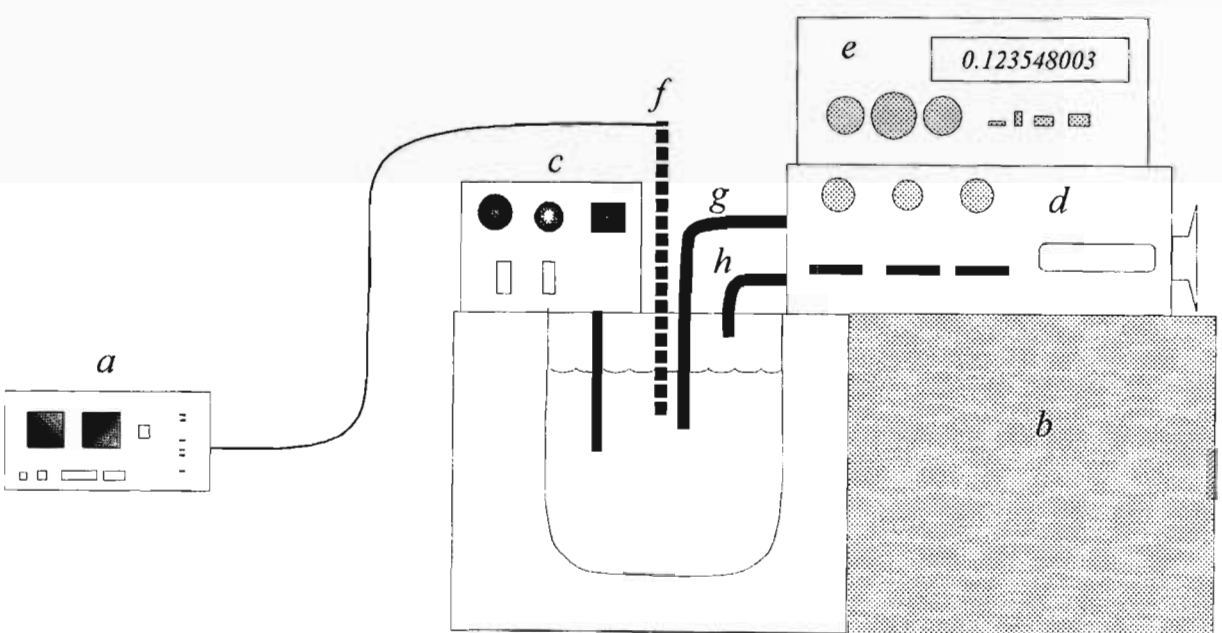

Figure 5.1. Schematic layout of the experimental apparatus. a. Hewlett-Packard thermometer, b. cooling unit, c. temperature control unit with heater and stirrer, d. external cell(contains oscillating u-tube), e. period meter, f. quartz temperature probe, g. water inlet pipe, h. outlet pipe.

5.3.2. Chemicals:

The chemicals used in this work and their purities are given in table 5.1 together with the experimental density and the literature value of the density.

Table 5.1. Details of chemicals: suppliers, purity and density, ρ, at 298.15 K.

Compound	Supplier	Purity	ρ^{25}	ρ^{25} (literature)	Reference
NMP	Sigma	>99 %	1.0278	1.0259	24
benzene	SAARchem	99 %	0.8735	0.8737	23
toluene	SAARChem	99 %	0.8628	0.8622	23
o-xylene	JANSSEN CHIMICA	99 %	0.8747	0.8759	23
m-xylene	Merck	99 %	0.8598	0.8601	23
p-xylene	JANSSEN CHIMICA	>99 %	0.8569	0.8566	23
mesitylene	Merck	98 %	0.8616	0.8611	23
ethyl benzene	ACROS	99 %	0.8625	0.8625	23

5.4. Results:

The excess molar volumes of mixing for mixtures of the type NMP + an aromatic hydrocarbon at 298.15 K are shown in table 5.2. and are plotted in figure 5.2. The Redlich-Kister equation (5.12.) was fitted to the experimental results by the method of unweighted least squares:[100]

$$V_m^E = x(1-x)\sum_{i=0}^{k} A_r(1-2x)^r \qquad (5.12)$$

The parameters A_0, A_1, A_2 and A_3 together with the standard deviation, σ, which were determined using the commercial computer package STATGRAPHICS are given in table 5.3. The Excess molar volume and excess molar enthalpy show the same functional dependance on x.

Table 5.2. Excess molar volumes at 298.15 K for the mixtures NMP (1) + an aromatic hydrocarbon (2).

x_1	V_m^E / cm³ mol⁻¹	x_1	V_m^E / cm³ mol⁻¹	x_1	V_m^E / cm³ mol⁻¹	x_1	V_m^E / cm³ mol⁻¹
benzene		toluene		o-xylene		m-xylene	
0.022	-0.0929	0.053	-0.1457	0.023	-0.0617	0.022	-0.0661
0.035	-0.1396	0.084	-0.2470	0.050	-0.1392	0.113	-0.2964
0.068	-0.2590	0.141	-0.4147	0.094	-0.2283	0.208	-0.4821
0.129	-0.4400	0.175	-0.5027	0.110	-0.2757	0.335	-0.6317
0.157	-0.5084	0.309	-0.7325	0.194	-0.4166	0.443	-0.6911
0.273	-0.7073	0.469	-0.8439	0.207	-0.4370	0.458	-0.6939
0.539	-0.7937	0.601	-0.7845	0.335	-0.5898	0.511	-0.6978
0.699	-0.6583	0.739	-0.6259	0.343	-0.6006	0.617	-0.6526
0.855	-0.3722	0.874	-0.3821	0.503	-0.6482	0.727	-0.5372
0.922	-0.2175	0.927	-0.2569	0.758	-0.5109	0.768	-0.5002
0.962	-0.1347	0.973	-0.1318	0.862	-0.3561	0.873	-0.3311
0.983	-0.0754			0.890	-0.3055	0.925	-0.2418
				0.940	-0.2009	0.983	-0.0473
				0.968	-0.1268		

Table 5.2. continued. Excess molar volumes at 298.15 K for the mixtures NMP (1) + an aromatic hydrocarbon (2).

x_1	V_m^E / cm³ mole⁻¹	x_1	V_m^E / cm³ mole⁻¹	x_1	V_m^E / cm³ mole⁻¹
p-xylene		mesitylene		ethyl benzene	
0.023	-0.0789	0.033	-0.0599	0.061	-0.1894
0.108	-0.3254	0.101	-0.1646	0.105	-0.3030
0.205	-0.5329	0.227	-0.3000	0.224	-0.5540
0.330	-0.7033	0.373	-0.3985	0.373	-0.7012
0.428	-0.7683	0.458	-0.4172	0.533	-0.7419
0.503	-0.7929	0.509	-0.4265	0.645	-0.6765
0.600	-0.7642	0.537	-0.4160	0.900	-0.3314
0.679	-0.6790	0.644	-0.3942	0.951	-0.1978
0.764	-0.5769	0.671	-0.3791	0.972	-0.1316
0.866	-0.3914	0.706	-0.3633	0.981	-0.0973
0.933	-0.1926	0.790	-0.3028		
0.979	-0.0842	0.879	-0.2127		
		0.940	-0.1305		
		0.986	-0.0347		

Table 5.3. Coefficients A_r and the standard deviations, σ, for the mixtures NMP (1) + an aromatic hydrocarbon (2) at 298.15 K.

Aromatic hydrocarbon	A_0	A_1	A_2	A_3	σ
benzene	-3.2321	-0.5326	-0.5019	-0.0088	0.0119
toluene	-3.3356	-0.5201	-0.1980	1.2007	0.0132
o-xylene	-2.5800	-0.0690	-0.6059	0.5878	0.0094
m-xylene	-2.7647	-0.2854	-0.3846	0.6443	0.0105
p-xylene	-3.1454	-0.0298	-0.2941	-0.0277	0.0105
mesitylene	-1.6788	-0.0244	-0.3695	0.3272	0.0048
ethyl benzene	-2.9379	-0.1985	-0.9246	0.8802	0.0123

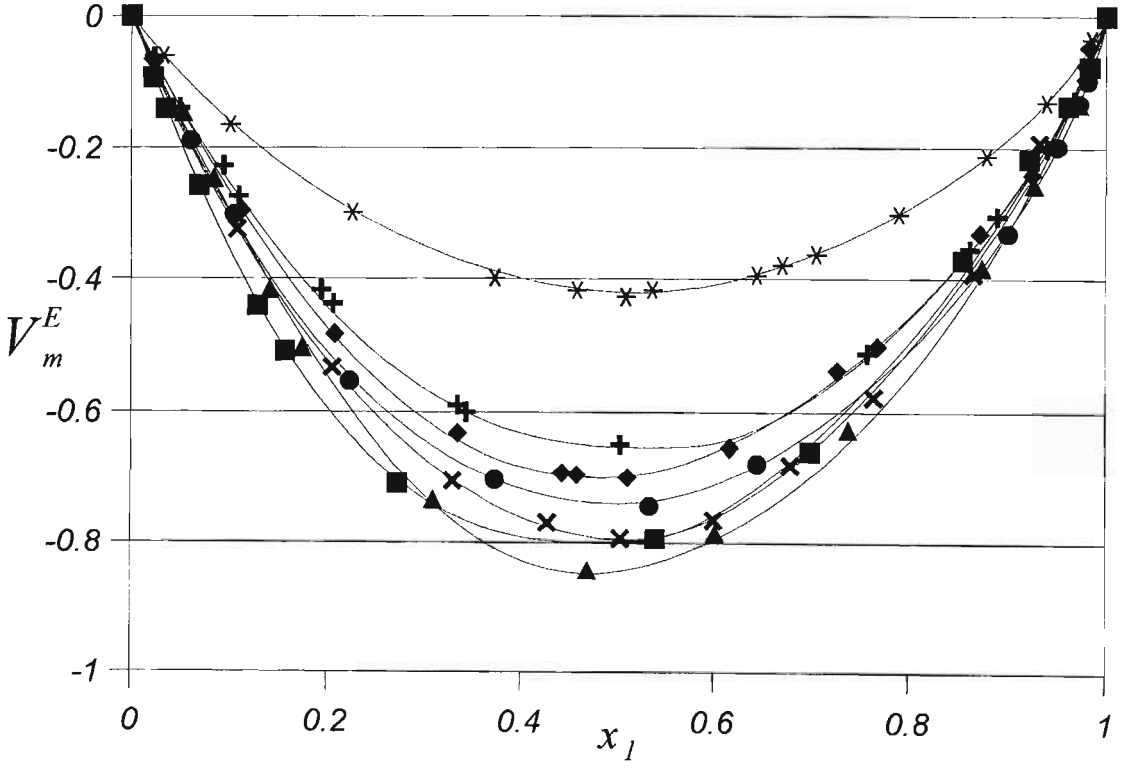

Figure 5.2. Excess molar volume (cm^3 mol^{-1}) at 298.15 K for the mixture NMP(1) + aromatic hydrocarbon (2).
Key : ■ = benzene, ▲ = toluene, ✚ = o-xylene, ◆ = m-xylene, ✖ = p-xylene, ✱ = mesitylene, ● = ethyl benzene.

5.5. Discussion:

5.5.1. Previous work:

High precision dilatometric work carried out by Liu *et al.*[102] (see figure 5.3) shows that V_m^E is negative over the complete mole fraction range for mixtures of the type NMP + an aromatic hydrocarbon, where the aromatic hydrocarbon is benzene or toluene or o-xylene or m-xylene or p-xylene or ethyl benzene. The curves shown in figure 5.3 are symmetrical and smooth. Their work shows that the sequence of excess molar volumes in terms of their absolute values at $x_1 = 0.5$ is : toluene > p -xylene > benzene > m-xylene > o-xylene ≈ ethyl benzene. Dilatometry does have a drawback in that errors tend to be accumulative and results can appear to have high precision (smooth curves).

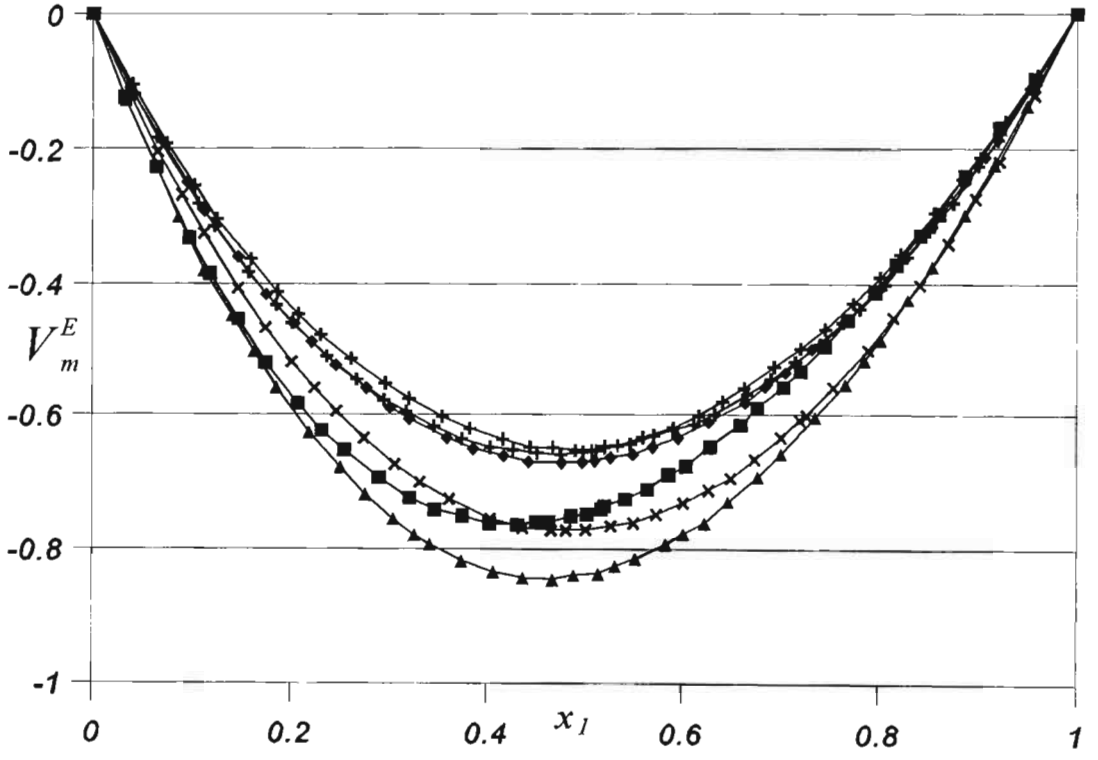

Figure 5.3. Excess molar volume (cm^3 $mole^{-1}$) at 298.15 K for the mixture NMP (1) + aromatic hydrocarbon (2). this work was done by Liu *et al.*[102]
Key : ■ = Benzene, ▲ = toluene, ✚ = o-xylene, ◆ = m-xylene, ✖ = p-xylene ,● = ethyl benzene.

Al-Mashhadani *et al.*[101] have measured V_m^E for the mixtures NMP + an aromatic hydrocarbon at 298.15 K where an aromatic hydrocarbon refers to benzene or toluene or o-xylene or m-xylene or p-xylene or mesitylene or ethyl benzene using densitometry. Their work is presented in figure 5.4. This shows that the sequence of excess molar volumes in terms of their absolute values at $x_1 = 0.5$ is : toluene > p -xylene > benzene ≈ m-xylene ≈ o-xylene ≈ ethyl benzene > mesitylene. The data presented by Liu *et al.*[102] appears to be better as the standard deviation of the work by Liu *et al.*[102] is better than 0.005 and the standard deviation of the work by Al-Mashhadani *et al.*[101] is only better than 0.02.

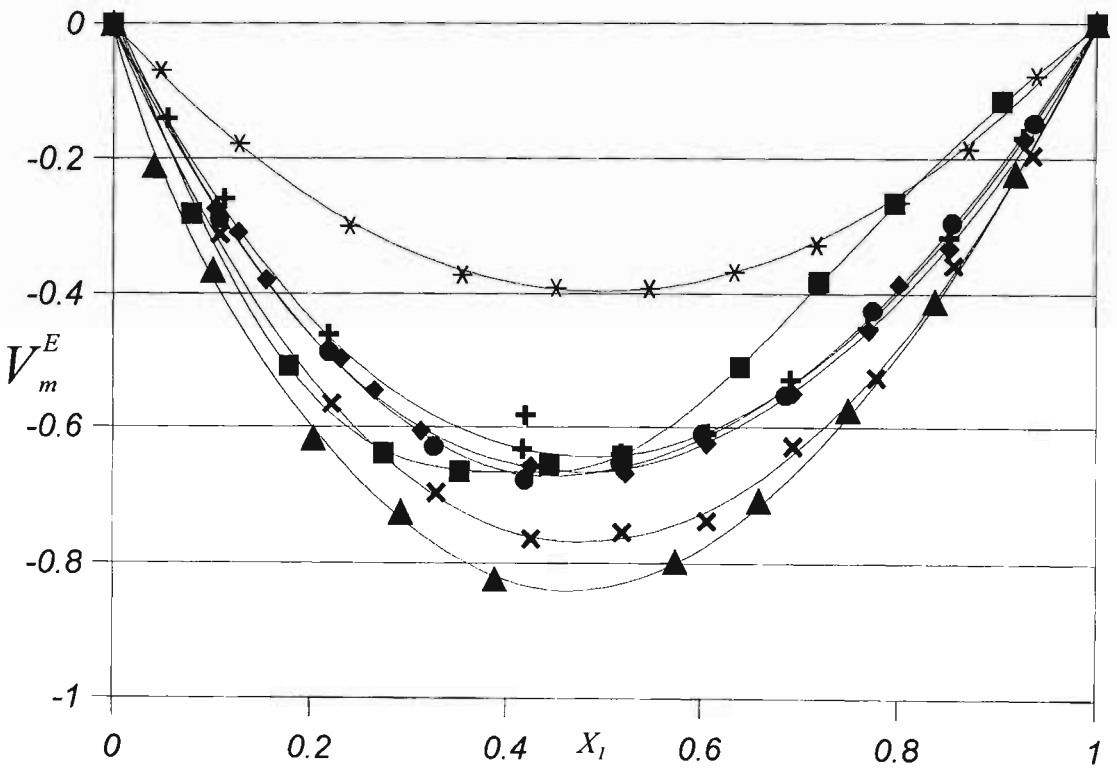

Figure 5.4. Excess molar volumes at 298.15 K for the mixture NMP (1) + an aromatic hydrocarbon reported by Al-Mashhadani *et al.*[101]
Key: ■ = benzene, ▲ = toluene, ✚ = o-xylene, ◆ = m-xylene, ✖ = p-xylene, ✱ = mesitylene, ● = ethyl benzene.

5.5.2. This work:

The excess molar volumes determined in this work are all negative over the entire composition range and relate well to the measurements made by Liu *et al.*[102] (see figures 5.5. to 5.10.) with the exception of the mixture NMP + ethyl benzene. Data reported by Liu *et al.*[102] has a better (lower) standard deviation than the data presented here.

Al-Mashhadani *et al.*[101] have determined V_m^E for the systems investigated in this work by densitometry. The data from their work is compared to the data from this work in figures 5.11 through figure 5.17. The standard deviation from their work is poorer (higher) than that reported here.

The negative excess molar volume could be as a result of packing and association between the polar NMP and the polarizable aromatic compound.

Mesitylene shows the smallest negative excess molar volume and toluene the largest negative excess molar volume.

The sequence of aromatic hydrocarbons in terms of the magnitude of V_m^E at $x_1 = 0.5$ is:

toluene > benzene ≈ p-xylene > ethyl benzene > m-xylene > o-xylene > mesitylene.

Increased methyl substitution on the benzene moiety results in a decrease in the magnitude of V_m^E. This effect could be due to packing (which includes the steric effects of increased methyl substitution) or due to inductive effects of methyl substitution. It is impossible to separate these effects. Benzene's behaviour is contrary to this pattern.

The association between NMP and the aromatic hydrocarbons that accounts for the negative enthalpic effect seen in chapter four also accounts for the dimunition (negative effect) in the molar excess volume results presented here.

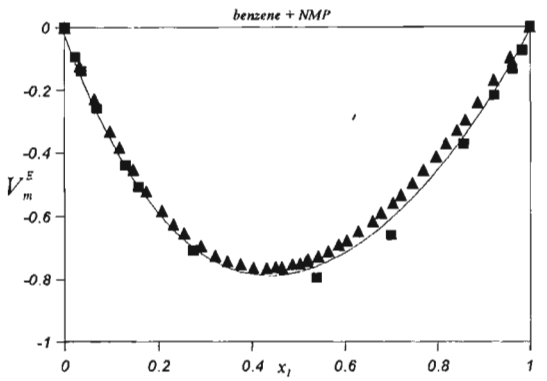

Figure 5.5. Comparison of the results of this work with literature data for NMP(1) + Benzene(2).
■ = this work, ▲ = Liu *et al.*[102]

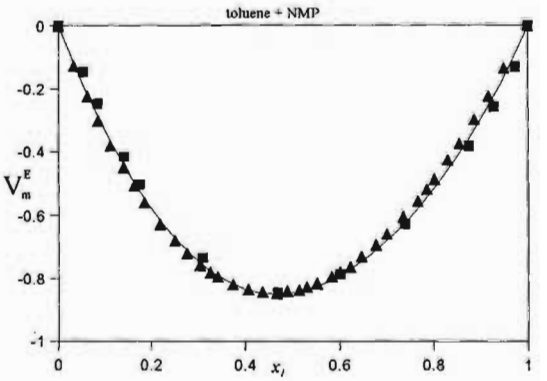

Figure 5.6. Comparison of the results of this work with literature data for NMP(1) + toluene(2).
■ = this work, ▲ = Liu *et al.*[102]

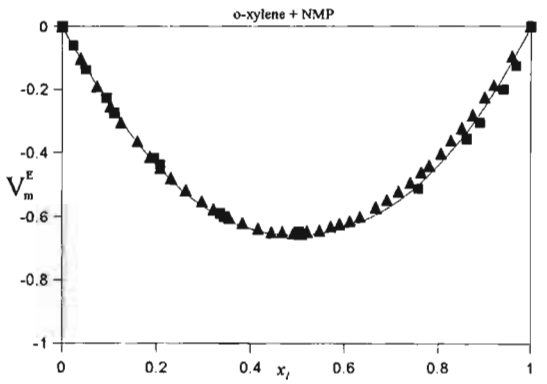

Figure 5.7. Comparison of the results of this work with literature data for NMP(1) + o-xylene(2).
■ = this work, ▲ = Liu *et al.*[102]

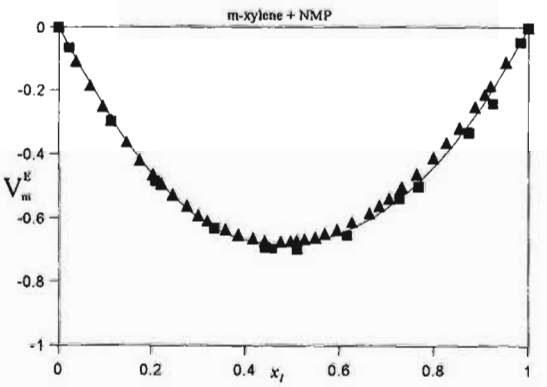

Figure 5.8. Comparison of the results of this work with literature data by for NMP(1) + m-xylene(2).
■ = this work, ▲ = Liu *et al.*[102]

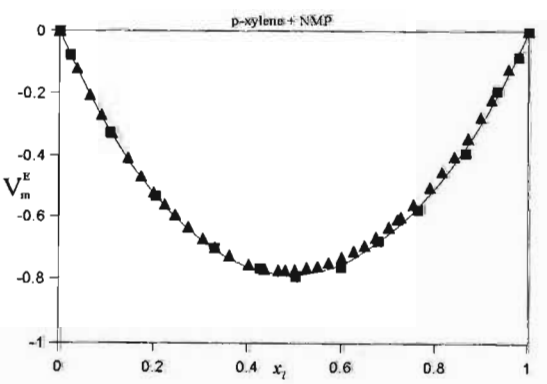

Figure 5.9. Comparison of the results of this work with literature data for NMP(1) + p-xylene(2).
■ = this work, ▲ = Liu *et al.*[102]

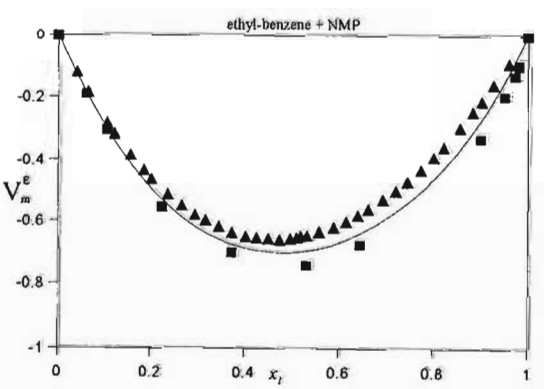

Figure 5.10. Comparison of the results of this work with literature data for NMP(1) + NMP(2).
■ = this work, ▲ = Liu *et al.*[102]

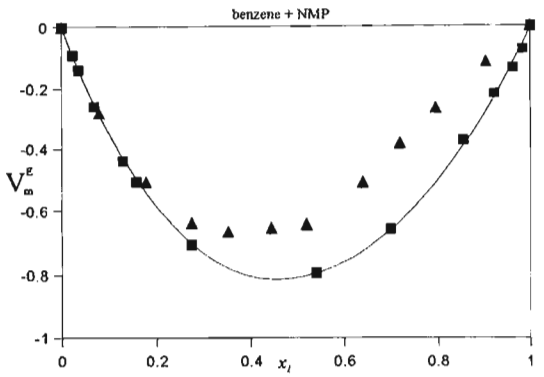

Figure 5.11. Comparison of the results of this work with the literature for the mixture NMP (1) + benzene(2).
Key : ■ = this work ▲ = Al-Mashhadani *et al.*[101]

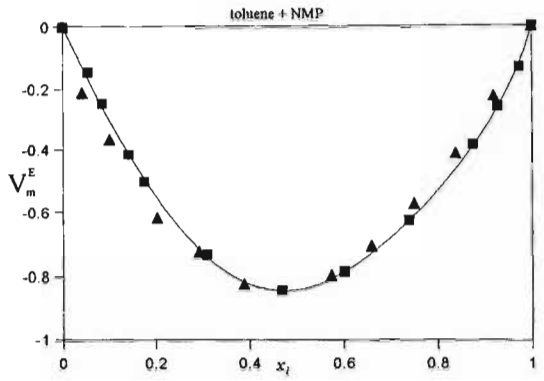

Figure 5.12. Comparison of the results of this work with the literature for the mixture NMP(1) + toluene(2).
Key: ■ = this work, ▲ = Al-Mashhadani *et al.*[101]

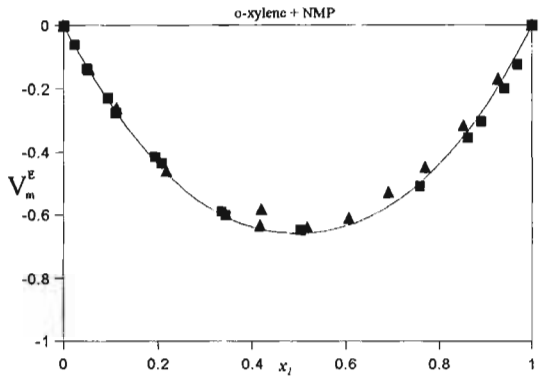

Figure 5.13. Comparison of the results of this work with the literature for the mixture NMP (1) + o-xylene(2).
Key: ■ = this work, ▲ = Al-Mashhadani *et al.*[101]

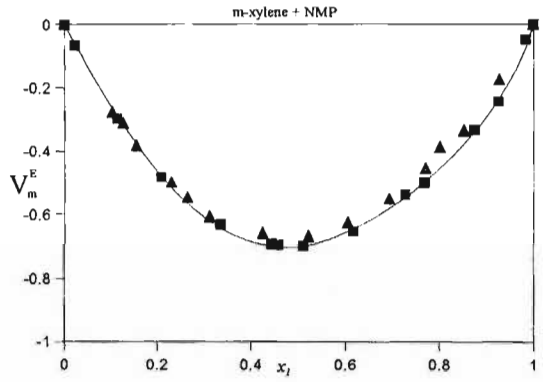

Figure 5.14. Comparison of the results of this work with the literature for the mixture NMP (1) + p-xylene(2).
Key: ■ = this work, ▲ = Al-Mashhadani *et al.*[101]

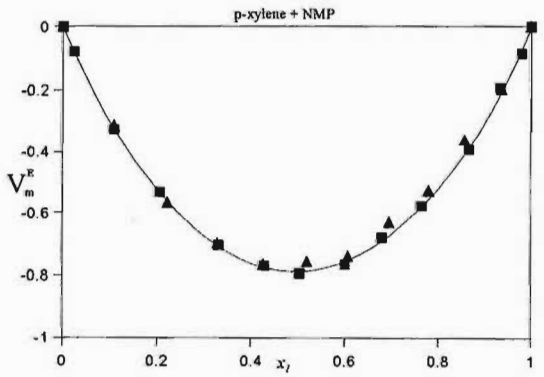

Figure 5.15. Comparison of the results of this work with the literature for the mixture NMP (1) + (2).
Key: ■ = this work, ▲ = Al-Mashhadani *et al.*[101]

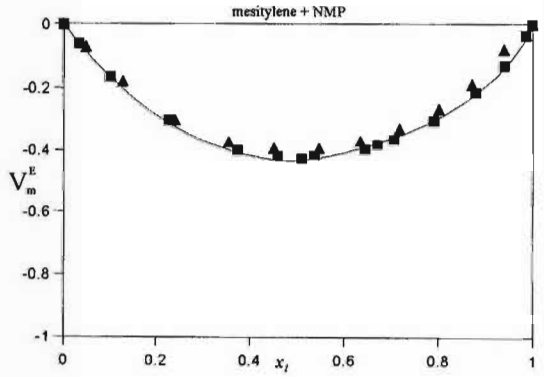

Figure 5.16. Comparison of the results of this work with the literature for the mixture NMP (1) + mesitylene(2).
Key: ■ = this work, ▲ = Al-Mashhadani *et al.*[101]

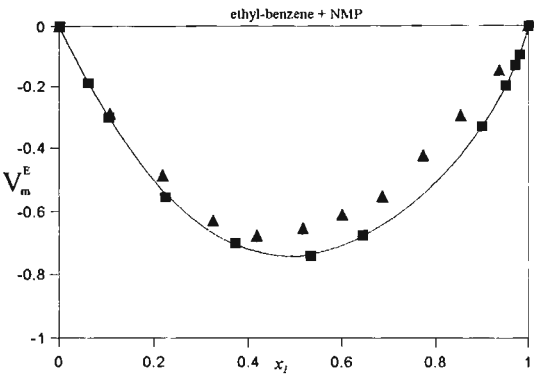

Figure 5.17. Comparison of the results of this work with the literature for the mixture NMP (1) + ethyl benzene(2).
Key: ■ = this work, ▲ = Al-Mashhadani *et al.*[101]

Chapter 6
Conclusion

The conclusions of this work are summarized below.

- The liquid-liquid equilibrium data presented here support the results presented by Ferreira *et al.*[12] for the mixture n-heptane + toluene + NMP at 298.2 K.

- New liquid-liquid equilibria data are presented for the mixtures given below at 298.2 K and 1 atmosphere pressure:
  - n-hexane + toluene + NMP
  - n-nonane +toluene + NMP
  - n-hexadecane + toluene + NMP
  - n-hexadecane + o-xylene + NMP
  - n-hexadecane + m-xylene + NMP
  - n-hexadecane + p-xylene + NMP
  - n-hexadecane + mesitylene + NMP
  - n-hexadecane + ethyl benzene + NMP.

- From the liquid-liquid equilibria work presented here, the phase equilibria for the mixtures n-alkanes + an aromatic hydrocarbon + NMP at a temperature of 298.2 K and a pressure of 1 atmosphere show a strong dependance on the chain length of the n-alkane (see figure 6.1a) and a very weak dependance on methyl substitution of the aromatic hydrocarbon (see figure 6.1b). An increase in the chain length of the n-alkane from C_6 (hexane) to C_{16} (hexadecane) results in an increase in the area defining the two phase region(see figure 6.1a).

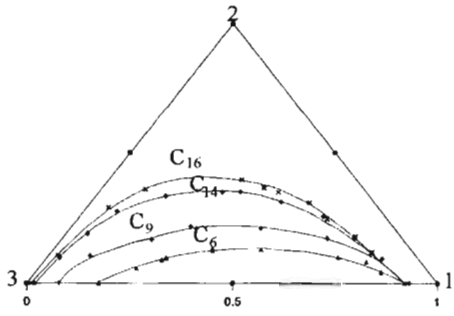

Figure 6.1a. Dependance of the area defining the two-phase region on n-alkane chain length.

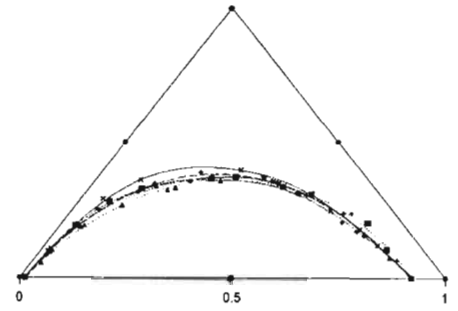

Figure 6.1b. Dependance of the area defining the two-phase region on the type of aromatic hydrocarbon.

- The slopes of the tie-lines on equilibrium phase diagrams for mixtures of the type an n-alkane + an aromatic hydrocarbon + NMP show that the aromatic compound is more soluble in NMP than in the alkane when the chain length of the alkane is short (C_6 to C_9), (see figure 6.2a) and the aromatic compound is more soluble in the n-alkane than in NMP when the chain length of the n-alkane is long (C_{14} to C_{16}), (see figure 6.2b). This could have an important bearing on the liquid-liquid extraction of aromatic hydrocarbons from mixtures containing n-alkanes and aromatic hydrocarbons using NMP. More work should be done to further investigate this property. Because of the importance of the slopes of the tie-lines, it would be important to investigate the effect of temperature and pressure on these slopes.

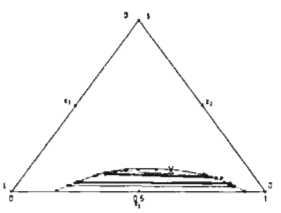

Figure 6.2a. Slope of tie-lines for n-hexane + toluene + NMP.

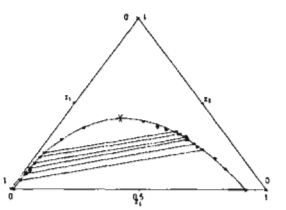

Figure 6.2b. Slope of tie-lines for hexadecane + toluene + NMP.

- The tie-line results indicate that it is probably viable to separate the individual n-alkanes from each other in mixtures containing n-alkanes and aromatic hydrocarbons using solvent extraction, but it is not possible to separate the aromatics from each other using this process.

- The $\gamma^{\infty}_{1,3}$ results presented for the n-alkanes or cycloalkanes in NMP supports the work by Muller *et al.*[33], Kikic *et al.*[34] and Surovy *et al.*[41].

- New $\gamma^{\infty}_{1,3}$ results are presented for cyclopentane or cyclooctane or 1-heptene or 1-octene or diethyl ether or diisopropyl ether in NMP at 298.15 K. These results can be used to predict the phase equilibria for mixtures containing NMP and these solutes. This has not been attempted here but should form the basis of further work.

- The γ^{∞}_{13} results presented here show a monotonic increase with carbon number for the n-alkanes or cycloalkanes or 1-alkenes in NMP at 298.15 K. This can be seen in figure 6.3.

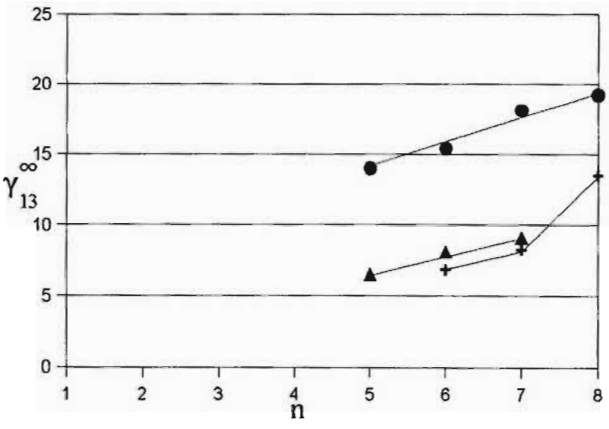

Figure 6.3. Plot of γ^{∞}_{13} versus carbon chain length.
Key: ● = n-alkanes, ▲ = cycloalkanes, ✚ = 1-alkenes.

- H^{E}_{m} results presented here for the mixture NMP + benzene supports the H^{E}_{m} results presented by Gustin and Renon[77] for the same mixture.

- New H^{E}_{m} results are presented for the mixtures NMP + toluene or m-xylene or p-xylene or mesitylene or ethyl benzene at 298.15 K.

- The H_m^E results presented here for the mixtures NMP + an aromatic hydrocarbon (where an aromatic hydrocarbon refers to benzene or toluene or o-xylene or m-xylene or p-xylene or mesitylene or ethyl benzene) show the effect that methyl substitution on the benzene ring has on the H_m^E. The more methyl groups on the benzene moiety the less negative is H_m^E, implying a reduction in the association between NMP and the aromatic hydrocarbon. This diminished association between NMP and the aromatic hydrocarbon could be due to steric effects which result from an increase in methyl substitution on the benzene moiety.

- The V_m^E results presented here for the mixtures NMP + an aromatic hydrocarbon (where an aromatic hydrocarbon refers to benzene or toluene or o-xylene or m-xylene or p-xylene or mesitylene or ethyl benzene) is in very good agreement with the dilatometric work carried out by Liu *et al.* [103] and in reasonably good agreement with the densitometric work carried out by Mashhadani *et al.*[102].

- V_m^E results presented here for the mixtures NMP + an aromatic hydrocarbon (where an aromatic hydrocarbon refers to benzene or toluene or o-xylene or m-xylene or p-xylene or mesitylene or ethyl benzene) show the effect that methyl substitution on the benzene moiety has on V_m^E. The more methyl groups on the benzene moiety, the less negative is the V_m^E implying a reduction in association between NMP and the aromatic hydrocarbon. This reduced association between NMP and the aromatic hydrocarbon could be due to the steric effects which result from an increase in methyl substitution on the benzene moiety or to inductive effects of the methyl groups.

- The H_m^E and V_m^E results presented here for mixtures NMP + an aromatic hydrocarbon (where an aromatic hydrocarbon refers to benzene or toluene or o-xylene or m-xylene or p-xylene or mesitylene or ethyl benzene) could be used to test mixing theories, such as UNIFAC, ERAS, NRTL. This has not been attempted here but could form the basis of further work.

Literature

1. Mueller E.; Hoefeld G.; *8th World Pet. Congress*, (1971), **4**, 213.
2. Mueller E.; Hoefeld G.; *7th World Pet. Congress*, (1967), **4**, 13.
3. Eisenlohr K. H.; Gross Hans W.; *Erdol Kohle Erdgas Pertrchem.*, (1965), **18**, 614.
4. Wuepper J. L.; Popov A. I.; *J. Am. Chem. Soc.*, (1969), **91**,4352.
5. Dyke J. D.; Sears P.G.; Popov A. I.; *J. Phys. Chem.*, (1967), **71**, 4140.
6. Breant M.; *Bull. Soc. Chim. Fr.*, (1971), 725.
7. Sowinski A. F.; Whitesides G. M.; *J. Org. Chem.*, (1979), **44**, 2369.
8. Kadum A. A.; Langan J. R.; Salmon G. A.; Edwards P. P.; *Radioanal. Nucl. Chem.*, (1986), **101**, 319.
9. Guarino G.; Ortona O.; Sartirio G. A.; Edwards P. P.; *J. Chem. Eng. Data*, (1985), **30**, 366.
10. Thornton J. D.; *Science and Practice of Liquid-Liquid Extraction Vol 1*, (1992),Claredon Press, Oxford, Great Britain.
11. Schweitzer P. A.; *Handbook of Separation Techniques for Chemical Engineers*, (1979), McGraw Hill, USA.
12. Ferreira P. O.; Ferreira J. B.; Medina A. G.; *Fluid Phase Equilibria*, (1984), **16**, 369-379.
13. Al-Zayied T. A.; Al-Sahhaf T. A.; Fahim M. A.; *Fluid Phase Equilibria*, (1990), **61**, 131-144.
14. Fabries J. F.; Gustin J. L.; Renon H.; *J. Chem. Eng. Data*, (1977), **22**(3), 303-308.
15. Ashton N. F. McDermott C.; Branch A.; *Handbook of Solvent Extraction*, (1983), Edited by Lo T. C.; Baird M. H. I.; Hansa C.; Wiley Interscience, New York.

16. Reinhardt H.; Rydeberg J.; *Acta Chemical Scandinavica*, (1969), **23**, 2773.

17. Liljenzin J. L.; *Proceedings of the International Solvent Extraction Conference*, (1979), ISEC 77, Vol. 1, CIM special vol. 21, 295, Canadian Institute of Mining and Metallurgy, Montreal, Canada.

18. Letcher T. M.; Wooten S.; Shuttleworth B.; Heyward C.; *J. Chem. Thermodynamics*, (1986), **18**, 1037-1042.

19. Newsham D. M. T.; Ng S. B.; *J. Chem. Eng. Data*, (1972), **17**, 205.

20. Briggs S. W.; Commings E.W.; *Ind. Eng. Chem.*, (1943), **35**, 411-415.

21. Malanowski S.; Bittrich H. J.; Lempe D.; Reinhardt K.; *Fluid Phase Equilibria*, (1994), **98**, 163-171.

22. Treybal R. E.; Webber L. D.; Daley J. F.; *Ind. Eng.Chem.*, (1946), **38**, 817-825.

23. *TRC Thermodynamic Tables*, (1988); Texas Engineering Experimental Station, Thermodynamic Research Centre, Texas A & M University system.

24. Riddick J. A.; Bunger W. B.; Sakano T. K.; *Organic solvents: Physical Properties and Methods of Purification*, (1986), Wiley Interscience, New York.

25. Atkins P. W.; *Physical Chemistry*, (1986), 3rd edition, Oxford University Press, Great Britain.

26. Sandler S. I.; *Chemical Thermodynamics*, (1940), Wiley, USA.

27. Smiley H. M.; *J. Chem. Eng. Data*, (1970), **15**, 413.

28. Hlavatý K.; *Coll. Czech. Chem. Commun.*, (1972), **37**, 4005.

29. Schultz D. M.; Crouse C. F. S.; *S. Afr. Stat. J.*, (1973), **7** , 143-144.

30. Letcher T. M.; Siswana P. M.; van der Watt P.; Radloff S.; *J. Chem. Thermodynamics*, (1989), **21**, 1053-1060.

31. Smiley H. M.; *J. Chem. Eng. Data*, (1970), **15**, 413.

32. Popescu R.; Blidisel I.; Papa E.; *Rev. Roum. Chim.*, (1967), **18**, 746.

33. Muller S.; Trieu N. B.; Bittrich H. J.; *Wiss. Z. Tech. Hochsch. Chem Leuna-Mersburg*, (1976), **18**, 587.

34. Kikic I.; Renon H.; *Sep. Sci.*, (1976), **11**, 45.

35. Vernier P.; Raimbault C.; Renon H.; *J. Chim. Phys.*, (1969), **66**, 429.

36. Wardencki W.; Tameesh A. H.; *J. Chem. Tech. Biotechnol.*, (1981), **31**, 86.

37. Leroi J. C.; Masson J. C.; Renon H.; Fabries J. F.; Sannier H.; *Ind. Eng. Chem. Process Des. Dev.*, (1977), **16**, 139.

38. Deal C. H.; Derr E. L.; *Ind. Eng. Process Des. Dev.*, (1964), **3**, 394.

39. Masalsccky T.; Popescu R.; *Rev. Chim.* (Bucharest), (1976), **27**, 292.

40. Tian F.; Jin S.; Wang X.; Zhao S.; Chen Z.; *SEPU*, (1986), **4**, 235.

41. Surovy J.; Oveckova J.; Graczova E.; *Collect. Czech. Chem. Commun.*, (1990), **55**, 1457.

42. Park J. H.; Hussam A.; Couasnom P.; Frity D.; Carr P. W.; *Anal. Chem.*, (1987), **59**, 1970.

43. Frost R.; Bittrich H. J.; *Wiss. Z. Tech. Hochsch. Chem Leuna-Mersburg*, (1974), **16**, 18.

44. DECHEMA Chemistry Data Series, *Activity coefficients at infinite dilution*, (1994), Vol. 1.

45. Malanowski S.; Anderko A.; *Modelling Phase Equilibria*, (1992), Wiley Series in Chemical Engineering. Wiley, USA.

46. Palmer D. A.; *Handbook of Applied Thermodynamics*, (1987), CRC Press, Boca Raton.

47. Schreiber L. B.; Eckert C. A.; *Ind. Chem. Eng. Process Design Development*, (1971), **10**, 572.

48. Reid R. C.; Prausnitz J. M.; Poling B. E.; *The Properties of Gases and Liquids*, (1986), McGraw-Hill, USA.

49. Letcher T. M.; *Activity Coefficients at Infinite Dilution Using GLC*, (1978), Chemical Thermodynamics : A Specialist Periodical Report Vol. 2, Chapter 2, Edited by M. L. McGlashan, Chemical Society London.

50. Trompe D. M.; Eckert C. A.; *J. Chem. Eng. Data*, (1990), **35**, 156.

51. Suleiman D.; Eckert C. A.; *J. Chem. Eng. Data*, (1994), **39**, 692.

52. Hussam A.; Carr P. W.; *Anal. Chem.*, (1985), **57**, 793.

53. Piridal K. A.; Bertigh A.; Sandler S. I.; *J. Chem. Eng. Data*, (1992), **37**, 484.

54. Hradertzky G.; Wobst M.; Vopel H.; Bittrich H. J.; *Fluid Phase Equilibria*, (1990), **54**, 133.

55. Thomas E. R.; Newman B. A.; Nicolaides G. L.; Eckert C. A.; *J. Chem. Eng. Data*, (1982), **27**, 233.

56. Thomas E. R.; Eckert C. A.; *Ind. Eng. Chem. Proc. Des. Dev.*, (1984), **23**, 194.

57. Wilson G. M.; *J. Am. Chem. Soc.*, (1964), **86**, 127.

58. Wilson G. M.; Deal C. H.; *Ind. Eng. Chem. Fundam.*, (1962), **1**, 20.

59. Redlich O.; Derr E. L.; Pierotti G.; *J. Am. Chem. Soc.*, (1959), **81**, 2283.

60. Derr E. L.; Papadopoulous M.; *J. Am. Chem. Soc.*, (1959), **81**, 2285.

61. Fredenslund A.; Jones L.; Prausnitz J. M.; *AIChe. J.*, (1975), **21**, 1086.

62. Abrams D. S.; Prausnitz J. M.; *AIChe. J.*, (1975), **21**, 116.

63. Magnussen T. P.; Rasmussen P.; Fredenslund A.; *Ind. Eng. Chem. Proc. Des. Dev.*, (1981), **20**, 331.

64. Ghmeling J.; Weidlich U.; *Fluid Phase Equilibria*, (1986), **242**, 171.

65. Larsen B. L.; Rasmussen P.; Fredenslund A.; *Ind. Eng. Chem. Proc. Des. Dev.*, (1987), **26**, 2274.

66. Elbro H. S.; Fredenslund A.; Rasmussen P.; *Report SEP 8819*, (1988), Instutitt for Kemiteknik DJH, Lyngby, Denmark.

67. Marin A. J. P.; Synge R. L.; *Biochem. J.*, (1941), **35**, 1358.

68. James A. T.; James A. J. P.; *Biochem. J.*, (1952), **50**, 679.

69. Martin A. J. P.; *Analyst*, (1956), **81**, 52.

70. Porter P. E.; Deal C. H.;Stross F. H.; *J. Am. Chem. Soc.*, (1956), **78**, 2999.

71. Everett D. H.; Stoddart C. T. H.; *Trans. Faraday Soc.*, (1961), **57**, 746.

72. Cruickshank A. J. B.; Gainey B. W.; Hicks C. P.; Letcher T. M.; Moody R. W.; Young C. L.; *Trans. Faraday Soc.*, (1968), **64**, 2667.

73. McGlashan M. L.; Potter D. J. B.; *Proc. Roy. Soc. A.*, (1962), **267**, 478.

74. Hudson G. H.; McCoubrey J. C.; *Trans. Faraday Soc.*, (1960), **56**, 761.

75. *C. R. C. Handbook of Chemistry and Physics*, (1984),Edited by R. C. Weast, **72nd Edition**, C.R.C. Press Inc., Boca Raton.

76. Gustin J. L.; Renon H.; *J. Chem. Eng.Data*, (1973), **18**, 164-166.

77. Schernbina E. I.; Tenenbaum A. E.; Gurarii L. L.; *Zh. Fiz. Khim.*, (1975), **49**, (English Translation), 450, (Russian Pages) 768.

78. Prausnitz J. M.; *Thermodynamics of Fluid Phase equilibria*, (1969), Englewood Cliffs, Prentice-Hall Inc., New Jersey.

79. Marsh K. N. M.; O'Hare P. A. G.; *Experimental Thermodynamics Vol IV, Solution Calorimetry*, (1994), IUPAC, Cambridge University Press, Great Britain.

80. Savini C. G.; Winterhalter D. R.; Van Ness H. C.; *J. Chem. Eng. Data*, (1966), **11**, 40.

81. Rose V. C.; Storvick T. S.; *J. Chem. Thermodynamics*, (1966), **18**, 359.

82. Stoesser P. R.; Gill S. J.; *Rev. Sci. Instrum.*, (1967), **38**, 422.

83. Monk P.; Wadsö I.; *Acta Chem. Scand.*, (1968), **22**, 1842.

84. Sturtevant J. M.; Lyons P. A.; *J. Chem. Thermodynamics*, (1969), **1**, 201.

85. Picker P.; Jolicoeur C.; Desnoyers J. E.; *J. Chem. Thermodynamics*, (1969), **1**, 469.

86. McGlashan M. L.; Stoeckli J. F.; *J. Chem. Thermodynamics*, (1969), **1**, 589.

87. Govender U. P.; *Ph D Thesis*, (1996), University of Natal, South Africa.

88. Mercer-Chalmers J. D.; *Ph D Thesis*, (1993), Rhodes University, South Africa.

89. McGlashan M. L.; *Experimental Thermochemistry*, Volume 2, Chapter 15, (1967), Edited by H. R. E. Skinner, Interscience, London.

90. Marsh K. N.; *Chemical Thermodynamics (Specialist Periodical Reports)*, (1978), Edited by M. L. McGlashan, The Chemical Society, London.

91. Marsh K. N.; *Ann. Rep. R.. S. C. Sect. C*, (1980), **77** , 101.

92. Marsh K. N.; *Ann. Rep. R.. S. C. Sect. C*, (1984), **81** , 209.

93. Becker F.; *Thermochimica Acta*, (1980), **40**, 1.

94. McGlashan M. L.; *Thermochimica Acta*, (1984), **72**, 55.

95. Mrazek R. V.; Van Ness H. C.; *Am. Inst. Chem. Eng Data J.*, (1961), **7**, 190.

96. Stokes R. H.; Marsh K. N.; Tomlins R. P.; *J. Chem. Thermodynamics*, (1969), **1**, 211.

97. Spink C.; Wadsö I.; *Calorimetry as an analytical tool in Biochemistry an Biology. Methods of Biochemistry.*, (1976), Vol. 23, Edited by D. Glick, Wiley, NewYork.

98. Wadsö I.; *Thermal and Energetic Studies of Cellular Biological Systems.*, (1987), Edited by A. M. James, Wright, Bristol.

99. Suurkuusk J.; Wadsö I.; *Chem. Scr.*, (1982), **20**, 257.

100. Redlich O.; Kister P.; *Ind. Eng. Chem.*, (1948), **40**, 345.

101. Al-Mashhadani A. M. A.; Awwad A. M.; *Thermochimica Acta*, (1985), **89**, 75.

102. Liu X.; Su Z.; Wang H.; Zhong X; *J. Chem. Thermodynamics*, (1996), **28**, 277-283.

103. Kanbour F. I.; Al-Madfai S. F.; Al-Assadi Z. A.; Alchi W. T.; *J. Pet. Res.*, (1982), **1**, 77.

104. Battino R.; *Chemical Reviews*, (1971), **71(1)**, 5.

105. Letcher T. M.; *Chem. S. A.*, (1975), **1**, 226.

106. Handa Y. P.; Benson G. C.; *Fluid Phase Equilibria*, (1979), **3**, 185.

107. Stokes R. H.; Marsh K. N.; *Ann. Rev. Phys. Chem.*, (1972), **23**, 65.

108. Kumaran M. K.; McGlashan M. L.; *J. Chem. Thermodynamics*, (1993), **25**, 949.

109. Bauer N.; Lewin S. Z. *Physical Methods of Organic Chemistry*, (1959), **Part 1**, Edited by Weissberger, Interscience, New York.

110. Wood S. E.; Brusie J. P.; *J. Am. Chem. Soc.*, (1953), **65**, 1891.

111. Scatchard G.; Wood S. E.; Mochel J. M.; *J. Am. Chem. Soc.*, (1945), **68**, 1957.

112. Ash Croft S. J.; Booker D. R.; Turner J. C. R.; *J. Chem. Soc. Faraday Trans.*(1990), **86(1)**, 145.

113. James A. M.; Prichard F. E.; *Practical Physical Chemistry*, (1974), Longman, London.

Appendix A

Table A. Experimental data for the calculation of $\gamma_{1,3}^{\infty}$ of the solutes in NMP (3) at 298.15 K.

Solute	t_G	t_R	n_3	U_o	p_i	p_o
	s	s	moles	$cm^3\ s^{-1}$	mmHg	mmHg
n-pentane	18.53	37.52	0.0049	0.719	760.83	751.50
n-hexane	18.39	79.34	0.0049	0.670	766.05	761.00
n-heptane	18.39	187.81	0.0049	0.670	766.05	761.00
n-octane	17.96	494.41	0.0049	0.743	757.28	752.10
cycloopentane	17.96	80.88	0.0049	0.739	764.48	759.30
cyclohexane	17.96	179.52	0.0049	0.740	764.48	759.30
cycloheptane	17.96	657.98	0.0049	0.742	764.48	759.30
1-hexene	17.64	117.98	0.0049	0.768	755.83	745.79
1-heptene	17.96	292.36	0.0049	0.743	764.48	759.30
1-octene	17.64	765.28	0.0049	0.771	765.28	755.51
diethyl ether	17.64	88.80	0.0049	0.773	755.25	744.91
diisopropyl ether	17.64	179.05	0.0049	0.773	755.24	744.91

Appendix B

Table B1. Experimental data for the mixture NMP(1) + benzene(2) at 298.15 K.

Mass of NMP	Mass of benzene	Time	Power	Flow rate	x_1	H^E_m
g	g	s	W	10^{-4} mol s^{-1}		J mol^{-1}
3.9494	11.6779	982	70.4	1.93	0.210	-365.11
6.3055	17.3580	1216	91.0	2.35	0.223	-387.13
3.9336	6.8489	804	74.3	1.58	0.312	-469.03
14.3368	15.9084	2726	68.1	1.28	0.415	-533.00
9.6576	9.2296	1047	111.3	2.06	0.452	-540.53
9.9327	8.8553	1007	115.4	2.12	0.469	-544.12
7.8258	6.5792	755	118.1	2.16	0.484	-546.40
19.2742	14.3513	1634	125.0	2.31	0.514	-540.11
9.8465	4.0308	775	91.8	1.95	0.658	-471.37
13.6226	4.7547	902	97.4	0.22	0.693	-443.05
18.5654	4.5828	999	88.3	2.46	0.761	-358.65
24.1545	3.5242	1310	52.3	0.22	0.844	-237.25

Table B2. Experimental data for the mixture NMP(1) + toluene(2) at 298.15 K.

Mass of NMP	Mass of toluene	Time	Power	Flow rate	x_1	H_m^E
g	g	s	W	10^{-4} mol s^{-1}		J mol^{-1}
5.5101	18.6188	2064	23.0	1.25	0.216	-184.25
7.9388	17.3548	1320	53.3	2.03	0.298	-262.09
7.1392	12.1410	1158	52.7	1.76	0.353	-299.46
6.9645	8.4239	1263	41.0	1.28	0.435	-320.28
9.1774	7.7956	886	63.1	0.02	0.522	-315.53
16.6310	13.4708	2951	33.1	1.06	0.534	-311.11
14.0296	8.3243	922	72.2	2.51	0.610	-287.09
18.1089	8.8137	1001	75.7	2.78	0.656	-272.25
13.4719	4.4156	1295	33.3	1.42	0.739	-234.59

Table B3. Experimental data for the mixture NMP(1) + o-xylene(2) at 298.15 K.

Mass of NMP	Mass of o-xylene	Time	Power	Flow rate	x_1	H_m^E
g	g	s	W	10^{-4} mol s^{-1}		J mol^{-1}
6.3186	23.2013	1175	9.9	0.24	0.226	-41.21
5.8502	20.5504	1040	9.9	2.43	0.234	-40.76
5.7704	9.6307	1102	12.2	1.35	0.391	-90.28
9.5659	14.4435	933	22.6	2.49	0.415	-90.68
10.7905	14.3395	1085	23.1	2.25	0.446	-102.76
10.7402	11.6387	1052	23.1	2.07	0.497	-111.49
10.6696	9.2273	1037	22.6	1.88	0.553	-120.44
7.3750	6.1754	707	22.8	1.87	0.561	-121.60
15.7689	10.2981	1554	19.8	1.65	0.621	-120.16
15.4784	7.3953	860	32.0	2.63	0.692	-121.88
15.0278	6.2502	729	35.2	2.89	0.720	-121.92
15.9982	3.5501	1568	12.2	1.24	0.828	-98.19

Table B4. Experimental data for the mixture NMP(1) + m-xylene(2) at 298.15 K.

Mass of NMP	Mass of m-xylene	Time	Power	Flow rate	x_1	H_m^E
g	g	s	W	10^{-4} mol s^{-1}		J mol^{-1}
4.3275	17.3419	889	-11.7	2.33	0.211	50.25
4.0283	15.5542	900	-10.4	2.08	0.217	50.02
4.0638	14.2482	1095	-7.6	0.16	0.234	47.50
3.6215	11.4258	1335	-5.3	1.08	0.253	49.08
4.0600	12.7905	839	-8.7	1.92	0.254	45.22
6.6147	14.7585	1218	-6.1	1.69	0.324	36.11
5.6535	11.0579	1013	-5.2	1.59	0.354	32.68
4.7275	7.3341	840	-3.6	1.39	0.408	25.90
5.5770	6.8552	1151	-1.0	1.05	0.466	9.53
9.7544	6.3714	936	0.3	1.69	0.621	-1.77
14.1300	6.1761	918	1.3	2.19	0.710	-5.95
17.6924	6.6703	978	2.2	2.47	0.740	-8.92
16.6344	5.4080	806	2.3	2.71	0.767	-8.47
21.8511	6.1873	943	2.7	2.96	0.790	-9.14
15.0945	3.3615	1520	1.3	1.21	0.828	-10.74

Table B5. Experimental data for the mixture NMP(1) + p-xylene(2) at 298.15 K.

Mass of NMP	Mass of p-xylene	Time	Power	Flow rate	x_1	H_m^E
g	g	s	W	10^{-4} mol s^{-1}		J mol^{-1}
5.3990	16.7475	1987	0.9	1.07	0.256	-8.42
4.0993	12.6491	1490	0.9	1.08	0.258	-8.36
6.4090	11.3580	660	10.2	0.26	0.377	-39.22
6.5513	10.8345	721	10.4	2.33	0.393	-44.60
9.4772	15.1288	1801	5.5	1.32	0.402	-41.60
7.7117	10.2066	795	12.0	2.19	0.447	-54.85
6.9123	7.9557	733	11.4	1.97	0.482	-57.76
7.1315	7.1984	911	9.5	1.53	0.515	-61.93
7.3013	6.6836	769	11.4	1.78	0.539	-64.17
9.1378	6.9156	878	12.1	1.79	0.586	-67.53
8.7252	6.0961	935	10.7	1.56	0.605	-68.79
10.3083	6.2394	795	13.5	2.05	0.639	-65.94
10.0138	5.0499	650	15.8	2.29	0.680	-69.12
8.1153	3.9836	905	8.8	1.32	0.686	-66.71
9.8865	4.4155	549	16.9	2.57	0.706	-65.65
12.3640	5.0217	600	18.1	2.87	0.725	-63.13
13.6785	3.0822	1396	5.7	0.12	0.826	-47.64
24.4400	3.4883	1551	6.9	0.18	0.882	-38.30

Table B6. Experimental data for the mixture NMP(1) + mesitylene(2) at 298.15 K.

Mass of NMP	Mass of mesitylene	Time	Power	Flow rate	x_1	H_m^E
g	g	s	W	10^{-4} mol s^{-1}		J mol^{-1}
4.5141	21.8378	1628	-33.1	0.14	0.200	237.15
5.7041	14.3488	1107	-51.0	0.16	0.325	319.10
7.1534	12.2624	918	-63.9	0.19	0.414	336.77
8.1574	10.5447	789	-72.5	2.15	0.484	336.44
12.4367	13.5682	790	-98.7	3.02	0.526	327.14
9.1750	9.5544	714	-78.9	2.41	0.537	327.43
11.4042	10.9180	722	-91.1	2.85	0.559	319.47
11.0974	9.6186	720	-83.8	2.67	0.583	314.29
11.9614	8.8225	662	-88.6	2.93	0.621	302.23
17.2590	11.1628	836	-93.2	3.19	0.652	291.84
14.1814	7.8271	898	-64.6	2.32	0.687	278.66
13.5684	5.5505	861	-52.2	2.13	0.748	245.52
16.3527	2.5159	1032	-23.1	0.18	0.887	128.24

Table B7. Experimental data for the mixture NMP(1) + ethyl benzene(2) at 298.15 K.

Mass of NMP	Mass of ethyl benzene	Time	Power	Flow rate	x_1	H_m^E
g	g	s	W	10^{-4} mol s^{-1}		J mol^{-1}
5.0674	29.2227	1125	5.6	0.29	0.157	-19.30
5.5165	14.4041	1075	7.0	1.78	0.291	-39.33
6.109	9.8842	801	11.7	1.93	0.398	-60.57
9.5955	11.9907	921	15.9	2.28	0.462	-69.82
8.8191	9.0336	675	18.3	2.58	0.511	-70.97
9.6430	9.4747	623	21.1	2.99	0.522	-70.48
9.2084	8.0261	600	19.9	2.81	0.551	-70.87
9.2989	7.8297	600	19.7	2.79	0.560	-70.55
11.5767	8.4562	640	21.6	3.07	0.595	-70.38
10.0250	6.8497	645	17.8	2.57	0.611	-69.31
9.5032	5.2516	600	15.7	2.42	0.660	-64.82
14.5358	5.9054	928	12.3	2.18	0.725	-56.44
13.8736	3.918	900	9.2	1.97	0.791	-46.82
21.7901	6.1541	1371	4.5	1.82	0.881	-24.73